The

Geophysical Journal

of the

Royal Astronomical Society

incorporating

the Geophysical Supplement to the Monthly Notices of the R. A. S.

Volume 2 No. 2 June 1959

Published and Sold by the

Royal Astronomical Society

Burlington House, London, W.1, England

Price £1; in U.S.A. $3 Annual Subscription £3; in U.S.A. $9

The Geophysical Journal
of the Royal Astronomical Society

Geophysical Secretary

R. A. Lyttleton, M.A., Ph.D., F.R.S., St. John's College, Cambridge

Geophysical Editors

A. H. Cook,
M.A., Ph.D., F.R.A.S., F.G.S.
National Physical Laboratory,
Teddington.

T. F. Gaskell,
M.A., Ph.D., F.R.A.S.
British Petroleum Company,
London.

The *Geophysical Journal* is a journal for the publication of research in geophysics and related subjects. In addition to original papers, short notes and letters to the Editors are accepted for publication.

The aims of the Editors are to publish papers of a high standard, to give them a wide international circulation and to assure authors of speedy publication.

Book reviews and reports of geophysical meetings are also published and the Editors are always glad to hear of such meetings and to receive short reports of them.

Notice to Authors

Authors of papers offered for publication need not be Fellows of the Society.

No charges of any kind are made for printing papers or articles accepted. Contributors are entitled to receive 25 reprints free and greater numbers are obtainable at moderate rates, e.g. 300 copies of a 12-page reprint (exc. plates) cost £11 14s. (U.S. $35). Special arrangements can be made for institutions requiring reprints of their contributions with covers, special pagination etc., for issue in their own series of publications.

Attention is drawn to the recommendations to authors printed on the inside of the back cover.

Papers offered for publication in the December issue should reach the Assistant Secretary of the Society by mid-August.

Volume 2 No. 3 September 1959

The following contributions have been accepted for publication in the above issue:

H. Charnock, Tidal friction from currents near the sea bed.

A. H. Cook, The external gravity field of a rotating spheroid to the order of e^3.

J. H. Piddington, The transmission of geomagnetic disturbances through the atmosphere and interplanetary space.

Progress Report on "Developments in Dynamical Geodesy" by A. H. Cook.

The Geophysical Journal

of the

ROYAL ASTRONOMICAL SOCIETY

Vol. 2 No. 2 June 1959

Torsional Oscillations of the Earth and some Related Problems

H. Takeuchi*

(Received 1958 December 5)

Summary

Variational calculus methods are applied to the problem of torsional oscillations of elastic spheres of variable densities and elasticities and the corresponding plane Love wave problem for vertically heterogeneous media. The methods work well and give the phase velocity curve shown in Figure 1 for the model Earth, the internal constitution of which was inferred by K. E. Bullen. The corresponding displacement distributions are shown in Figure 2.

1. Introduction

Torsional oscillations of elastic spheres of variable densities and elasticities have been studied by several authors. Recently, Matsumoto & Sâto (1954) have studied the torsional oscillations of a sphere consisting of the mantle and core, each of which is homogeneous. N. Jobert (1956) has studied the torsional oscillation of spherical harmonic degree 2 type of the Earth, the internal constitution of which was inferred by K. E. Bullen. Making use of the calculus of variations, she has got the period of 43·54 min for the Earth thus assumed. All of these authors are concerned with the oscillations of rather lower modes. As was pointed out by J. H. Jeans as early as in 1923, by making the wave number larger and larger in this kind of problem, we arrive at the corresponding surface wave problem. Thus the study of torsional oscillation of the Earth may throw some light on the nature of the G wave.

2. Variational method

From the mathematical point of view, the problem of torsional oscillations of elastic spheres of variable densities and elasticities is reduced to solving the

* Seismological Laboratory, California Institute of Technology. On leave from Geophysical Institute, Tokyo University.

The Geophysical Journal

of the

ROYAL ASTRONOMICAL SOCIETY

Vol. 2 No. 2 June 1959

Torsional Oscillations of the Earth and some Related Problems

H. Takeuchi*

(Received 1958 December 5)

Summary

Variational calculus methods are applied to the problem of torsional oscillations of elastic spheres of variable densities and elasticities and the corresponding plane Love wave problem for vertically heterogeneous media. The methods work well and give the phase velocity curve shown in Figure 1 for the model Earth, the internal constitution of which was inferred by K. E. Bullen. The corresponding displacement distributions are shown in Figure 2.

1. Introduction

Torsional oscillations of elastic spheres of variable densities and elasticities have been studied by several authors. Recently, Matsumoto & Sâto (1954) have studied the torsional oscillations of a sphere consisting of the mantle and core, each of which is homogeneous. N. Jobert (1956) has studied the torsional oscillation of spherical harmonic degree 2 type of the Earth, the internal constitution of which was inferred by K. E. Bullen. Making use of the calculus of variations, she has got the period of 43·54 min for the Earth thus assumed. All of these authors are concerned with the oscillations of rather lower modes. As was pointed out by J. H. Jeans as early as in 1923, by making the wave number larger and larger in this kind of problem, we arrive at the corresponding surface wave problem. Thus the study of torsional oscillation of the Earth may throw some light on the nature of the G wave.

2. Variational method

From the mathematical point of view, the problem of torsional oscillations of elastic spheres of variable densities and elasticities is reduced to solving the

* Seismological Laboratory, California Institute of Technology. On leave from Geophysical Institute, Tokyo University.

differential equation

$$\mu\left\{\frac{d^2l}{d\xi^2}-\frac{n(n+1)}{\xi^2}l\right\}+\frac{d}{d\xi}\left(\frac{dl}{d\xi}-\frac{2}{\xi}l\right)+\rho p^2a^2l=0 \tag{2.1}$$

under the boundary conditions

$$\frac{dl}{d\xi}-\frac{2}{\xi}l=0 \text{ at } \xi=1 \tag{2.2}$$

and

$$\mu\left(\frac{dl}{d\xi}-\frac{2}{\xi}l\right) \text{ and } l \text{ are continuous at } \xi=\xi_0, \text{ say.} \tag{2.3}$$

In (2.1), ρ and μ are density and rigidity, each being assumed to be a function of ξ, n the degree of spherical harmonic, p the frequency, e^{ipt} being understood throughout the equations. ξ is the distance r from the centre of the sphere divided by the radius of the sphere a. ξ_0 in (2.3) is ξ corresponding to some surface of discontinuity within the sphere, if one exists. The first and second conditions in (2.3) correspond to the continuities of displacement and stress, respectively, whereas (2.2) shows the vanishing of stress at the free surface $r=a$. (2.1)–(2.3) will be obtained by putting

$$r=a\xi, \qquad \xi^{n+1}L_n=l \tag{2.4}$$

in (102) and (104) in a previous paper (Takeuchi 1950).

We can easily find the variational equation equivalent to (2.1)–(2.3), which, after a little transformation, is reduced to

$$\int_0^1 \rho p^2a^2l\,\delta l\,d\xi - \int_0^1 \mu\left[\left\{-\frac{d^2l}{d\xi^2}+\frac{n(n+1)}{\xi^2}l\right\}\delta l+\frac{d}{d\xi}\left\{\left(\frac{dl}{d\xi}-\frac{2}{\xi}l\right)\delta l\right\}\right]d\xi=0. \tag{2.5}$$

As the trial function in (2.5), we take

$$l=\sum_m A_m\,l(m,\xi) \tag{2.6}$$

where the A_m are some constants to be determined and each $l(m,\xi)$ or simply $l(m)$ is chosen so as to satisfy the conditions (2.2) and (2.3). We understand also that the variation process is applied only to the undetermined constants A_m. In this case, (2.5) are reduced to m equations of the following type

$$\int_0^1 \rho p^2a^2l\,l(m)\,d\xi - \int_0^1 \mu\left[\left\{-\frac{d^2l}{d\xi^2}+\frac{n(n+1)}{\xi^2}l\right\}l(m)+\frac{d}{d\xi}\left\{\left(\frac{dl}{d\xi}-\frac{2}{\xi}l\right)l(m)\right\}\right]d\xi=0 \tag{2.7}$$

for the assumed $l(m)$ of number m in all. In fact, putting (2.6) into (2.7), we get m

simultaneous equations among m unknown A_m. Putting the determinant formed by the coefficients equal to zero will give the value of p required.

In our calculations, we take into account the existence of the fluid core and assume no surface of discontinuity within the mantle. Thus the condition (2.3) becomes

$$\frac{dl}{d\xi} - \frac{2}{\xi} l = 0 \quad \text{at} \quad \xi = \frac{6370 - 2900}{6370} = 0{\cdot}544741. \tag{2.8}$$

As the trial function $l(m)$ which satisfies (2.2) and (2.8), we take

$$l(m) = \xi^m \left(1 - \frac{m-2}{m-1} \cdot \frac{984}{347} \xi + \frac{m-2}{m} \cdot \frac{637}{347} \xi^2 \right) \tag{2.9}$$

where m is some positive integer. Since the boundary conditions are independent of the wave number n, $l(m)$ in (2.9) may be a trial function for any n. This will make our calculation quite short. In our practical calculations, we use only three functions $l(2)$, $l(6)$ and $l(20)$. The reason why we use discrete values of m as above is as follows. As is seen after a little numerical calculation, $l(3)$ and $l(4)$, for example, will give almost the same distribution (mode) as $l(2)$. Thus, if we use $l(2)$, $l(3)$ and $l(4)$ in our calculation, for example, we lose almost all significant figures and get no reliable final result. In the calculation of $l(2)$, $l(6)$ and $l(20)$ also, we must take care not to lose significant figures. This we can do by keeping fractional expressions for numbers as late as possible.

3. Trial results

Using the method described in the last section, we shall at first check the results obtained by Matsumoto and Sâto. The calculation proceeds as follows. We at first calculate the values of $l(2)$, $l(6)$, $l(20)$ and their derivatives at ξ corresponding to the depths of 0, 200, 400, 700, 1 000, 1 400, 1 800, 2 350 and 2 900 km in the Earth. Next, using Simpson's method of numerical integration, we calculate the integrals in (2.7). In the present case, ρ and μ are assumed to be constant, so they go out of the integral. The results of calculations are expressed as follows.

$$\begin{aligned} \widehat{2\,2}\, A_2 + \widehat{6\,2}\, A_6 + \widehat{20\,2}\, A_{20} &= 0 \\ \widehat{2\,6}\, A_2 + \widehat{6\,6}\, A_6 + \widehat{20\,6}\, A_{20} &= 0 \\ \widehat{2\,20}\, A_2 + \widehat{6\,20}\, A_6 + \widehat{20\,20}\, A_{20} &= 0 \end{aligned} \tag{3.1}$$

where the coefficient $\widehat{2\,2}$, for example, is

$$\widehat{2\,2} = 47{\cdot}8392\, P - 159{\cdot}9777 N + 319{\cdot}6554$$

$$N = n(n+1), \qquad P = \frac{pa}{V_{s,0}}, \qquad V_{s,0} = \sqrt{\left(\frac{\mu_0}{\rho_0}\right)} \tag{3.2}$$

μ_0 and ρ_0 being μ and ρ at the surface. $\widehat{2\,2}$, together with other coefficients, is shown in a self-explanatory way in Table 1. The coefficients are symmetrical with respect to the diagonal. So we have, for example, $\widehat{2\,6} = \widehat{6\,2}$. Putting the determinant formed by these coefficients equal to zero, we have the eigen value P for given N. We shall call the results obtained by using $\widehat{2\,2}$; $\widehat{2\,2}$, $\widehat{2\,6}$, $\widehat{6\,6}$; $\widehat{2\,2}$,

$\widehat{2\ 6}$, $\widehat{6\ 6}$, $\widehat{2\ 20}$, $\widehat{6\ 20}$, $\widehat{20\ 20}$ as the first, second and third approximations, respectively. The first, second and third approximations of P for $n = 2$, 3, 4 and ∞ are shown in Table 2. In Table 2, are shown also the exact P obtained by Matsumoto and Sâto. We see that our second approximations give values of P almost

Table 1

	P	N	l
$\widehat{2\ 2}$	47·8392	−159·9777	319·9554
$\widehat{2\ 6}$	−1·013227	1·703042	−3·406082
$\widehat{2\ 20}$	−0·5048223	0·8250114	−1·650023
$\widehat{6\ 6}$	0·0377500	−0·0693672	−2·188851
$\widehat{6\ 20}$	0·019604738	−0·02950595	−1·317838
$\widehat{20\ 20}$	0·011661966	−0·01950237	−1·621529

identical to theirs. Our second approximations give one more P. They are $P = 8{\cdot}758$, 9·372 and 10·32 for $n = 2$, 3 and 4, which agree quite well with the exact values $P = 8{\cdot}18$, 8·9 and 9·9 obtained by Matsumoto and Sâto. By the reason which will be given later, we must have $P = 1{\cdot}0\ n$ as n tends to infinity. Our second and third approximations give $P = 1{\cdot}075\ n$ and $P = 1{\cdot}032\ n$ as n tends to infinity, which are not so good. The reason why we get rather poor result in this case is simply that $l(m)$ with $m = 2$, 6 and 20 are not good approximations to the mode for this case. We are sure to get better approximations by using $l(m)$ with larger m, but we shall not try to do so here. As is well known, approximate values by using the variational calculus here are always larger than the true values. We see in the above this is always the case.

Table 2

$$P = \frac{pa}{V_{s,0}} = \frac{2\pi a}{TV_{s,0}}$$

n	1st	2nd	3rd	Exact
2	2·423	2·413		2·415
3	3·831	3·795		3·79
4	6·933	5·055		4·99
∞	$1{\cdot}212\ n$	$1{\cdot}075\ n$	$1{\cdot}032\ n$	$(1{\cdot}0\ n)$

4. Results for Bullen's Earth model

Having seen the efficiency of our method in this kind of calculation, we shall now calculate P for the model Earth, the internal constitution of which is inferred by K. E. Bullen. The numerical data are taken from Bullard's text book (1954) and are shown in Table 3.

In Table 3, surface values are obtained by extrapolation from those in the deeper part. Thus we do not take into account the existence of the Earth's crust. This may be allowed in this kind of calculation. The calculation proceeds as in the last

Table 3

Properties of Earth model

Depth $= a-r$ km	ρ g/cm	μ 10^{12} dyne/cm
0	3·3	0·6
200	3·47	0·74
400	3·63	0·89
700	4·33	1·52
1 000	4·68	1·89
1 400	4·91	2·15
1 800	5·13	2·39
2 350	5·415	2·73
2 900	5·68	3·03

section except that we have now variable density and elasticity. Corresponding to Tables 1 and 2, we have now Tables 4 and 5.

Table 4

	P	N	l
$\overset{\frown}{2\ 2}$	36·3870	−53·4030	106·8061
$\overset{\frown}{2\ 6}$	−0·874861	0·982992	−1·965984
$\overset{\frown}{2\ 20}$	−0·452904	0·5080651	−1·016130
$\overset{\frown}{6\ 6}$	0·0330281	−0·0382040	−0·755642
$\overset{\frown}{6\ 20}$	0·01792547	−0·01974089	−0·6230995
$\overset{\frown}{20\ 20}$	0·010914097	−0·01177460	−0·974379

Table 5

Convergence of approximations to P

$$P = \frac{pa}{V_{s.0}} = \frac{2\pi a}{TV_{s.0}}$$

n	1st	2nd	3rd
2	3·658	3·601	3·601
4	7·758	7·287	7·285
8	15·30	12·97	12·92
16	30·05	23·34	22·29
32	59·37	44·52	39·50
∞	1·829 n	1·353 n	1·127 n

In the present case, we have no exact value to compare with. However, as the successive approximate values converge quite well, we are sure to get reliable approximations for P, especially for smaller n. In the present case also, we must get $P = 1{\cdot}0\ n$ as n tends to infinity. Our third approximation gives $P = 1{\cdot}127\ n$ as n tends to infinity, which is not so good. The reason why we get poor results

here again is the same as at the end of the last section. This will be understood as follows. Putting the coefficient $\widehat{20\ 20}$ for $n = 32$, for example, equal to zero, we get $P = 39{\cdot}74$, which is very close to the third approximation $P = 39{\cdot}50$ shown in Table 5. This result shows that $l(m)$ with $m = 20$ is a good approximation to the mode for $n = 32$ and we shall have a better result by using this one in the first approximation and some other $l(m)$ with m larger than 20 in the second and third approximations. However, we shall not try to do so here. We know in the next section that even the results for $n = 16$ and 32 in Table 5 are good enough for our present purpose. Putting $a = 6\,370$ km and $V_{s.0} = 4{\cdot}26$ km/s, which is obtained from μ and ρ at the surface, into the third approximations in Table 5, we get the periods T shown in Table 6. We see that the period for $n = 2$ is 43·4 min, which agrees well with 43·54 min obtained by N. Jobert. The asymptotic expression for the Legendre function $P(\theta)$ shows that the wave length λ for large n is equal to $2\pi a$ divided by $n+\frac{1}{2}$. Dividing this wave length by the period in Table 6, we get

Table 6

Wavelength, λ, Phase, C, and Period, T

n	λ km	C km/s	T min
2	16 000	6·140	43·43
4	8 888	6·903	21·48
8	4 706	6·481	12·11
16	2 424	5·761	7·02
32	1 231	5·181	3·96

the corresponding phase velocity C. Although the above procedure is valid only for large n, we show in Table 6 the values of λ and C obtained in this way. The reason why we must have $P = 1{\cdot}0n$ as n tends to infinity is now clear. Since $P/(n+\frac{1}{2})$ is equal to $C/V_{s.0}$ the above requirement is another way of stating the well known fact that the phase velocity of Love waves for very short wave length is equal to the shear wave velocity at the surface of the Earth.

The results in Table 6, together with some of the results which will be obtained in the next section, are shown in Figure 1. From this figure, we see that the phase velocity C has a maximum of about 6·9 km/s for the period T of about 1 300 s or for the wave length λ of about 9 000 km. That C becomes smaller for wave length longer than this critical one shows the existence of some lower (shear wave) velocity layer in the deeper depth. In the present case, this lower velocity layer is nothing but the Earth core. The core boundary is at 2 900 km depth. The scale ratio, wave length/depth, is about 3, a plausible one. In the following way, we get the scale ratio of this order of magnitude for other wave lengths. The phase velocity C for $n = 8$ (or $\lambda = 4\,706$ km) is 6·481 km/s. The depth at which the shear wave velocity takes this value is at about 1 200 km within the Earth. The scale ratio in this case is about 4. Similarly, for $n = 16$ and 32, we have the scale ratios of about 4 and 3. This kind of scale ratio consideration is sometimes very useful, especially when we want to get a rough idea of the dispersion curve for complicated structures.

In this connection, it will be interesting to see the displacement distribution with the depth, or vibration mode for each n. This we can do by solving (3.1)

and putting the results thus obtained into (2.6) and finally into

$$u_r = 0, \qquad u_\theta = -l\frac{\partial S_n^m(\theta,\phi)}{\xi \sin\theta\, \partial\phi}, \qquad u_\phi = l\frac{\partial S_n^m(\theta,\phi)}{\xi\, \partial\theta}, \tag{4.1}$$

$$S_n^m(\theta,\phi) = P_n^m(\theta)\begin{matrix}\cos m\phi \\ \sin m\phi\end{matrix}$$

u_r, u_θ and u_ϕ in (4.1) show (r, θ, ϕ) components of displacement in spherical coordinates. Since we are treating here the free oscillation problem, we cannot

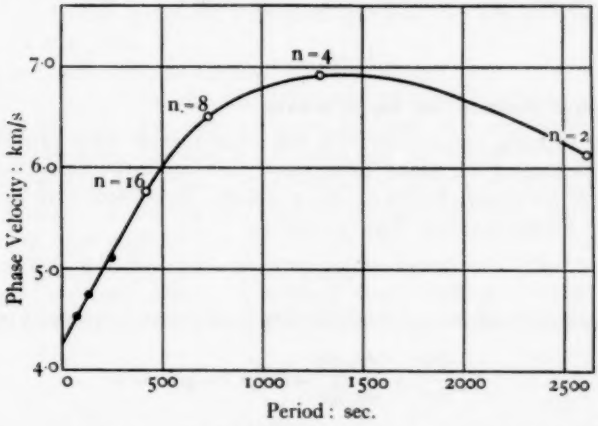

FIG. 1.—Theoretical phase velocity curve of the mantle Love wave.

expect to get an absolute value for the displacement. Thus we show in Figure 2 the distribution of l/ξ against depth, taking its value at the surface as unity. We see from this figure that the shorter the wave length, the shallower the depth to

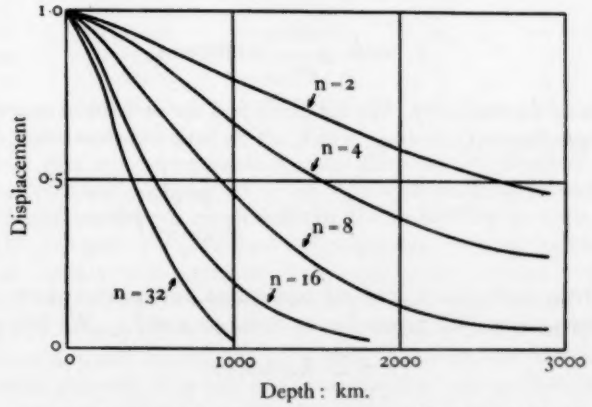

FIG. 2.—Displacement distributions within the Earth. n is the degree of the corresponding spherical harmonic.

which the corresponding displacement penetrates. This, of course, must be the case. For very short wave lengths, we have surface waves in the usual meaning.

For $n = 8$, 16 and 32 in Figure 2, the displacements almost vanish within the mantle. Thus for these waves or oscillations, the existence of the core of the Earth has almost no influence. For $n = 4$, the displacement at the core boundary is about $\frac{1}{4}$ of that at the surface, which is not negligible. Thus in this type of oscillation we can expect some effect of the existence of the Earth's core. This is exactly what we had in the above.

To find values of C not calculated above, Figure 1 may be used. We can find C for $n = 6$, for example, as follows. First, we have the wave length $\lambda = 6\,154$ km. We try next to find C and T which are on the smooth curve in Figure 1 and the product of which is equal to 6 154 km. Thus we get $T = 900$, $C = 6{\cdot}75$ approximately.

5. Variational method for Love waves

In order to make connection with the usual surface wave problem, we shall study in this section the plane Love wave problem in vertically heterogeneous media. There are many studies on this problem. References may be made to the text book by Ewing & others (1957). Putting

$$v \propto e^{ik(Ct-x)} \tag{5.1}$$

in their equation (7.69), we get the following fundamental equations to be studied.

$$\mu\frac{d^2v}{dz^2} + \frac{d\mu}{dz}\frac{dv}{dz} + k^2(\rho C^2 - \mu)v = 0. \tag{5.2}$$

The boundary conditions are the vanishing of stress at the free surface $z = 0$ and continuities of displacement and stress at some surface of discontinuity if it exists. These conditions are satisfied by putting

$$\frac{dv}{dz} = 0 \quad \text{at} \quad z = 0 \tag{5.3}$$

and

$$v \quad \text{and} \quad \mu\frac{dv}{dz} \quad \text{continuous} \tag{5.4}$$

at the surface of discontinuity. We can easily find the variational equation (Jeffreys 1934) corresponding to (5.1)–(5.4), which, after a little transformation, is reduced to

$$\int_0^{+\infty} \rho C^2 v\,\delta v\,dz - \int_0^{+\infty} \mu\left(v\delta v + \frac{1}{k^2}\frac{dv}{dz}\frac{d\delta v}{dz}\right)dz = 0. \tag{5.5}$$

We consider the half-space in the $+z$ region and assume that there is no surface of discontinuity there. We proceed as in Sections 2 and 3. We first put

$$v = \sum_m A_m\, v(m, kz) \tag{5.6}$$

where A_m are some undetermined constants, and as $v(m, z)$, each satisfying (5.3), we shall take

$$v(m, kz) = e^{-mkz} - 0{\cdot}5\,e^{-2mkz}. \tag{5.7}$$

Variations in A_m will give equations similar to (3.1). The coefficient of $A_{m'}$

in the mth equation may be put in the form

$$\int_0^\infty \left[\rho C^2 v(m', kz)v(m, kz) - \mu\left\{v(m', kz)v(m, kz) + \frac{dv(m', kz)}{d(kz)}\frac{dv(m, kz)}{d(kz)}\right\}\right] d(kz). \quad (5.8)$$

The reason why we take kz as the independent variable rather than z is that we can then carry out almost all calculations independently of the wave number k. The consideration of k comes only at the last step when we form the products including ρ and μ. The distributions of ρ and μ in the kz space are different for different k. In our practical numerical calculus, we use $m = 0{\cdot}5$, $1{\cdot}0$ and sometimes $m = 0{\cdot}25$, $2{\cdot}0$.

In order to check the efficiency of our method, we first apply it to the case studied by Wilson (1940, see also the text book by Ewing & others, p. 214). That is the typical Love wave problem, a superficial layer on a semi-infinite medium. The rigidity in the lower medium is $1{\cdot}8$ times that in the upper layer. The shear wave velocities in the upper and lower layers are $3{\cdot}6$ and $4{\cdot}6$ km/s, respectively. As there is a surface of discontinuity in the region considered, our method described above seems not to be applicable to the present case. But by replacing the discontinuity surface by a thin continuous layer in which rigidity and shear wave velocity change rapidly, we may apply our method here. Taking $v(0{\cdot}5, kz)$ as a trial function, and carrying out the integration, we get the results in Table 7.

Table 7

$\frac{2\pi}{kH}$	$\int_{kH}^{\infty} v^2 d(kz)$	$\int_{kH}^{\infty} \left(\frac{dv}{d(kz)}\right)^2 d(kz)$	Our C	Exact C
			km/s	km/s
0·00	0·0	0·0	3·76	3·60
1·72	0·023215956	0·0051717190	3·83	3·80
2·84	0·086799923	0·016788801	4·02	4·00
4·27	0·16283787	0·027316495	4·22	4·20
6·86	0·25141526	0·035677655	4·42	4·40
10·02	0·30955991	0·039073316	4·54	4·50
16·24	0·36368226	0·040879418	4·64	4·56
∞	0·45833333	0·041666667	4·81	4·60

Table 7 shows that our approximate method gives almost identical results with Wilson's except for $kH \to 0$ and $kH \to \infty$, thus justifying the replacement of the surface of discontinuity by a continuous layer. In order to remedy rather poor results for $kH \to 0$ and $\to \infty$, we have only to replace our trial function $v(0{\cdot}5, kz)$ by $v(0{\cdot}25, kz)$. In fact by using $v(0{\cdot}25, kz)$, we get for $kH \to 0$ and $\to \infty$, $C = 3{\cdot}64$ and $4{\cdot}65$ km/s, respectively, which agree well with the exact results $C = 3{\cdot}60$ and $4{\cdot}60$ km/s. Thus we may expect very good agreement in the second approximation by using $v(0{\cdot}5, kz)$ and $v(0{\cdot}25, kz)$. We shall, however, not try to do so here. For our present purpose, it is sufficient to know that our method works well.

6. Results for mantle waves

Having thus checked the efficiency of our method, we shall now apply the method to the plane boundary problem corresponding to the case discussed in

Section 4. The density and rigidity distributions are shown in Table 3. We restrict our study to the case when there is no need to know the distributions within the core. The computation proceeds as follows. We first calculate the values of $v(0{\cdot}5, kz)$, $v(1{\cdot}0, kz)$, $v(2{\cdot}0, kz)$ and their derivatives (with respect to kz) for several values of kz, and then form the products like $v(0{\cdot}5, kz)\, v(1{\cdot}0, kz)$ and

$$\frac{dv}{dkz}(0{\cdot}5, kz)\frac{dv}{dkz}(1{\cdot}0, kz).$$

Substituting values of k will give the corresponding distributions of ρ and μ for each kz. Forming products like $\rho v(0{\cdot}5, kz)\, v(1{\cdot}0, kz)$, we carry out the numerical integration. The coefficients, which have meanings similar to those in Table 4, for $1/k = 200$, 100 and 50 km are shown in Table 8. The wave lengths for these waves are 1 257, 628 and 314 km respectively.

Table 8

	$(C/V_{s.0})^2$	1	$(C/V_{s.0})^2$	1	$(C/V_{s.0})^2$	1
$\overset{\frown}{0{\cdot}5\ 0{\cdot}5}$	1·495349	−2·164886	1·425821	−1·764019	1·400108	−1·625459
$\overset{\frown}{0{\cdot}5\ 1{\cdot}0}$	0·9490493	−1·327204	0·9246861	−1·175540	0·9143637	−1·114840
$\overset{\frown}{1{\cdot}0\ 1{\cdot}0}$	0·7157905	−1·126688	0·7031800	−1·031734	0·6972855	−0·9883948
$1/k$	200 km		100		50	

In the similar way as in Sections 3 and 4, we have the first and second approximations of $C/V_{s.0}$ for each k as shown in Table 9. Since they show fairly good convergence, multiplying the second approximation by $V_{s.0} = 4{\cdot}26$ km/s, we may get the value of C for each k as shown also in Table 9. These results are shown

Table 9

$1/k$	$C/V_{s.0}$ 1st	$C/V_{s.0}$ 2nd	C	λ	T
200 km	1·203	1·199	5·11 km/s	1 257 km	246 s
100	1·112	1·110	4·73	628	133
50	1·077	1·069	4·55	314	69

in Figure 1 by black circles. The smooth curve in this part of Figure 1 is drawn by connecting the point corresponding to $n = 16$ and the point ($T = 0$, $C = V_{s.0} = 4{\cdot}26$ km/s). The merging of the results obtained in this Section and in Section 4 into each other will assure us of the validity of our methods of study.

Figure 1 shows that the phase velocity C is almost linear against the period T for T less than 400 s. This result agrees well with the study of G waves by Sâto (1958). In this connection, it will be interesting to work out the corresponding group velocity U. Assuming that C is linear against T between $T = 0$ and 400 s, we get

$$\frac{dC}{dT} = \frac{5{\cdot}70 - 4{\cdot}26}{400 - 0} = 0{\cdot}0036\ \text{km/s}^2. \tag{6.1}$$

The formula

$$U = \frac{C}{1+(T/C)(dC/dT)}, \tag{6.2}$$

then gives $U = 4{\cdot}29$, $4{\cdot}35$, $4{\cdot}44$ and $4{\cdot}55$ km/s for $T = 100$, 200, 300 and 400 s. These are about the values of group velocities usually observed in this period interval. We must take care, however, not to attach much importance to these figures. The calculation has not taken into account the existence of the Earth's crust. Furthermore, $V_{s.0} = 4{\cdot}26$ km/s in the Jeffreys and Bullen model is a little far from the truth. Recent studies in explosion seismology indicate that $V_{s.0}$ is about $4{\cdot}7$ km/s. In the present paper, we are concerned with rather large-scale characteristics of the Earth, so it is sufficient for our present purpose to get figures roughly in accord with the observational data. The approximate method in this and the last Section, however, is one of the most effective in discussing minor structures in the upper mantle and the crust. So after getting enough data, we hope to study this interesting problem in the near future. Taking care not to apply rashly the usual wave concepts to the vibrations of the longer periods, we calculate the values of U for $T = 600$, 800, 1 000 and 1 200 s. Use is made of Figure 1 and (6.2). The results are $U = 5{\cdot}15$, $5{\cdot}71$, $6{\cdot}16$ and $6{\cdot}54$ km/s for the above periods, respectively. No flattening of the dispersion curve is seen here as is found in the mantle Rayleigh waves (Ewing & Press 1954, Benioff & Press 1958). The flattening of the dispersion curve of mantle Rayleigh waves around the period of 500 s is considered to be due to the existence of the core. By the present study, this inference is a little doubtful. The wave of period 500 s is of too small scale to be influenced by the existence of the Earth's core. As is said in Section 4, it is only at $n = 4$ or $T = 1\,300$ s that the wave or vibration is influenced by the existence of the core. It may be said against this argument that the situation is different in the case of the mantle Rayleigh waves from the mantle Love waves studied here. In order to make this point clear, it will be best to study the statical deformation of the Earth as a whole by normal traction at the surface. This is a deformation of the dilatational type, and as the statical deformation penetrates deeper than the corresponding dynamical deformation, the study will be one of the crucial tests for the above problem. This kind of study will be made in a forthcoming paper.

7. Conclusions and acknowledgments

Periods of oscillations and corresponding phase velocities have been calculated for the torsional oscillations of the Earth, the internal constitution of which was inferred by K. E. Bullen. The fundamental period calculated is $43{\cdot}4$ min agreeing closely with that obtained by N. Jobert. By making the wave number larger, we get the phase velocity curve for the G wave. The calculated results agree roughly with the observations. The variational calculus method used in the present study is very effective and makes the problems considered here matters of computational interest. Modern digital computers will be of help in making the computations. In connection with the present study, several problems suggest themselves. Among them are the problem of statical deformations of the Earth as a whole by normal traction at the surface, the study of structures in the crust and in the upper mantle and the application of the variational calculus method to the study of dilatational oscillations of the Earth and the corresponding mantle Rayleigh waves.

This study was carried out at the Seismological Laboratory of the California Institute of Technology. The author wishes to thank Dr Frank Press for giving him the opportunity to visit there and for making valuable suggestions throughout the study. The author also wishes to thank the Alfred P. Sloan Foundation for financial support.

Seismological Laboratory
California Institute of Technology
Pasadena, California,

(*Division of the Geological Sciences, Contribution No.* 906).

1958 *November* 17.

References

Benioff, H. & Press, F., 1958. *Geophys. J.* **1**, 208.
Bullard, E. C., 1954. *The earth as a planet* (edited by G. P. Kuiper). University of Chicago Press.
Bullen, K. E., 1953. *An introduction to the theory of seismology*. Cambridge University Press.
Ewing, M., Jardetzky, W. S. & Press, F., 1957. *Elastic waves in layered media*. McGraw-Hill.
Ewing, M. & Press, F., 1954. *Bull. Seismol. Soc. Amer.*, **44**, 127.
Jeans, J. H., 1923. *Proc. Roy. Soc. A.* **102**, 554.
Jeffreys, H., 1934. *Mon. Not. Roy. Astr. Soc. Geophys. Suppl.* **3**, 253.
Jobert, N., 1956. *C.R. Acad. Sci., Paris.* **243**, 1230.
Matsumoto, T. & Sâto, Y., 1954. *Bull. Earthq. Res. Inst.*, **32**, 248.
Sâto, Y., 1958. *Bull. Seismol. Soc. Amer.*, **48**, 231.
Takeuchi, H., 1950. *Trans. Amer. Geophys. Un.* **31**, 651.
Wilson, J. T. 1940. *Ball. Seismol. Soc. Amer.*, **30**, 273-301.

The Distortion of Pulse-like Earthquake Signals by Seismographs

M. Landisman, Y. Satô, and M. Ewing

(Received 1958 December 8)

Summary

A numerical method for calculating the seismogram of any seismograph for an arbitrary continuous ground disturbance is used to investigate the effect of instruments with various physical constants on both theoretical and actual impulsive signals. This calculation solves the equations of motion of the pendulum–galvanometer system by a fourth-order Runge–Kutta process. Variation of instrumental constants produces conspicuously different seismograms, in several cases of practical interest.

In order to resolve the apparent discrepancy between the observations of Satô, and those of Benioff and Press for the group velocity of long period Love waves, certain computed seismograms of the long period Love wave arrival, G_1, from the New Guinea shock of 1938 February 1, were compared with the linear strain recording of this signal. The results of this study confirm the observations of Satô, that the group velocity of Love waves is essentially flat in the long period range to several hundred seconds. The distortion introduced by instruments whose magnification changes rapidly with period is great enough to mask any small dispersion that might be associated with these pulse-like signals.

1. Introduction

In order to determine precisely the effects of seismographs with various physical constants on the pulse-like signals from earthquakes, a systematic investigation has been made of the modification of certain theoretical pulses, as well as signals from earthquakes, using an IBM 650 electronic data processing machine. Modifications of seismic ground motion, which are produced by the recording instrument, have been discussed previously in many studies of near earthquakes, and of teleseisms, for both body and surface waves.* However, the method presented here is more powerful, and does not require the use of the arbitrary integration constants which are needed to reduce a seismic trace to ground motion.

Although instrumental distortion affects the entire seismic signal, a quantitative measure of this effect is especially important at present in the case of surface

* See Akima & Nagamune (1956), Birkenhauer (1945), Bryan (1936), Byerley (1942), Coulomb (1952), Dyk (1935), Ewing & Press (1952), McComb & Ruge (1937), McComb & Wenner (1936), Neumann & others (1943), Ruge (1936), Satô (1958), Sharpe (1935), Tsuboi (1931), Walter (1945), Wilson (1932), Wilson (1940).

waves, because for these waves signal character as well as arrival time is used to study the physical properties of the Earth. In one study of well-dispersed Rayleigh wave trains, it was shown (Ewing & Press 1952), after comparing data from seismograms with different physical constants, that it is neither necessary to integrate the seismograms to true ground motion nor to eliminate instrumental phase shifts for the periods studied and the precision required.

There are, however, surface wave signals with small dispersion. A particularly striking example of a pulse-like teleseismic signal is the long-period Love wave, named the *G* wave by Byerly (1926) after Gutenberg, for his pioneer work on this phase (Sieberg & Gutenberg 1924). His studies, as well as most other investigations of this wave* indicated that it shows little dispersion, since its pulse-like character is preserved at great distances. These studies demonstrated that the Love wave group velocity curve is essentially flat in the long period range to several hundred seconds, with a group velocity near 4·48 km/s. For a summary of dispersion data on Love waves of shorter periods, see Ewing, Jardetzky & Press (1957).

In a recent study, Benioff and Press (1958) suggested, on the basis of seismograms from a new instrument, that the previous studies of the *G* wave had resulted in poor group velocity determinations, and that the Love wave group velocity curve has a true maximum, with a decrease in velocity for periods greater than about two minutes. The more pronounced dispersion of mantle Rayleigh waves which show a maximum for periods near one minute and a decrease in velocity to a minimum for periods near four minutes, has permitted determination of the group velocity and associated maximum and minimum to be made from the seismograms of many instruments (Ewing & others 1957, Ewing & Press 1954(a), (b)). In addition, the group velocities obtained from studies of the direct wave agreed with determinations based on multiple passages of these waves around the earth, although the wave train had been strongly altered by its conspicuous dispersion. The agreement of these determinations shows that effect of the instruments on mantle Rayleigh waves is small compared to that of the dispersion.

The essentially constant *G* wave group velocities were determined by Satô (1958), exclusively by the measurement of differences in phase which were obtained by Fourier analysis of the arrivals $G3$, $G1$, and $G4$, $G2$. In this manner, the effects of the instrument and of the spectrum of the source are completely removed.

The group velocities of long-period surface-wave signals provide a means of studying the mantle which is independent of body wave studies, and it is therefore quite important to get reliable surface wave group velocity data, as the derived mantle structures are sensitive to changes in the observed dispersion curves.

After an investigation of the effect of seismographs on theoretical signals, calculations were made of the seismograms which would be produced by various instruments upon reception of the $G1$ signal from the New Guinea earthquake of 1938 February 1, which had been used by Satô for his group velocity determination.

Our calculations have shown that the instruments significantly influence the shape of pulse-like signals (see Figures 1 and 3) in cases of practical interest. Such changes in wave shape will cause measurable changes in the observed group velocity for signals with slight dispersion unless instrumental effects are removed. The modification of the $G1$ signal by the four pendulum–galvanometer systems described in Figure 4, which is similar to the distortion of the test signals in Figure 3, indicates that the effect of the recording system on these pulse-like signals is

* See Coulomb (1952), Di Filippo (1950), Ewing & Press (1956), Imamura (1937), Satô (1958), Sieberg & Gutenberg (1924), Wilson (1940).

quite important. Since this is the same G wave signal which, after elimination of the effects of the recording system and of the spectrum of the source, did not produce a maximum in the group velocity (Satô 1958), the earlier determinations of an essentially flat Love wave group velocity curve for long periods up to several hundred seconds are confirmed. This Love wave group velocity curve is useful for testing structures proposed for the upper mantle. An extensive programme of study of the upper mantle, using surface waves and body waves is nearing completion at the Lamont Geological Observatory, and the results will soon be published (Landisman, Satô & Ewing).

The present investigation of seismograph distortion of pulse-like ground motions indicates that, for best results, dispersion curves for pulse-like signals should be constructed from the seismograms of instruments whose magnification changes very gradually with period. In addition, this study emphasizes the fact that the transient response of instruments whose magnification changes rapidly with period can be important in studies of wave propagation.

2. Method

The transient response of various types of seismographs to pulse-like signals will be considered. The equations of motion of these systems, with suitable initial conditions, provide a complete description of their behaviour.

One type of system is the linear strain as recorded by a galvanometer by means of a velocity pickup. The response, R, of a directly recorded strain rod, for harmonic components much longer than the rod, has been shown by Benioff (1935, 1955) to be

$$R_T = \frac{L}{c} \sin\alpha \cos\alpha \frac{\partial z}{\partial t} \tag{1}$$

for transverse waves, and

$$R_L = -\frac{L}{c} \cos^2\alpha \frac{\partial z}{\partial t} \tag{2}$$

for longitudinal waves,

where R = displacement of the free end of the horizontal strain rod relative to the earth beneath the free end,
z = horizontal particle displacement,
L = length of strain rod,
c = horizontal phase velocity,
α = angle between strain rod and the azimuthal direction of approach of the waves.

Figure 1 in the study of Benioff & Press (1958) shows that in practical cases, changes of phase velocity of the order of 1 km/s produce negligible changes of magnification. When phase velocity is treated as a constant and the time derivative of R, as obtained from a velocity pickup, is recorded on a galvanometer, the magnification is similar to that of a simple pendulum with the same period and damping as the galvanometer. The pendulum obeys the well-known equation

$$\ddot{x} + 2\epsilon_0\dot{x} + \omega_0^2 x = -\ddot{z}, \tag{3}$$

where x = pendulum displacement with respect to the ground,
z = absolute ground displacement,

waves, because for these waves signal character as well as arrival time is used to study the physical properties of the Earth. In one study of well-dispersed Rayleigh wave trains, it was shown (Ewing & Press 1952), after comparing data from seismograms with different physical constants, that it is neither necessary to integrate the seismograms to true ground motion nor to eliminate instrumental phase shifts for the periods studied and the precision required.

There are, however, surface wave signals with small dispersion. A particularly striking example of a pulse-like teleseismic signal is the long-period Love wave, named the *G* wave by Byerly (1926) after Gutenberg, for his pioneer work on this phase (Sieberg & Gutenberg 1924). His studies, as well as most other investigations of this wave* indicated that it shows little dispersion, since its pulse-like character is preserved at great distances. These studies demonstrated that the Love wave group velocity curve is essentially flat in the long period range to several hundred seconds, with a group velocity near 4·48 km/s. For a summary of dispersion data on Love waves of shorter periods, see Ewing, Jardetzky & Press (1957).

In a recent study, Benioff and Press (1958) suggested, on the basis of seismograms from a new instrument, that the previous studies of the *G* wave had resulted in poor group velocity determinations, and that the Love wave group velocity curve has a true maximum, with a decrease in velocity for periods greater than about two minutes. The more pronounced dispersion of mantle Rayleigh waves which show a maximum for periods near one minute and a decrease in velocity to a minimum for periods near four minutes, has permitted determination of the group velocity and associated maximum and minimum to be made from the seismograms of many instruments (Ewing & others 1957, Ewing & Press 1954(a), (b)). In addition, the group velocities obtained from studies of the direct wave agreed with determinations based on multiple passages of these waves around the earth, although the wave train had been strongly altered by its conspicuous dispersion. The agreement of these determinations shows that effect of the instruments on mantle Rayleigh waves is small compared to that of the dispersion.

The essentially constant *G* wave group velocities were determined by Satô (1958), exclusively by the measurement of differences in phase which were obtained by Fourier analysis of the arrivals G_3, G_1, and G_4, G_2. In this manner, the effects of the instrument and of the spectrum of the source are completely removed.

The group velocities of long-period surface-wave signals provide a means of studying the mantle which is independent of body wave studies, and it is therefore quite important to get reliable surface wave group velocity data, as the derived mantle structures are sensitive to changes in the observed dispersion curves.

After an investigation of the effect of seismographs on theoretical signals, calculations were made of the seismograms which would be produced by various instruments upon reception of the G_1 signal from the New Guinea earthquake of 1938 February 1, which had been used by Satô for his group velocity determination.

Our calculations have shown that the instruments significantly influence the shape of pulse-like signals (see Figures 1 and 3) in cases of practical interest. Such changes in wave shape will cause measurable changes in the observed group velocity for signals with slight dispersion unless instrumental effects are removed. The modification of the G_1 signal by the four pendulum–galvanometer systems described in Figure 4, which is similar to the distortion of the test signals in Figure 3, indicates that the effect of the recording system on these pulse-like signals is

* See Coulomb (1952), Di Filippo (1950), Ewing & Press (1956), Imamura (1937), Satô (1958), Sieberg & Gutenberg (1924), Wilson (1940).

quite important. Since this is the same G wave signal which, after elimination of the effects of the recording system and of the spectrum of the source, did not produce a maximum in the group velocity (Satô 1958), the earlier determinations of an essentially flat Love wave group velocity curve for long periods up to several hundred seconds are confirmed. This Love wave group velocity curve is useful for testing structures proposed for the upper mantle. An extensive programme of study of the upper mantle, using surface waves and body waves is nearing completion at the Lamont Geological Observatory, and the results will soon be published (Landisman, Satô & Ewing).

The present investigation of seismograph distortion of pulse-like ground motions indicates that, for best results, dispersion curves for pulse-like signals should be constructed from the seismograms of instruments whose magnification changes very gradually with period. In addition, this study emphasizes the fact that the transient response of instruments whose magnification changes rapidly with period can be important in studies of wave propagation.

2. Method

The transient response of various types of seismographs to pulse-like signals will be considered. The equations of motion of these systems, with suitable initial conditions, provide a complete description of their behaviour.

One type of system is the linear strain as recorded by a galvanometer by means of a velocity pickup. The response, R, of a directly recorded strain rod, for harmonic components much longer than the rod, has been shown by Benioff (1935, 1955) to be

$$R_T = \frac{L}{c} \sin\alpha \cos\alpha \frac{\partial z}{\partial t} \tag{1}$$

for transverse waves, and

$$R_L = -\frac{L}{c} \cos^2\alpha \frac{\partial z}{\partial t} \tag{2}$$

for longitudinal waves,

where R = displacement of the free end of the horizontal strain rod relative to the earth beneath the free end,
z = horizontal particle displacement,
L = length of strain rod,
c = horizontal phase velocity,
α = angle between strain rod and the azimuthal direction of approach of the waves.

Figure 1 in the study of Benioff & Press (1958) shows that in practical cases, changes of phase velocity of the order of 1 km/s produce negligible changes of magnification. When phase velocity is treated as a constant and the time derivative of R, as obtained from a velocity pickup, is recorded on a galvanometer, the magnification is similar to that of a simple pendulum with the same period and damping as the galvanometer. The pendulum obeys the well-known equation

$$\ddot{x} + 2\epsilon_0\dot{x} + \omega_0^2 x = -\ddot{z}, \tag{3}$$

where x = pendulum displacement with respect to the ground,
z = absolute ground displacement,

ϵ_0 = damping constant of the pendulum,
ω_0 = natural frequency of the pendulum.

We may obtain the ground acceleration from a simple pendulum record (Bryan 1936) by solving the equation

$$\ddot{z} = \kappa_1\ddot{x} + \kappa_2\dot{x} + \kappa_3 x, \tag{4}$$

where

$$\kappa_1 = -1, \qquad \kappa_2 = -2\epsilon_0, \quad \text{and} \quad \kappa_3 = -\omega_0^2.$$

The derivatives may be found numerically, using differences (Hildebrand 1956, Scarborough 1950).

For a pendulum–galvanometer system, such as the Galitzin seismograph or similar instruments, where a mechanical pendulum drives a galvanometer through a velocity pickup, we may write the equations of motion (Coulomb & Grenet 1935) in notation similar to that of Chakrabarty (1949):

$$\ddot{x} + 2\epsilon_0\dot{x} + \omega_0^2 x - \sigma_0\dot{\theta} = -\ddot{z} = +w, \tag{5}$$

$$\ddot{\theta} + 2\epsilon_g\dot{\theta} + w_g^2\theta - \sigma_g\dot{x} = 0, \tag{6}$$

where

θ = galvanometer deflection,
w = negative ground acceleration,
ϵ_0 = pendulum damping constant,
ϵ_g = galvanometer damping constant,
ω_0 = pendulum natural frequency,
ω_g = galvanometer natural frequency,
σ_0 = coupling of galvanometer to pendulum,
σ_g = coupling of pendulum to galvanometer.

It can easily be shown (Byerly 1942, Walter 1945) that the ground acceleration, $\ddot{z} = -w$, can be found if θ, its first three derivatives, and first integral with respect to time are known.

$$\ddot{z} = -w = \kappa_0\dddot{\theta} + \kappa_1\ddot{\theta} + \kappa_2\dot{\theta} + \kappa_3\theta + \kappa_4\int_0^t \theta\, dt, \tag{7}$$

where t = time on record,

$$\begin{aligned}
\kappa_0 &= -\sigma_g^{-1}, \\
\kappa_1 &= -2(\epsilon_0 + \epsilon_g)/\sigma_g, \\
\kappa_2 &= -(\omega_0^2 + 4\epsilon_0\epsilon_g + \omega_g^2 - \sigma_0\sigma_g)/\sigma_g, \\
\kappa_3 &= -2(\epsilon_0\omega_g^2 + \epsilon_g\omega_0^2)/\sigma_g, \\
\kappa_4 &= -\omega_0^2\omega_g^2/\sigma_g.
\end{aligned} \tag{8}$$

To obtain ground displacement we must solve

$$\dot{z} = \int_0^t \ddot{z}\, dt, \qquad z = \int_0^t \dot{z}\, dt. \tag{9}$$

When a linear strain record is to be compared with that produced by a pendulum–galvanometer system, it is best to use equation (4) to deduce earth accelerations and equations (5) and (6) to compute the comparison seismogram. The equation (7) is only presented to show the method of intercomparison between various pendulum-galvanometer combinations. The computation of equation (4) will be referred to in future discussion as the inverse seismograph computation.

To obtain a seismogram from the ground displacement or acceleration, one must solve the equations of motion (5) and (6). Many authors have contributed valuable studies concerning the effect of instrumental constants on the response of the instrument*, but it is often difficult to imagine what type of seismogram will correspond to a certain response curve and a given ground disturbance.

We have adopted one of the Runge–Kutta methods, which has been derived by Gill (1951), to solve these differential equations numerically. We consider a system of $n+1$ simultaneous first-order differential equations

$$\frac{dy_i}{dy_0} = f_i(y_0, y_1, ..., y_n), \quad i = 0, 1, ... n, \tag{10}$$

where $f_0 \equiv 1$, and $y_0 = t$.

For such a set of equations, Gill has derived a numerical method of solution which is a fourth-order Runge–Kutta process, and in which, for each step of iteration over interval h, the error is of order h^5. The process has the advantage that it may be started at any place in the iteration, and that the functions f_i must be evaluated only at the ends of the interval and twice in the middle of the interval, which is convenient for interpolation or differentiation.

The following set of equations, (11), which may be found in Gill's study (his equation 26) are his solution for maximum accuracy. The equations are computed in the order shown, i.e.

$$\begin{aligned}
&k_{i0}, \quad \text{then} \quad r_{i1} \quad \text{for} \quad i = 1, ... n,\\
&y_{i1}, \quad \text{then} \quad q_{i1} \quad \text{for} \quad i = 1, ... n,\\
&\qquad \vdots \qquad\qquad \vdots \qquad\quad \vdots\\
&y_{i4}, \quad \text{then} \quad q_{i4} \quad \text{for} \quad i = 1, ... n.
\end{aligned}$$

The first of the two subscripts refers to the identification number of each member of the set of first-order differential equations, while the second refers to each of the four stages of the iteration process, which together constitute one complete step of interval h. When each of the sixteen equations, (11), have been computed for each member of the set of first-order differential equations, in the order mentioned above, the iteration has proceeded through one step of interval h. The q_{ij} and r_{ij} have been introduced to keep the errors, $e(r_{ij})$, at each stage of the iteration process to a minimum. To preserve the accuracy from one step, h, to the next, it is necessary to make the q_{i4} of one interval equal to the q_{i0} of the next, and to round q_{i0} and q_{i4} in opposite directions. At the start of the first interval of iteration q_{i0} may be set equal to zero. With this introduction we may now consider the set of equations (11).

* See Chakrabarty (1949), Coulomb & Grenet (1935), Eaton (1957), Hagiwara (1958), Matsumoto (1958), Sutton & Oliver (in press).

$$
\left.\begin{aligned}
k_{i0} &= hf_i(y_{00}, y_{10}, \ldots), & r_{i1} &= \tfrac{1}{2}k_{i0} - q_{i0} + e(r_{i1}),\\
y_{i1} &= y_{i0} + r_{i1}, & q_{i1} &= q_{i0} + 3r_{i1} - \tfrac{1}{2}k_{i0},\\
k_{i1} &= hf_i(y_{01}, y_{11}, \ldots), & r_{i2} &= [1 - \sqrt{(\tfrac{1}{2})}](k_{i1} - q_{i1}) + e(r_{i2}),\\
y_{i2} &= y_{i1} + r_{i2}, & q_{i2} &= q_{i1} + 3r_{i2} - [1 - \sqrt{(\tfrac{1}{2})}]k_{i1},\\
k_{i2} &= hf_i(y_{02}, y_{12}, \ldots), & r_{i3} &= [1 + \sqrt{(\tfrac{1}{2})}](k_{i2} - q_{i2}) + e(r_{i3}),\\
y_{i3} &= y_{i2} + r_{i3}, & q_{i3} &= q_{i2} + 3r_{i3} - [1 + \sqrt{(\tfrac{1}{2})}]k_{i2},\\
k_{i3} &= hf_i(y_{03}, y_{13}, \ldots), & r_{i4} &= \tfrac{1}{6}(k_{i3} - 2q_{i3}) + e(r_{i4}),\\
y_{i4} &= y_{i3} + r_{i4}, & q_{i4} &= q_{i3} + 3r_{i4} - \tfrac{1}{2}k_{i3}.
\end{aligned}\right\} \quad (11)
$$

A complete discussion of the method may be found in the original study by Gill (1951).

Equations (5) and (6) were adapted to this method as follows:

Let

$$t = y_0, \qquad x = y_1, \qquad \dot{x} = y_2, \qquad \theta = y_3, \qquad \dot{\theta} = y_4.$$

Then, $\dot{y}_1 = y_2$,

or

$$\frac{dy_1}{dy_0} = f_1(y_0, y_1, y_2, y_3, y_4, w),$$

or

$$\boxed{f_1 = y_2}. \qquad (5A)$$

Also,

$$\dot{y}_2 = [-2\epsilon_0 y_2 - \omega_0^2 y_1 + \sigma_0 y_4 + w],$$

or

$$\frac{dy_2}{dy_0} = f_2(y_0, y_1, y_2, y_3, y_4, w),$$

or

$$\boxed{f_2 = -2\epsilon_0 y_2 - \omega_0^2 y_1 + \sigma_0 y_4 + w}. \qquad (5B)$$

Similarly, $\dot{y}_3 = y_4$, or

$$\frac{dy_3}{dy_0} = f_3(y_0, y_1, y_2, y_3, y_4, w),$$

or

$$\boxed{f_3 = y_4}. \qquad (6A)$$

Finally,

$$\dot{y}_4 = [-2\epsilon_g y_4 - \omega_g^2 y_3 + \sigma_g y_2],$$

or

$$\frac{dy_4}{dy_0} = f_4(y_0, y_1, y_2, y_3, y_4, w),$$

or

$$\boxed{f_4 = -2\epsilon_g y_4 - \omega_g^2 y_3 + \sigma_g y_2}. \qquad (6B)$$

In order to find the acceleration, $\ddot{z} = -w$, from the displacement z, the differentiated forms of the Stirling and Bessel central difference interpolation formulae

to fourth-order differences (Hildebrand 1956, Scarborough 1950) were used to calculate $w = -\ddot{z}$.

$$w_0 = -\frac{1}{h^2}[-0{\cdot}0833\,3333\,3z_2 + 1{\cdot}3333\,3333\,3z_1 - 2{\cdot}50z_0 + 1{\cdot}3333\,3333\,3z_{-1} - 0{\cdot}0833\,3333\,3z_{-2}], \quad (12)$$

and

$$w_{\frac{1}{2}} = -\frac{1}{h^2}[-0{\cdot}1041\,6666\,7z_3 + 0{\cdot}8125\,0z_2 - 0{\cdot}7083\,3333\,3z_1 - 0{\cdot}7083\,3333\,3z_0 + 0{\cdot}8125\,0z_{-1} - 0{\cdot}1041\,6666\,7z_{-2}],$$

where w_0 is at the start, and $w_{\frac{1}{2}}$ is in the middle of an interval of iteration. The factor h is the interval of time between the various values of displacement, z; z_0 is the displacement at time t; z_1, z_2 and z_3 are later values of displacement, while z_{-1} and z_{-2} are earlier values. If it is desired to use an acceleration input, the interpolation formula becomes:

$$w_0 = -\ddot{z}_0, \quad (13)$$

and

$$w_{\frac{1}{2}} = -[+0{\cdot}0117\,1875\,0\ddot{z}_3 - 0{\cdot}0976\,5625\,0\ddot{z}_2 + 0{\cdot}5859\,3750\ddot{z}_1 + 0{\cdot}5859\,3750\ddot{z}_0 - 0{\cdot}0976\,5625\,0\ddot{z}_{-1} + 0{\cdot}0117\,1875\,0\ddot{z}_{-2}].$$

At the start of the iteration process the central difference formulae, (12) and (13) must be replaced by Gregory–Newton forward difference formulae to fourth-order differences. Thus at $t = 0$, $\frac{1}{2}h$, h and $\frac{3}{2}h$ we have, for a displacement input:

$$w_0 = -\frac{1}{h^2}[+0{\cdot}9166\,6666\,7z_4 - 4{\cdot}6666\,6666\,7z_3 + 9{\cdot}50z_2 - 8{\cdot}6666\,6666\,7z_1], \quad (12A)$$

$$w_{\frac{1}{2}} = -\frac{1}{h^2}[+0{\cdot}2916\,6666\,7z_4 - 1{\cdot}6666\,6666\,7z_3 + 4{\cdot}250z_2 - 4{\cdot}6666\,6666\,7z_1],$$

$$w_1 = -\frac{1}{h^2}[+0{\cdot}9166\,6666\,7z_5 - 4{\cdot}6666\,6666\,7z_4 + 9{\cdot}50z_3 - 8{\cdot}6666\,6666\,7z_2 + 2{\cdot}9166\,6666\,7z_1],$$

$$w_{\frac{3}{2}} = -\frac{1}{h^2}[+0{\cdot}2916\,6666\,7z_5 - 1{\cdot}6666\,6666\,7z_4 + 4{\cdot}250z_3 - 4{\cdot}6666\,6666\,7z_2 + 1{\cdot}7916\,6666\,7z_1].$$

For an acceleration input, we must use:

$$w_0 = 0, \quad (13A)$$

$$w_{\frac{1}{2}} = -[-0{\cdot}0390\,6250\ddot{z}_4 + 0{\cdot}2187\,50\ddot{z}_3 - 0{\cdot}5468\,750\ddot{z}_2 + 1{\cdot}0937\,50\ddot{z}_1],$$

$$w_1 = -\ddot{z}_1,$$

$$w_{\frac{3}{2}} = -[-0{\cdot}0390\,6250\ddot{z}_5 + 0{\cdot}2187\,50\ddot{z}_4 - 0{\cdot}5468\,750\ddot{z}_3 + 1{\cdot}0937\,50\ddot{z}_2 + 0{\cdot}2734\,3750\ddot{z}_1].$$

For values of $t \geq 2h$ the central difference formulae are utilized.

These equations, (4) for the inverse seismograph computation, and (11), (5A), (5B), (6A), (6B), (12), (12A), (13) and (13A) for the Runge–Kutta seismograph computation were coded for solution by the IBM 650 electronic data processing machine.

A computation was made in which sinusoidal ground displacement signals were used as an input to a seismograph having the constants $T_0 = 30$ s, $\epsilon_0 = 4{\cdot}5\omega_0$, $T_g = 100$ s, $\epsilon_g = \omega_g$, $\sigma_0\sigma_g = 0$, which is one of the instruments in use at the Lamont Geological Observatory (Sutton & Oliver 1959). It will be referred to

hereafter as the 30–100 instrument. The steady-state response was the same as that calculated by Sutton & Oliver using the Laplace transform method of Chakrabarty (1949). See Figure 1, circles on curve *c*.

A transient test signal was then made:

$$S_1(t) = \begin{cases} \frac{1}{2}\left[1-\cos\frac{2\pi}{20}t\right]; & t_0 < t \leqslant t_0+10\text{s}. \\ \cos\frac{2\pi}{40}(t-10); & t_0+10\text{s} < t \leqslant t_0+30\text{s} \\ -\frac{1}{2}\left[1-\cos\frac{2\pi}{20}(t-30)\right]; & t_0+30\text{s} < t \leqslant t_0+40\text{s}. \end{cases} \tag{14}$$

This ground displacement signal was used in a calculation with the same 30–100 seismograph, and Fourier analysis of the input and output was performed (Matsumoto 1958), with a Fourier analysis programme built for another study.

The amplitude response to this transient

$$G_\theta(T) = \frac{A_0(T)}{A_i(T)}, \text{ where } T = \text{period}, \tag{15}$$

was then calculated, and is also shown in Figure 1 as curve *c*. The Fourier amplitude spectrum, $A_i(T)$, of the test signal $S_1(t)$ is also shown in Figure 1, as curve *a*,

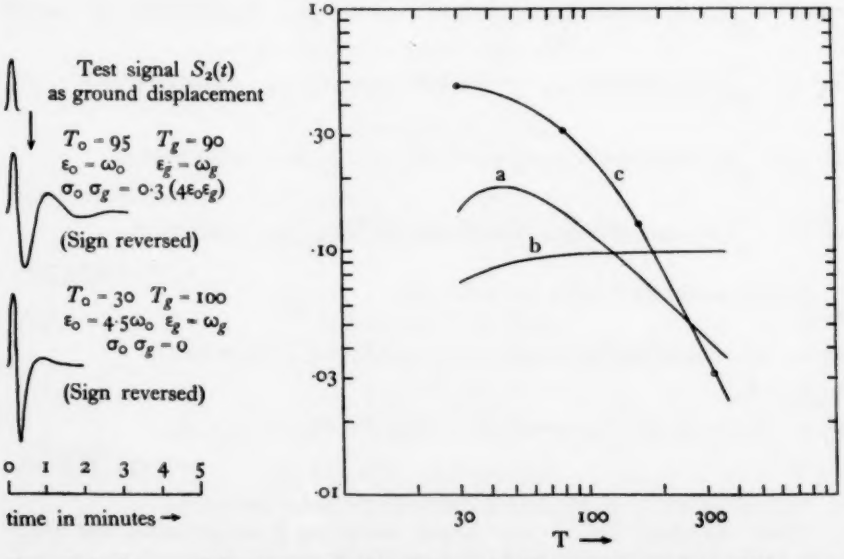

FIG. 1.—Left: Seismograms produced by pulse-like ground motion, $S_2(t)$, on a narrow-band and a broad-band seismograph.

Right:
(a) Fourier amplitude spectrum of test signal $S_1(t)$.
(b) Fourier amplitude spectrum of test signal $S_2(t)$. Amplitudes times 0·1.
(c) Amplitude response vs. period of 30–100 seismograph. Circles show results of steady-state tests, curve is the result of transient test.

and $A_0(T)$ is the amplitude spectrum of the resulting galvanometer deflection, not shown. As can be seen in Figure 1, the transient response of the system is identical to that for steady-state signals.

This same test signal was used to calculate the response curves shown in Figure 2, and the input and output signals for the various instruments are shown in Figure 3. The sign has been reversed where shown to facilitate comparison. Seismographs are normally connected so that an upward deflection of the trace implies that the ground moved up, east or north.

The inverse seismograph computation programme was also tested with this signal. The resulting response curve for the linear strain recorder is shown in Figure 2, and the input and output time functions are shown in Figure 3. The resulting acceleration was then used as the acceleration input of the seismograph computation. The resulting seismograms are shown in Figure 3. The non-symmetrical ground acceleration shown in Figure 3 is that required by a 70 second pendulum in order to produce a seismogram equal to $S_1(t)$ (see equation (4)). By Fourier analysis of the 100–90 seismograms of Figure 3, and of the corresponding acceleration, the response curves for the 100–90 instruments, shown in Figure 2, were obtained.

In addition, Laplace transform calculation of the steady-state response at $T = 60$ s was performed for the strain seismograph, and for the 95–90 and 100–90 instruments with $\sigma_0\sigma_g = 0$. These responses agreed with those found by Fourier analysis of the test signals, and are shown in Figure 2.

From an assumed seismogram, $S_1(t)$, the acceleration was computed with equation (4). Then the computed seismogram which resulted, when a simple pendulum having the same constants received this acceleration as an input, was used to test the entire system of computation. The computed pendulum displacement signal was the same as the original input. Upon comparison, the first four leading digits of both signals were found to be identical. A similar test in which the test signal was first used as an acceleration, also reproduced the same acceleration to a corresponding number of digits. This means that the computed seismogram is the same as that which would be produced by the equivalent seismograph. The "noise" in the computed record is at least an order of magnitude less than the smallest deflections which can be plotted or observed.

Another test signal,

$$S_2(t) = \frac{1}{2}\left[1 - \cos\frac{2\pi}{20}t\right] \quad (t_0 < t \leqslant t_0 + 20\text{s}) \tag{16}$$

was used as a displacement input to the 30–100 seismograph and the 95–90 instrument with coupling. The resulting signals are shown in Figure 1, and the Fourier amplitude spectrum of $S_2(t)$ appears as curve b in Figure 1. For signals which begin gradually, such as these, central difference formulae which start at $t_0 \neq 0$ give equivalent results to forward difference formulae which start at $t_0 = 0$, to the precision required. Both methods were used and the results were equivalent.

When it was clear that both computation programmes were working properly, calculations were made using an earthquake signal. A linear strain seismogram of the $G1$ signal from the New Guinea shock of 1938 February 1, as recorded at Pasadena, which was sampled every six seconds by Satô (1958) for his study of the G wave, was reduced to ground acceleration, and this acceleration was then used as an input for various approximations to the Gilman instrument discussed by

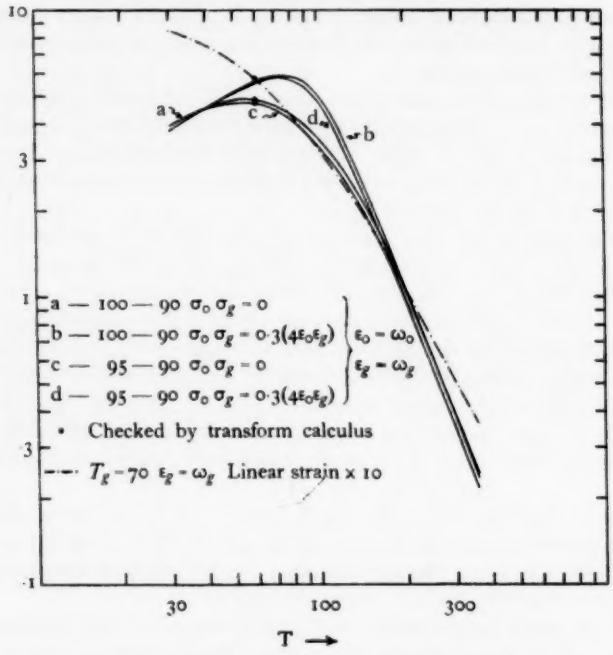

FIG. 2.—Amplitude response vs. period for linear strain, $T_g = 70$ s, $\epsilon_g = \omega_g$, and four seismographs whose amplitude response changes rapidly with period.

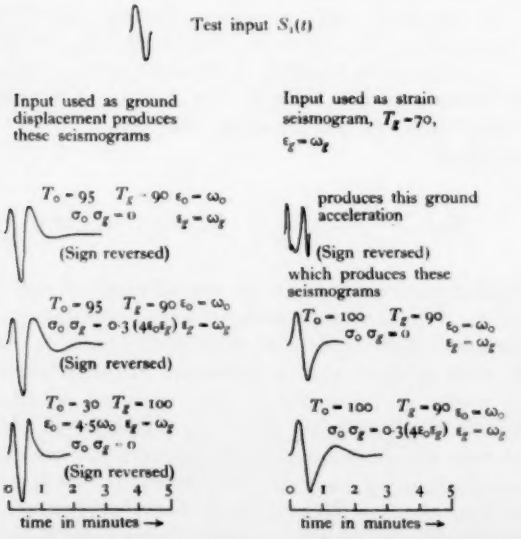
Test input S₁(t)
Input used as ground displacement produces these seismograms
Input used as strain seismogram, T_g = 70, ε_g = ω_g
T₀ = 95 T_g = 90 ε₀ = ω₀ σ₀ σ_g = 0 ε_g = ω_g
(Sign reversed)
produces this ground acceleration
(Sign reversed)
which produces these seismograms
T₀ = 95 T_g = 90 ε₀ = ω₀ σ₀ σ_g = 0·3(4ε₀ε_g) ε_g = ω_g
(Sign reversed)
T₀ = 100 T_g = 90 ε₀ = ω₀ σ₀ σ_g = 0 ε_g = ω_g
T₀ = 30 T_g = 100 ε₀ = 4·5ω₀ ε_g = ω_g σ₀ σ_g = 0
(Sign reversed)
T₀ = 100 T_g = 90 ε₀ = ω₀ σ₀ σ_g = 0·3(4ε₀ε_g) ε_g = ω_g
0 1 2 3 4 5
time in minutes →
0 1 2 3 4 5
time in minutes →

FIG. 3.—Test input $S_1(t)$ used as ground displacement, left, and as strain seismogram, right. The 100–90 seismograms would be produced by the same acceleration that produces $S_1(t)$ on the linear strain.

Benioff & Press (1958). The results are shown in Figure 4. The overshoot displayed by the transient signals in Figure 3 is evident in the resulting seismograms of Figure 4. The records in Figure 4 are those which would be obtained if all four pendulum–galvanometer instruments and the original strain seismograph were recording simultaneously. A comparison of the lower four seismograms shows

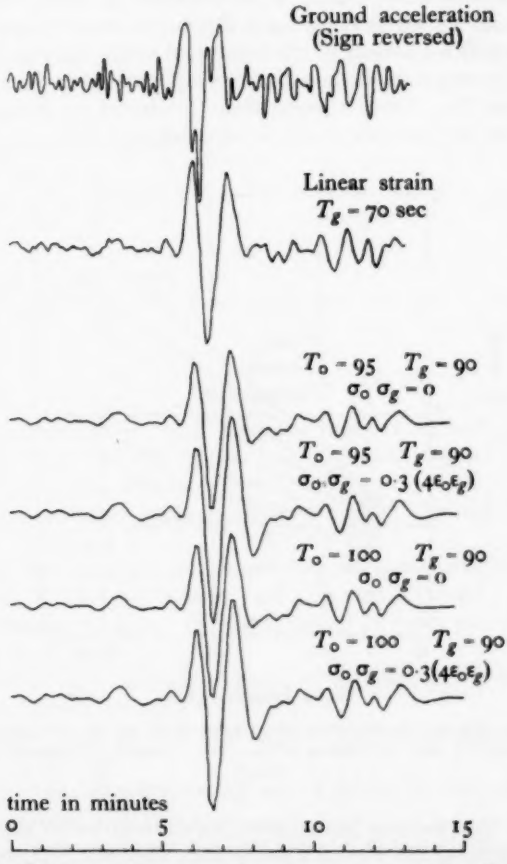

FIG. 4.—Linear strain record, $T_g = 70$ s, $\epsilon_g = \omega_g$, of the $G1$ signal from the New Guinea shock of 1938 February 1, as recorded at Pasadena (courtesy of Prof. H. Benioff) reduced to ground acceleration, above. The four seismograms produced by four approximations to the Gilman seismograph, below, display overshoot similar to that of the test pulses in Figure 3.

that slight changes in the pendulum period have negligible effect, which is also shown by the response curves in Figure 2. The effect of changing the coupling from $\sigma_0\sigma_g = 0$ to 0·3 ($4\epsilon_0\epsilon_g$) produces slightly increased distortion, for instruments whose pendulum and galvanometer periods are as close as these, but it is clearly evident that all four instruments have conspicuously distorted the seismic signal.

Figure 4 should be compared with Figure 8 in the study of Benioff & Press (1958). The record shown there, produced by a Gilman seismograph, is virtually identical with the computed seismograms in Figure 4. It was concluded by Benioff and Press that the group velocity of Love waves displays a maximum with a decrease in group velocity for periods greater than about two minutes, since the long period disturbance of the trace in Figure 8 of their study continued from the arrival of the G wave until the arrival of the Rayleigh wave train. The original strain seismogram, shown in Figure 4 of this paper, was the same one which was used by Satô (1958) for a study of the G wave, in which the response of the instrument and the spectrum of the source were subtracted out by taking differences $G3$–$G1$, and $G4$–$G2$. These computations produced an essentially flat group velocity curve for long periods, which is reproduced in Figure 5. We are thus led

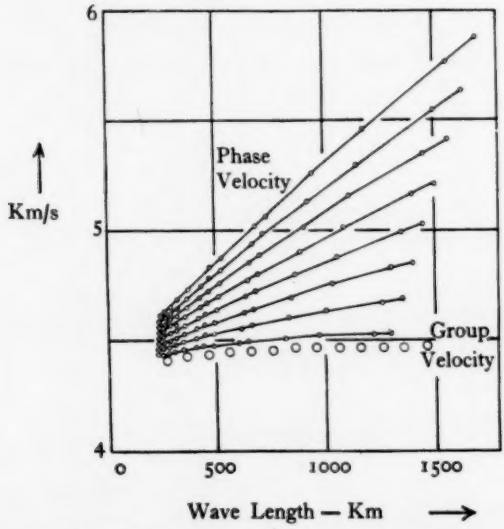

FIG. 5.—Phase velocity and group velocity of the G wave obtained by using $G3$ and $G1$ phases of the New Guinea earthquake (after Satô).

to the conclusion that the long period disturbance recorded by the Gilman instrument after the arrival of a G wave is a purely instrumental effect, and is not related to the physical properties of the earth.

3. Conclusions

For best results, dispersion curves for pulse-like signals should be constructed from the seismograms of instruments whose magnification changes very gradually with period. This study also emphasizes that the transient response of instruments, whose magnification changes rapidly with period, may be important in studies of wave propagation.

In the long period range up to several hundred seconds, there is no evidence for appreciable dispersion of the G wave, and earlier observations of an essentially flat group velocity curve remain valid.

4. Acknowledgments

The authors are especially grateful to Jack Oliver, not only for his constructive criticism, but also for his valuable suggestions when this study was begun. It is a pleasure to thank the Electronic Research Laboratories and the Watson Scientific Computing Laboratory of Columbia University for the use of their computing facilities, Betty Quest for drafting the figures for this study, and George Sutton and Stefan Mueller for helpful discussions of the manuscript. This research was supported by the American Petroleum Institute, Grant 49, the Office of Naval Research, Contract N-onr-266 (53), and the Air Force Cambridge Research Centre, Contract AF 19 (604) 4144.

Lamont Geological Observatory,
(Columbia University)
Palisades, New York
1958 *December.*

Lamont Geological Observatory
Contribution No. 339.

References

Akima, T. S. & Nagamune, T., 1956. Dispersion of seismic surface waves and the structure of continents and oceans. *Bur. Central Seismol. Internat. Pubs., Sér. A, Travaux Sci., No.* 19, 223–228.

Benioff, H., 1935. A linear strain seismograph. *Bull. Seismol. Soc. Amer.*, **25,** 283–309.

Benioff, H., 1955. Earthquake seismographs and associated instruments. *Advances in Geophysics*, **2,** 220–275. (New York: Academic Press.)

Benioff, H. & Press, F., 1958. Progress report on long period seismographs. *Geophys. J.* **1,** 208–215.

Birkenhauer, H. F., 1945. A study of house vibrations from quarry blasts. *Bull. Seismol. Soc. Amer.*, **35,** 99–115.

Bryan, A. B., 1936. True ground motion from mechanical seismograph records. *Geophysics*, **1,** 340–346.

Byerly, P., 1926. The Montana earthquake of June 28, 1925, G.M.C.T. *Bull. Seismol. Soc. Amer.*, **16,** 209–265.

Byerly, P., 1942. *Seismology*, 256 p. (New York: Prentice-Hall).

Chakrabarty, S. K., 1949. Response characteristics of electromagnetic seismographs and their dependence on the instrumental constants. *Bull. Seismol. Soc. Amer.*, **39,** 205–218.

Coulomb, J., 1952. Love waves of the Queen Charlotte Islands earthquake of August 22, 1949. *Bull. Seismol. Soc. Amer.*, **42,** 29–36.

Coulomb, J. & Grenet, G., 1935. Nouveaux principes de construction des séismographes électromagnétiques. *Ann. Phys. (Paris) Sér. XI*, **3,** 321–369.

Di Filippo, D., 1950. L'Onda "*G*" di Gutenberg nel terremoto delle Azzorre del 25 Novembre 1941. *Ann. Geofis.* **3,** 39–45.

Dyk, Karl, 1935. On the reduction of seismograms obtained in shaking-table experiments. *Bull. Seismol. Soc. Amer.*, **25,** 119–137.

Eaton, J. P., 1957. Theory of the electromagnetic seismograph. *Bull. Seismol. Soc. Amer.*, **47**, 37–75.

Ewing, M., Jardetzky, W. S. & Press, F., 1957. *Elastic waves in layered media*. 380 p. (New York: McGraw-Hill).

Ewing, M. & Press, F., 1952. Crustal structure and surface wave dispersion, Part II: Solomon Islands earthquake of July 29, 1950. *Bull. Seismol. Soc. Amer.*, **42**, 315–325.

Ewing, M. & Press, F., 1954(a). An investigation of mantle Rayleigh waves. *Bull. Seismol. Soc. Amer.*, **44**, 127–147.

Ewing, M. & Press, F., 1954(b). Mantle Rayleigh waves from the Kamchatka earthquake of November 4, 1952. *Bull. Seismol. Soc. Amer.*, **44**, 471–479.

Ewing, M. & Press, F., 1956. Surface waves and guided waves. *Encyclopedia of Physics*, **47**, 125 p. (Berlin: Springer).

Gill, S., 1951. A process for the step-by-step integration of differential equations in an automatic digital computing machine. *Proc. Camb. Phil. Soc.*, **47**, 96–108.

Hagiwara, T., 1958. A note on the theory of the electromagnetic seismograph, *Bull. Earthqu. Res. Inst.*, **36**, 139–164.

Hildebrand, F. B., 1956. *Introduction to numerical analysis*, 511 p. (New York: McGraw-Hill).

Imamura, A., 1937. *Theoretical and practical seismology*. p. 293 (Tokyo: Maruzen).

Landisman, M., Satô, Y., & Ewing, M., Shear wave velocities in the upper mantle. (In preparation).

Matsumoto, T., 1958. Calibration of an electromagnetic seismograph by means of the frequency analysis. *Bull. Earthqu. Res. Inst.*, **36**, 55–64.

McComb, H. E. & Ruge, A. C., 1937. Tests of earthquake accelerometers on a shaking table. *Bull. Seismol. Soc. Amer.*, **27**, 325–329.

McComb, H. E. & Wenner, F., 1936. Shaking-table investigations of teleseismic seismometers. *Bull. Seismol. Soc. Amer.*, **26**, 291–316.

Neumann, Frank & others, 1943. The determination of true ground motion by integration of strong-motion records: A symposium. *Bull. Seismol. Soc. Amer.*, **33**, 1–63.

Ruge, A. C., 1936. A machine for reproducing earthquake motions direct from a shadowgraph of the earthquake. *Bull. Seismol. Soc. Amer.*, **26**, 201–205.

Satô, Y., 1958. Attenuation, dispersion, and the wave guide of the *G* wave. *Bull. Seismol. Soc. Amer.*, **48**, 231–251.

Scarborough, J. B., 1950. *Numerical mathematical analysis*, 511 p. (Baltimore: Johns Hopkins Press).

Sharpe, J. A., 1935. Motion of the surface of the earth in the compressional phase of a deep-focus earthquake, and the effects of a layered crust. *Bull. Seismol. Soc. Amer.*, **25**, 199–222.

Sieberg, H. & Gutenberg, B., 1924. Das Erdbeben in der Chilenischen Provinz Atacama am November 10, 1922. *Veröff. der Reichsanstalt für Erdbebenforschung in Jena*, Heft 3.

Sutton, G. & Oliver, J. Seismographs of high magnification at long periods. *Ann. Geophys.* (In press).

Tsuboi, C., 1931. On the possibility of finding the permanent crust dislocation caused by an earthquake by means of its seismogram. *Proc. Imp. Acad. Japan*, **7**, 371–374.

Walter, E. J., 1945. An extension of the method of numerical integration of seismograms to include a third integration. *Bull. Seismol. Soc. Amer.*, **35**, 71–79.

Wilson, H. A., 1932. Calculation of the motion of the ground from seismograms. *Physics*, **12**, 196–199.

Wilson, J. T., 1940. The Love waves of the South Atlantic earthquake of August 28, 1933. *Bull. Seismol. Soc. Amer.*, **30**, 273–301.

The Determination of Virgin Strata Temperatures from Observations in Deep Survey Boreholes

L. R. Cooper and C. Jones

(Received 1959 January 22)

Summary

When a survey borehole is drilled downwards from the surface of the Earth the temperature is disturbed by the circulating drilling fluid, but fluid and adjacent strata gradually attain the local virgin strata temperature when drilling is stopped. Temperature equilibrium is approached most quickly near the bottom of the hole where the time of disturbance has been the least. Observations of the fluid temperature at this position may be made over a period of a day during a normal week-end break in drilling. Cylindrical heat flow theory is used in this paper to show that, with a knowledge of the thermal properties of the fluid and surrounding strata, the virgin strata temperature at the depth reached can be calculated from such observations. New and inexpensive equipment using a thermistor temperature measuring probe has been developed for making the observations of temperature and it has been tested successfully down to depths of 1 060 m (3 480 ft) in Hopton Pool Borehole in the Cannock Chase area. The paper also describes the equipment and gives the virgin strata temperatures for the Hopton Pool Borehole. It also gives observations of the temperature of the borehole fluid at various depths taken on one day several days after the borehole drilling had ceased and shows that these could not be regarded as reliable measures of the virgin strata temperature.

Symbols used in the text

θ_v	Virgin strata temperature.
θ_0	Borehole fluid temperature at a time $t = 0$.
θ	Borehole fluid temperature at time t.
T	Temperature indicated by the probe (in °K).
a	Radius of the borehole.
t	Time.
k, ρ, c	Thermal conductivity, density and specific heat, respectively, of the strata.
ρ_1, c_1	Density and specific heat of the fluid within the borehole.
K	Thermal diffusivity of the strata ($= k/\rho c$)
R	Electrical resistance of the thermistor in the probe (in ohms).

A, B Thermistor characteristic constants.

H The reciprocal of the thermal contact resistance per unit area between the fluid in the borehole and the surrounding strata.

$$\tau = Kt/a^2, \qquad \alpha = 2\rho c/\rho_1 c_1, \qquad n = (\theta - \theta_0)/(\theta_v - \theta_0), \qquad h = k/aH.$$

The units used throughout the report are in both the metric and foot-pound-second systems.

1. Introduction

When a coal mine is to be opened to bring coal from the warm strata deeper than 900 m (2 950 ft) it is necessary to know, as early as possible, whether the strata temperature is high enough to create an uncomfortable working climate. The earliest opportunity for obtaining information occurs when boreholes are being drilled downwards from the Earth's surface to locate the depths and nature of the coal seams. During the progress of the borehole there are usually short breaks in the drilling during which temperature measuring equipment can be lowered into the hole. This paper describes new equipment which has been developed for measuring the temperature of the fluid at any depth in a borehole and also shows how the measurements very near the bottom of the hole can be converted to the virgin strata temperature at that depth.

During the course of the work here described, it came to the authors' notice that a similar programme was in progress for the Dutch State Mines but as far as is known to the authors no information has been issued on the results of the work and it is, therefore, not yet possible to make a comparison between the two cases.

If a long hole of small diameter is quickly drilled vertically into virgin strata and the hole is immediately filled with a fluid which is cooler than the strata there will be a flow of heat into the fluid. At the bottom of the hole the heat flows from the sides of the hole and also from the base of the hole. However, it is not possible to lower a temperature measuring device to this position because the drilling rods require some time for withdrawal, especially from the deeper holes, and during this time the solid matter in the drilling fluid settles to the bottom. It is therefore not possible to measure the fluid temperature at the bottom and readings have to be taken a short distance above the base. In this position the heat flows into a short length of a cylinder of fluid and if the measuring position is twelve or more hole diameters above the bottom of the hole it has been shown (Blackwell 1956) that the heat flow is entirely radial towards the centre of the hole. For the special case of a survey borehole any theory associated with such temperature measurements must apply for different sizes of hole, for the diameter is decreased from about 24 to 12 cm (9 to 5 in.) as the hole proceeds downwards, and it must also take into account the thermal properties of the surrounding strata which change considerably, particularly in the coal measures.

Normally, the effect of the drilling fluid on the strata temperature will penetrate some distance into the strata during the long drilling process and Bullard (1947) has shown that some time would be required after drilling ceased for the recovery from the temperature disturbance. However, near the bottom of a rapidly-drilled hole, around which the strata have experienced little or no temperature change, Bullard has indicated that the fluid temperature may approach quite near to the virgin strata temperature (V.S.T.) within as little as a day from the

end of the drilling. This paper confirms this finding and shows that observations at even shorter intervals may be corrected to give V.S.T.

2. Theory

The radial flow of heat from an infinite region surrounding a cylindrical borehole to the fluid within it has been discussed theoretically (Jaeger 1956) and as long as there is no heat flow along the axis of the cylinder then

$$\frac{\theta-\theta_v}{\theta_0-\theta_v} = F(h, \alpha, \tau)$$

where

$$F(h,\alpha,\tau) = \frac{4\alpha}{\pi^2}\int_0^\infty \frac{\exp(-\tau u^2)\,du}{u\{[uJ_0(u)-(\alpha-hu^2)J_1(u)]^2+[uY_0(u)-(\alpha-hu^2)Y_1(u)]^2\}}$$

in which $J_N(u)$ and $Y_N(u)$ are the Bessel functions of order N of the first and second kinds.

When a cool fluid is introduced into the borehole and its temperature rise is observed over a period of time it is more useful to study the ratio $n = (\theta-\theta_0)/(\theta_e-\theta_0)$ as this ratio approaches unity with increasing time.

Let

$$n = \frac{\theta-\theta_0}{\theta_v-\theta_0} = 1-\frac{\theta-\theta_v}{\theta_0-\theta_v} = 1-F(h,\alpha,\tau).$$

For the case of a survey borehole in which the fluid is mainly water in good thermal contact with the wall of the hole then $h = 0$. Values of $F(0, \alpha, \tau)$ have been evaluated (Jaeger 1956) and a graph of the values is reproduced in Figure 1

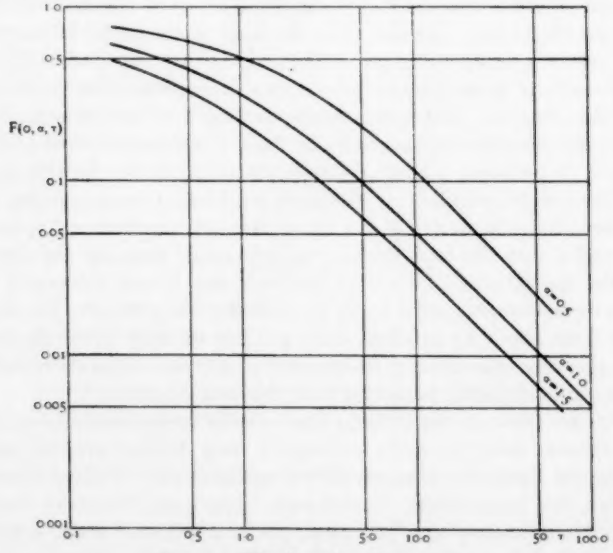

FIG. 1.—The function $F(0, \alpha, \tau)$.
Absissa: τ

for three values of α, namely 0·5, 1·0 and 1·5. For a borehole of known diameter containing water in a medium of known or assumed thermal properties at a higher temperature than the water, observations of the water temperature, θ, (initially $\theta = \theta_0$) can be measured at a series of times, t. It is then possible to evaluate $F(0, \alpha, \tau)$ from Figure 1, and hence n, for each of the times. The V.S.T., θ_v, can therefore be obtained for each time as $\theta_v = \theta_0 + (1/n)(\theta - \theta_0)$ and the values should be constant whatever the time. It is important to note that at a time $t = 0$ the strata surrounding the borehole must be at uniform temperature. This method of temperature correction is the same as that used in other heat flow problems (Bullard 1954, Bullard, Maxwell & Revelle 1956).

3. Experimental results

That the above theory could be used very near the bottom of a hole was first established in the laboratory using an approximately quarter-scale model of the bottom of a deep borehole. The theory was then used in the determination of the V.S.T. surrounding the Hopton Pool Borehole in Cannock down to a depth of about 1 060 m (3 480 ft).

3.1. *Examination of the theory by means of a laboratory scale model experiment*

A large block of sandstone of thermal conductivity 5×10^{-3} cal cm^{-1} s^{-1} (deg C)$^{-1}$ (0·00033 B.t.u. ft^{-1} s^{-1} (deg F)$^{-1}$, and about 1 m (yard) cube, was left to stand in a room until it has acquired a uniform temperature, the same as the surrounding air temperature. That this was so was checked by the readings of several thermocouples, some placed near and on the faces of the sandstone and others inserted into very narrow holes drilled to various depths into the rock. A larger vertical hole of 4 cm (1½ in.) diameter had been drilled downwards and centrally in the top of the block to reach just below the centre of the block. As soon as the temperatures in the block were uniform and steady the hole was filled with chilled slurry and a thermocouple was placed in the slurry eight hole diameters above the bottom of the hole. Figure 2 (full line) shows the temperature of the slurry over a period of time as it gained heat from the block. Table 1 shows the observations and the way they were corrected as described above to give the V.S.T. (chain dotted line in Figure 2) within 0·05°C of the measured V.S.T. which was 20·25°C (68·45°F).

Satisfactory results were obtained after about half an hour of temperature readings. On a full scale borehole one would therefore expect to obtain similarly satisfactory results after about eight hours, the time changing with the square of the hole diameter ($\tau = Kt/a^2$). It thus appeared quite possible to observe temperatures very near the bottom of a survey borehole for less than a day and so determine the V.S.T. Fortunately, it is possible to do this at the weekend break in drilling which usually lasts for about 24 hours.

3.2. *Field trials at Hopton Pool Borehole*

An opportunity to make observations of temperature in a survey borehole occurred in the Cannock Chase area where the National Coal Board is carrying out a programme of coal seam surveying. This borehole, known as the Hopton Pool Borehole and some 5 km (3 miles) north-east of Stafford, commenced in 1956 April and terminated at 1 060 m (3 480 ft) at the end of 1957 September.

Table 1

Results of laboratory scale model experiment

Measured V.S.T. = 20·25 °C (68·45 °F). Initial slurry temperature θ_0 = 2·9 °C (37·2 °F)

Time (hr)		0·083	0·167	0·250	0·333	0·416	0·500	0·584	0·666	0·750	0·830	1·00	1·50
θ	°C	12·2	15·8	17·05	17·7	18·2	18·55	18·85	19·0	19·15	19·3	19·4	19·6
	°F	54·0	60·4	62·7	63·9	64·8	65·4	65·9	66·2	66·5	66·7	66·9	67·3
τ				2·35	3·13	3·92	4·70	5·48	6·26	7·05	7·83	9·40	14·1
$F(o, \alpha, \tau)$				0·17	0·135	0·11	0·095	0·084	0·074	0·066	0·060	0·051	0·034
n				0·83	0·865	0·89	0·905	0·916	0·926	0·934	0·940	0·949	0·966
$\theta-\theta_0$	°C			14·15	14·8	15·3	15·65	15·95	16·1	16·25	16·4	16·5	16·7
	°F			25·5	26·7	27·6	28·2	28·7	29·0	29·3	29·5	29·7	30·1
θ_v	°C			20·0	20·05	20·15	20·2	20·3	20·3	20·3	20·3	20·3	20·2
	°F			68·0	68·1	68·3	68·4	68·5	68·5	68·5	68·5	68·5	68·4

For about the first 150 m (500 ft), when the surrounding strata were water-bearing sand and pebbles, the hole was some 25 cm (10 in.) in diameter and was punched out. From 150 to 340 m (500 to 1 100 ft) the strata were red marl with subsidiary sandstone and the diameter of the hole was decreased to 18 cm (7 in.). Between 340 and 450 m (1 100 and 1 500 ft) the strata changed to a mudstone which was impervious to water. Below 450 m (1 500 ft) the strata changed to the grey coal measures which were impervious to water and below 520 m (1 700 ft) they were predominantly mudstone with 21 coal seams between 520 and 860 m (1 700 and 2 840 ft), varying in thickness from 15 cm (6 in.) to 2·2 m (7 ft 4 in.).

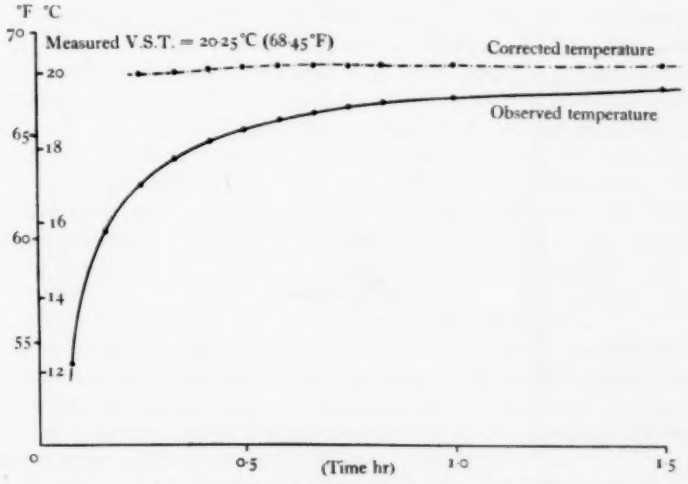

FIG. 2.—Laboratory-scale model experiment.

Roller drilling began at about 150 m (500 ft) and core drilling commenced some 300 m (1 000 ft) deeper and continued to the bottom of the hole with a diameter just under 12 cm (5 in.). The hole was lined with a steel casing but as this never came nearer to the bottom of the hole than 30 m (100 ft), and was often much further away than this, the probe used for temperature measurements was always surrounded only by strata. The fluid used for core drilling was a mixture of bentonite and water to give a specific gravity in the region 1·1 to 1·2, the higher figure being appropriate to the greater depths. Zero time was taken as the time when the drill rods were passing the depth at which observations of temperature were made. A short time elapsed while the rods drilled the short distance below the measuring point and some hours were required for all the rods to be removed from the hole and for the temperature probe to be lowered to its position near the bottom. This delay was timed as it entered into the correction to be made to the observed temperature.

Before the field trials were commenced a theoretical estimate was made of the rise in temperature with time of fluid standing in boreholes of different diameters and surrounded by strata of different conductivities. As mentioned above, the Hopton Pool Borehole changed in diameter from 25 cm (10 in.) down to about 12 cm (5 in.) and the strata varied from sandstone to coal, giving a change in the

diffusivity in the ratio of about five to one. Figure 3 shows the ratio of the rise in temperature of the fluid to the initial temperature difference between strata and fluid obtained from calculations based on the theory given earlier. For a hole of 12 cm ($4\frac{3}{4}$ in.) in rock this ratio is greater than 0·98 at the end of 24 hours but some 160 hours are needed to achieve the same value for coal. The value of 0·98 is selected here because for all values of the ratio greater than this the fluid temperature, θ, is within 0·5 °C (1 °F) of the V.S.T., θ_v, as long as $\theta_v - \theta_0$ is less than 28 °C (50 °F).

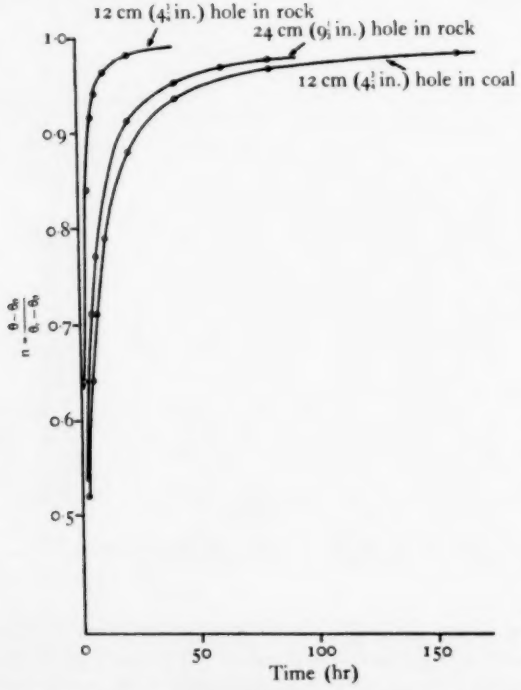

FIG. 3.—Rise in temperature of the drilling fluid for different boreholes.

Figure 3 also shows the effect of a larger hole in rock and, again, a longer time of some 100 hours is needed to achieve the ratio of 0·98. When the hole was large in diameter in the Hopton Pool Borehole at least 27 hours and up to 260 hours were available for observations and the difference between the virgin strata and drilling fluid temperatures was then the lowest, both being factors that reduced the temperature correction.

3.2.1. *The apparatus used for measuring the temperature of the borehole fluid*

The complete equipment is made up of the temperature probe, by which the borehole fluid temperature is measured, the measuring circuit by which the resistance of the thermistor in the probe can be determined, the cable connecting the two, the motorized winch and associated equipment for raising and lowering the probe and cable and, finally, a depth measuring device on the cable.

Maximum and minimum thermometers were discarded in this project as it is necessary to observe changes in temperature over short times when it is neither desirable nor is there sufficient time to lower and raise the thermometers a sufficient number of times. Thermocouples were rejected as they would require compensating leads due to the steady change of temperature down a borehole, and the spurious voltages which occur in boreholes, which are referred to later, would upset the readings of the couples. Also taking into account abrasion resistance and weight of cable the use of thermocouples is not a practical proposition. The choice of a temperature measuring device therefore rests between a thermistor and a wire resistance thermometer such as platinum, copper or nickel. Because the resistance of the latter is usually of the same order as the connecting cable it is necessary to use three or four leads to make full compensation for changes in cable resistance due to temperature changes. With a high resistance thermistor any change of cable resistance with temperature is negligible compared with the change in thermistor resistance and a cable with two conductors is all that is required. For the final design of temperature probe a type M.1512/300 thermistor made by Standard Telephones and Cables was used. Separate laboratory tests over a long period* justified the use of this type of thermistor. Figure 4 shows a simplified section of the probe, of 2 cm ($\frac{3}{4}$ in.) diameter, the thermistor, having a copper base, being placed in direct thermal contact with the stainless steel case of the probe. The cable with its cable gland is detachable for transit purposes. The overall length of the assembled probe is 160 cm (63 in.) and it is weighted with a lead filling to give a total weight of 2½ kg (5½ lb).

The thermistor head was calibrated before and on several occasions during use against a standard thermometer in a bath of silicone oil, the thermistor resistance, R, and the absolute temperature, T, being related by the law $R = A \exp(B/T)$ where A and B are constants. During the field work described in this report no significant change occurred in the thermistor calibration.

The cable had to satisfy two separate requirements, one with regard to mechanical strength and the other with regard to its electrical properties. With a thermistor of about 100 000 ohms at normal temperature a change of 0·05 °C (0·1 °F) in the temperature changed its resistance by about 250 ohms. The series resistance of the cable wire, therefore, was satisfactory if it never changed by more than 100 ohms. Similarly, a shunt resistance greater than 100 megohms changed the effective measured resistance by less than 100 ohms. The cable had to withstand a safe load of 45 kg (100 lb) (the maximum pull required to remove the probe from the mud) over and above its own weight at the full depth of the hole. The one finally selected was a special winch cable made by Johnson and Phillips and designated Type SS1A. It was made up of a central core of 7 tinned copper wires insulated with polythene and two armoured wrappings of galvanized steel wire. Its weight was 34 kg/km (23 lb/1 000 ft), loop resistance 128 ohms/km (39 ohms/1 000 ft), shunt resistance greater than 5 500 megohms/km (5 000 megohms/1 000 yards) and its minimum breaking load was 410 kg (900 lb).

The measuring circuit consisted of a Wheatstone bridge (Figure 5), the probe thermistor forming one arm of the bridge, with a light-spot type suspended coil galvanometer having a sensitivity of 250 mm/μA. When the bridge was in use it was found that stray voltages were observed of sufficient magnitude to deflect the galvanometer off scale. It is believed that these were caused by electrochemical potentials developed along the length of the armouring which formed

* made by L. R. Cooper.

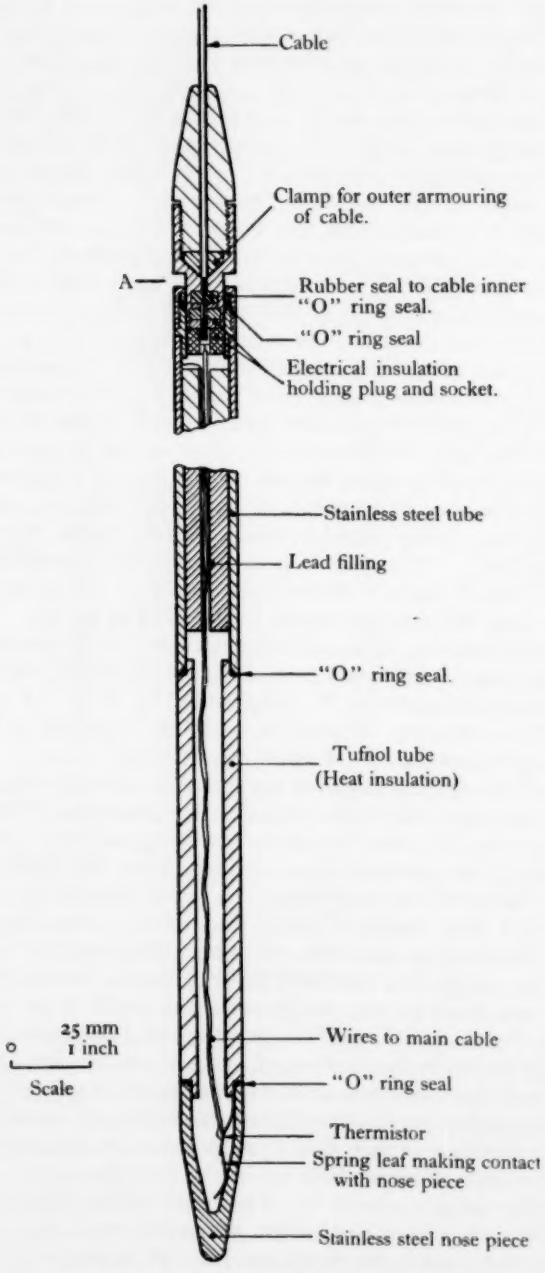

FIG. 4.—Simplified section of probe.

one of the two conductors to the thermistor, and which was immersed in the corrosive and chemically active water in the borehole. By means of an additional battery and variable resistance an opposing voltage of the same magnitude was injected into the bridge circuit. Figure 5 shows this battery at B_2 with the added resistances $R_{5,6,7,8,9}$. The external potentials were backed off by adjusting the potentiometer R_8 to return the galvanometer spot to the mid point of its scale. During this operation the backing off battery key, K_3, and the galvanometer key, K_2, were closed, the bridge battery key, K_1, was open. The final balance was then obtained, with K_2 and K_3 still closed, by adjusting the decade resistances R_1 until there was no change of deflection of the galvanometer on opening and closing K_1. The resistance of the thermistor probe was then read off from the dials of R_1.

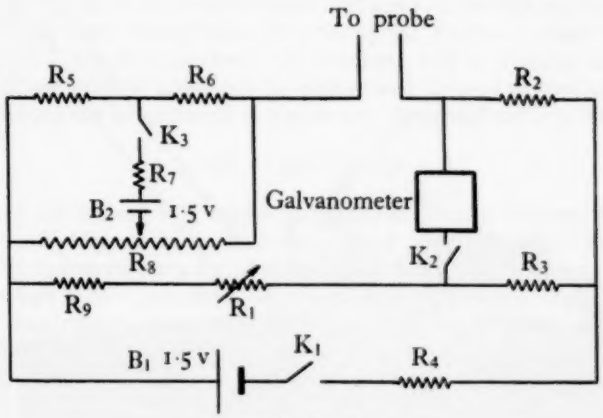

FIG. 5.—Bridge circuit.

R_1 decade	10Ω to 211 100Ω
R_2 & R_3	100 000Ω
R_4	4 700Ω
R_5 & R_6	50Ω
R_7	20Ω
R_8	500Ω
R_9	70Ω

That the added circuit did not affect the accuracy can be seen by noting that the bridge balance was obtained by observing the effect on the circuit only of battery B_1. The other e.m.f.'s played no part in this operation. Considering the circuit with all e.m.f.'s other than B_1 replaced by short circuits the condition for balance is that of a four-arm Wheatstone bridge. It is then seen that the resistance R_9 is practically equal to the resistance of the circuit $R_{5,6,7,8}$, at all values of R_8 and thus the main circuit is unaffected. The overall accuracy of the bridge in measuring temperature was better than 0·03 °C (0·05 °F).

A builder's power winch was specially adapted for the field work by the manufacturers. It consisted of a two-stroke engine which drove, via a four-speed gear box (three forward speeds for raising the probe and one reverse for lowering), a pair of cork covered rollers. The drum which carried the cable normally rested against brake pads but, on depressing the control handle, the drum moved off the brakes on to the cork driving rollers. There was thus a "dead man's handle" effect for quick stopping. The weight of the winch with cable was about 136 kg

(300 lb). The pull was 160 kg (350 lb) at a minimum speed of 8 m/min (25 ft/min). A depth indicator was added to show the amount of cable paid out, its smallest indicated unit being $7\frac{1}{2}$ cm (3 in.). Figure 6 (Plate I) shows the apparatus assembled for use.

3.2.2. *The borehole temperature measurements*

Because of the probable interchange of water between the strata and the borehole down to about 150 m (500 ft) no figures are included to this depth in this paper although the apparatus was given preliminary tests at the depth of 50 m (160 ft). The first reliable figures, capable of correction in accordance with the theory, were obtained below the water-bearing strata.

It was not possible to measure the temperature of the drilling fluid as the drill passed the depth at which the probe was subsequently positioned and it was therefore not possible to give a value to θ_0. However, it is not necessary to know this value as long as several observations of the probe temperature are measured over a period of a few hours. It was shown in Section 2 of the paper that

$$\theta = \theta_0 + (\theta_v - \theta_0)[1 - F(h, \alpha, \tau)]$$

and so it is possible to plot the observed values of θ against the corresponding values of $\{1 - F(h,\alpha,\tau)\}$. By least squares the best straight line through the observed points can be obtained and this will have a gradient and an intercept from which the virgin strata temperature can be evaluated. This technique, when applied to the results of the last hour of the scale model experiments in Table 1, gave the value of 20·3 °C (68·5 °F) for θ_v compared to the measured value of 20·25 °C (68·45 °F). The technique was adopted with the borehole temperature measurements.

At the depth of 156 m (510 ft) the probe gave a steady temperature of 10·7 °C (51·3 °F) for some 16 hours of observations. As these observations were commenced ten days after the drill rods had been withdrawn the correction to be made to the observed reading was negligibly small (Figure 3) and the value of 10·7 °C (51·3 °F) was accepted for θ_v.

At the depth of 302 m (990 ft) the probe was lowered near to the bottom of the hole ten hours after the drill rods had drilled past this depth. The observed temperature was steady at 13·3 °C (55·9 °F) for 22 hours and the analysis of the observations gave θ_v as 13.3 °C (55·9 °F) there being no correction on this occasion.

When the probe was lowered on a later occasion to 500 m (1 640 ft) the bottom of the hole was smaller in diameter and was passing through grey coal measures. Figure 7, curve (a), gives the observed temperatures for a period of two hours and the correction required to give the V.S.T. of 17·45 °C (63·4 °F). Curve (b) gives corresponding figures for the borehole when at a depth of 786 m (2 580 ft) and $\theta_v = 29{\cdot}05$ °C (84·3 °F) and curve (c) gives $\theta_v = 31{\cdot}6$ °C (88·9 °F) at 878 m (2 880 ft). In these three cases the probe readings were commenced some 11 or 12 hours after the drill rods had drilled past the depths at which observations were made. The hole was just under 12 cm (5 in.) in diameter and the strata were predominantly mudstone with coal layers.

The last opportunity for taking temperatures in the Hopton Pool Borehole occurred when the hole ceased at 1 060 m (3 480 ft). Before the probe could be lowered to the bottom it was necessary for Schlumberger to carry out two traverses

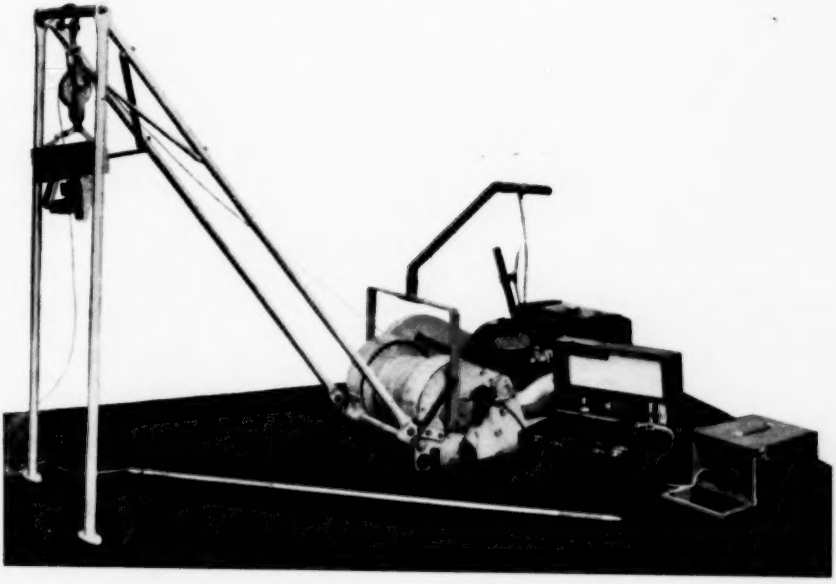

FIG. 6.—Apparatus assembled for use.

[*Facing page* 126

to the bottom of the hole and for this the borehole had to be flushed with freshly made slurry. Unfortunately for the probe measurements the hole was continuously flushed, without drilling, for just over two days prior to the withdrawal of the rods. Some cooling of the strata must therefore have occurred and it was expected that the results would not be so satisfactory on this occasion. Observations were therefore carried out for as long as was possible, some 17 hours, and the maximum observed reading was 37·45 °C (99·4 °F), the rate of increase of temperature at the end of the observations being 0·5 °C (1 °F) in 10 hours. It was

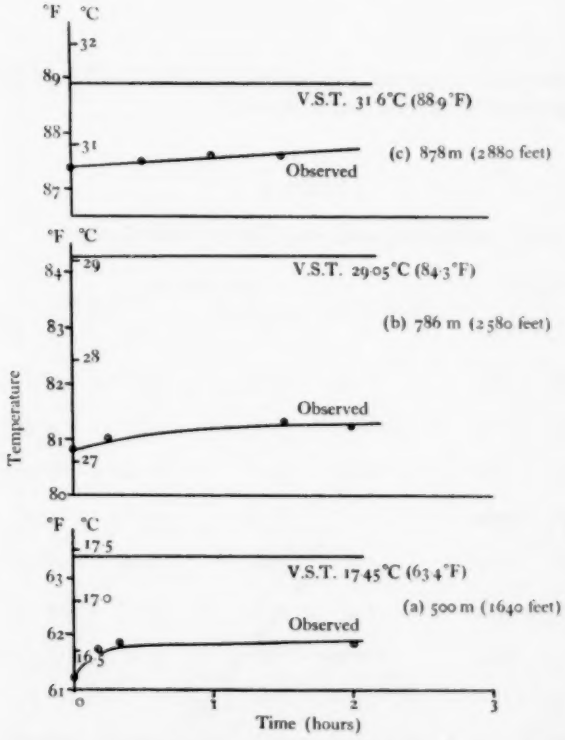

FIG. 7.—Examples of the Hopton Pool Borehole temperatures.

considered that on this occasion the theory could not be applied. It does not give a temperature change of the order observed, which was unusually high, and the preliminary flushing of the borehole should have reduced the heat flow below the theoretical value. It is certain, however, that the maximum observed temperature was below V.S.T. and from previous experience at other depths it is likely that this temperature should be increased by at least 1 °C (2 °F) to give a value of 39 °C (102 °F), which is probably not far removed from the V.S.T. at 1060 m (3480 ft). Such a value fits the general trend of the graph of temperature and depth for the coal measures (Figure 8) which one would not expect to change unless there was a marked change in the strata conductivity.

3.2.3. *An underground measurement of virgin strata temperature at Brereton Colliery*

During the drilling of the Hopton Pool Borehole an opportunity was taken to make one measurement of V.S.T. in the coal face at Brereton Colliery using a different technique to be reported elsewhere (Harris & Jones). Brereton Colliery gives the nearest underground access for comparison with the borehole figures. It lies about 16 km (10 miles) south-east of Stafford and a little more than this distance from the borehole. A V.S.T. of 13.4 °C (56·1 °F) was observed at 317 m (1 040 ft).

4. Discussion of results

The results described above are summarized in Table 2 and Figure 8 shows the V.S.T. plotted graphically against depth of cover.

Table 2

Virgin strata temperature at Hopton Pool Borehole

Depth		Temperature			
		Maximum observed		V.S.T.	
m	ft	°C	°F	°C	°F
156	510	10·7	51·3	10·7	51·3
302	990	13·3	55·9	13·3	55·9
500	1640	16·55	61·8	17·45	63·4
786	2580	27·4	81·3	29·05	84·3
878	2880	30·9	87·6	31·6	88·9
1060	3480	37·45	99·4	39	102
317	1040	Brereton Colliery		13·4	56·1

Also shown on Figure 8, as crosses, are the temperatures observed with the probe at different depths as it was raised from the bottom of Hopton Pool Borehole on the last visit. The probe was rested at each depth for some minutes until its reading was constant. It will be seen from Figure 8 that the temperatures obtained during this vertical traverse through the borehole fluid lie below the V.S.T. line at greater depths and above it towards the surface. One would expect this sort of result for during the long time of drilling a borehole the strata towards the bottom are cooled by the drilling fluid and those at the top are therefore heated, a phenomenon generally appreciated by users of temperature logging equipment when used in seam survey (Leonardon 1936). Such readings are therefore of only small value when accurate V.S.T. is required unless, of course, the hole can be left undisturbed for some time (Bullard 1947), two or three weeks if accuracy within 0·5 °C (1 °F) is required. When times of a few hours only are available in which to determine V.S.T. it is therefore necessary to observe

temperature as quickly as possible very near the bottom of the hole, as described in this paper, repeating the observation as the bottom reaches various depths.

Figure 8 also indicates that the geothermic gradient is not constant and varies, for the Hopton Pool Borehole, from about 50 to 26 m/deg C (90 to 48 ft/deg F) between

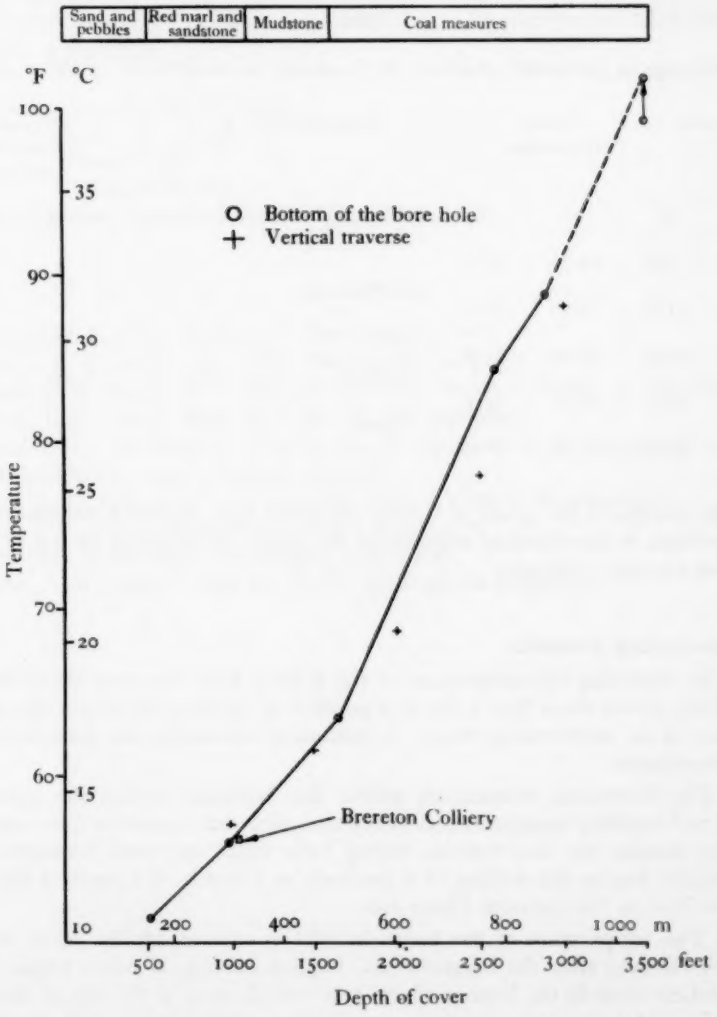

FIG. 8.—Virgin strata temperatures at Hopton Pool Borehole.

the depths of 300 and 1 060 m (1 000 and 3 500 ft). It is of interest to compare this change with the calculated value when the thermal conductivity of the strata changes, the Earth's radial heat flow remaining the same. Table 3 gives the geothermic gradient assuming the Earth's heat flow (Benfield 1939) is 10^{-6} cal $cm^{-2}s^{-1}$ ($3{\cdot}7 \times 10^{-6}$ B.t.u./ft^2 s) and using estimated values of the thermal conductivity of

the strata between the depths tabulated. The conductivities are as realistic as possible, short of actual measurement *in situ*, and are based on a knowledge of the geology of the strata obtained during boring and on laboratory measurements of strata thermal conductivities (Benfield 1939, Godridge 1956, Lomax 1957).

Table 3

Change in geothermic gradient due to change in conductivity of the strata

Depth		Strata temperature		Strata conductivity		Calculated geothermic gradient	
m	ft	°C	°F	cal/cm s deg C	B.t.u./ft hr deg F	m/deg C	ft/deg F
302	990	13·35	56·0				
				0·006	1·45	73	133
351	1150	14·0	57·2				
				0·005	1·21	50	91
473	1550	16·45	61·6				
				0·0033	0·80	33	61
525	1720	18·0	64·4				
				0·003	0·72	30	54
1060	3480	36·05	96·9				

The change in the gradient is very similar to that observed, confirming that the gradient is considerably affected by the lower conductivity of the strata in the coal bearing measures.

5. Concluding remarks

(a) By observing the temperature of the drilling fluid very near the bottom of a borehole for no more than a day it is possible to calculate the virgin strata temperature of the surrounding strata. A method of calculation has been developed for this purpose.

(b) The thermistor temperature probe, the resistance bridge, the motorized winch and ancillary equipment, all newly designed and inexpensive, are satisfactory for making the observations, having been tested on many occasions quite successfully during the drilling of a borehole to a depth of 1060 m (3480 ft) at Hopton Pool in the Cannock Chase area.

(c) The temperature of the borehole fluid at various depths, taken on one day several days after the borehole had finished drilling, is below virgin strata temperature towards the bottom of the hole and above it at the top of the hole. Borehole fluid temperature can become a direct measure of the virgin strata temperature only if the hole has been left standing for some time.

(d) At the Hopton Pool Borehole the virgin strata temperature changed with depth in a manner which was not linear, from 10·5 °C (51 °F) at 156 m (510 ft) to about 39 °C (102 °F) at 1060 m (3480 ft). The geothermic gradient changed from about 55 to 26 m/°C (100 to 48 ft/°F) for the same change in depth, due probably to the reduction in the thermal conductivity of the strata in the lower coal measures.

6. Acknowledgments

The authors wish to thank Mr H. J. Widdowson, General Manager in No. 2 (Cannock Chase) Area of the National Coal Board, and members of his staff for the assistance and facilities so generously provided. The work described in this paper was carried out as part of the research programme of the Scientific Department of the National Coal Board and is published by permission of the Director-General of Research.

Mining Research Establishment,
National Coal Board,
Worton Hall,
Isleworth, Mx.
1959 *January* 20.

References

Blackwell, J. H., 1956. *Canad. J. Phys.*, **34**, 412–417.
Benfield, A. E., 1939. *Proc. Roy. Soc. A*, **173**, 428–450.
Bullard, E. C., 1947. *Mon. Not. R. Astr. Soc. Geophys. Suppl.*, **5**, 127–130.
Bullard, E. C., 1954. *Proc. Roy. Soc. A*, **222**, 408–429.
Bullard, E. C., Maxwell, A. E. & Revelle, R., 1956. *Adv. in Geophys.*, **3**, 153–181.
Godridge, A. M., 1956. *Fuel*, **35**, 379–381.
Harris, A. D. & Jones, C. (To be published in *Colliery Engineering*.)
Jaeger, J. C., 1956. *Australian J. Phys.*, **9**, 167–179.
Leonardon, E. G., 1936. *Geophysics*, **1**, 115–126.
Lomax, E. G., 1957. Thesis for Ph.D., Nottingham University.

Rayleigh-Wave Dissipation Functions in Low-Loss Media

J. Ross Macdonald

(Received 1959 March 3)

Summary

A simple formula is derived relating the specific dissipation factors for Rayleigh, compressional, and shear waves in relatively low-loss materials. Calculations and a table are presented which allow an unknown specific dissipation factor to be obtained directly from the two known factors for the other types of waves. Results apply for any realizable ratio of any two of the three elastic phase velocities.

1. Introduction

The surface Rayleigh waves which travel in a solid half-space in addition to body compressional and shear waves are of particular importance for earthquake detection at large distances, where they predominate over three-dimensional body waves. As Press & Healy (1957) have pointed out, it is of interest to relate the absorption coefficients of Rayleigh waves to those of shear and compressional waves for materials showing energy dissipation and dispersion. These authors have derived a useful expression for this purpose for low-loss media which we shall here simplify, slightly generalize, and reduce to numerical applicability.

It will prove most convenient to deal with the specific dissipation factor, $1/Q$, for each type of wave, where $2\pi/Q$ is the ratio of energy dissipated per stress cycle to the peak energy stored (Knopoff & MacDonald 1958). The quantity $1/Q$ is a useful quantity for comparison with experiment because it is independent of the detailed mechanism of energy dissipation.

2. Dispersion and absorption

Whenever dissipation occurs, the resulting dispersion makes it necessary to distinguish between three kinds of wave velocities: the elastic velocities in the absence of dissipation, the corresponding phase velocities with dissipation, and the complex velocities. Using the subscripts A, B, and C to denote quantities relating to compressional, shear, and Rayleigh waves, the elastic velocities may be obtained from

$$v_A = [(\lambda+2\mu)/\rho]^{\frac{1}{2}}, \tag{1}$$

$$v_B = [\mu/\rho]^{\frac{1}{2}}, \tag{2}$$

$$[2-(v_C/v_B)^2]^4 = 16[1-(v_C/v_A)^2][1-(v_C/v_B)^2], \tag{3}$$

where ρ is the density and λ and μ are Lamé's moduli.

A damped harmonic wave travelling in the x direction involves the factor $\exp[i\omega t - \gamma x]$, where $\gamma \equiv \alpha + i\beta$ and α and β are the attenuation and phase factors respectively of the wave. For a given type of wave, the phase velocity V is given by ω/β while the complex velocity is $V' = \omega/(-i\gamma) \equiv \omega/k$. Further, when dispersion is present, the real equation (3) is replaced by the corresponding equation involving the complex velocities V_i'. Following Press & Healy, this complex equation can be used to determine a relation between $1/Q_A$, $1/Q_B$, and $1/Q_C$ in low-loss materials. It is assumed in the following that these three quantities refer to waves all having the same period.

From their definitions, it can be shown that

$$V_i/V_i' = 1 - i(\alpha_i/\beta_i), \tag{4}$$

$$1/Q_i = 2(\alpha_i/\beta_i)/[1 - (\alpha_i/\beta_i)^2]. \tag{5}$$

Now if the dissipation is relatively low so that $1/Q \leqslant 0{\cdot}1$, (5) can be expanded and simplified to yield, with negligible error,

$$V_i/V_i' \cong 1 - i(1/2Q_i), \tag{6}$$

where terms in $(1/2Q_i)^2$ have been neglected. To the same order of approximation, it can be shown that for either the Voigt dissipation model considered by Press & Healy or for loss arising from creep (Lomnitz 1957) $V_A \cong v_A$ and $V_B \cong v_B$. Taking $V_C \cong v_C$ as well and defining

$$a \equiv (v_C/v_A)^2, \; b \equiv (v_C/v_B)^2, \tag{7}$$

the complex-velocity Rayleigh equation becomes

$$\left[2 - b\left\{\frac{1 - i(1/2Q_B)}{1 - i(1/2Q_C)}\right\}^2\right]^4 = 16\left[1 - b\left\{\frac{1 - i(1/2Q_B)}{1 - i(1/2Q_C)}\right\}^2\right]\left[1 - a\left\{\frac{1 - i(1/2Q_A)}{1 - i(1/2Q_C)}\right\}^2\right]. \tag{8}$$

When (8) is expanded retaining terms up to $1/Q_i$ only, one obtains an equation from the real part identical with (3) and an equation from the imaginary part involving the $1/Q_i$'s. By using (3) to simplify the latter, or by taking imaginary parts of the logarithms of (8), one finally finds

$$\frac{1}{Q_C} = (1 - m)\frac{1}{Q_B} + m\frac{1}{Q_A}, \tag{9}$$

where

$$m = \frac{a(2-b)(1-b)}{a(2-b)(1-b) - b(1-a)(2-3b)}. \tag{10}$$

Although it is obtained more generally, Equation (9) is a simplified but equivalent form of the equation obtained by Press & Healy (1957).

The result (9) is a simple linear equation connecting the $1/Q_i$'s and is valid to high approximation when none of them exceed $0{\cdot}1$. This equation can be used to obtain any unknown $1/Q_i$ given the other two and knowledge of m. It is interesting to note that $1/Q$ is a more sensitive measure of loss than is dispersion of the velocities which, to the present approximation, is negligible.

In order to make (9) useful, the quantity m, which is a complicated function of v_A, v_B, and v_C, has been calculated, using a digital computer, as a function of v_B/v_A and is presented in Table 1 and Figure 1. Table 1 also gives v_C/v_B as a function of v_B/v_A, and the resulting curve is shown in Figure 1 with its ordinate

on the right. Now, if any two of the elastic phase velocities are known, the third can be obtained using the Figure or the Table. Then, after the corresponding value of m is obtained, the unknown $1/Q_i$ can be obtained using (9) and known values of the other $1/Q_i$'s.

Table 1

Numerical results

v_B/v_A	v_C/v_B	m
0	0·95531	0
0·05	0·95516	$3{\cdot}2411 \times 10^{-4}$
0·10	0·95469	$1{\cdot}3233 \times 10^{-3}$
0·15	0·95389	$3{\cdot}0823 \times 10^{-3}$
0·20	0·95271	$5{\cdot}7570 \times 10^{-3}$
0·25	0·95112	$9{\cdot}6002 \times 10^{-3}$
0·30	0·94903	$1{\cdot}5008 \times 10^{-2}$
0·35	0·94633	$2{\cdot}2597 \times 10^{-2}$
0·40	0·94286	$3{\cdot}3347 \times 10^{-2}$
0·45	0·93837	$4{\cdot}8851 \times 10^{-2}$
0·50	0·93253	$7{\cdot}1789 \times 10^{-2}$
0·55	0·92476	0·10685
0·60	0·91419	0·16257
0·65	0·89937	0·25512
0·70	0·87785	0·41586
0·75	0·84549	0·70455

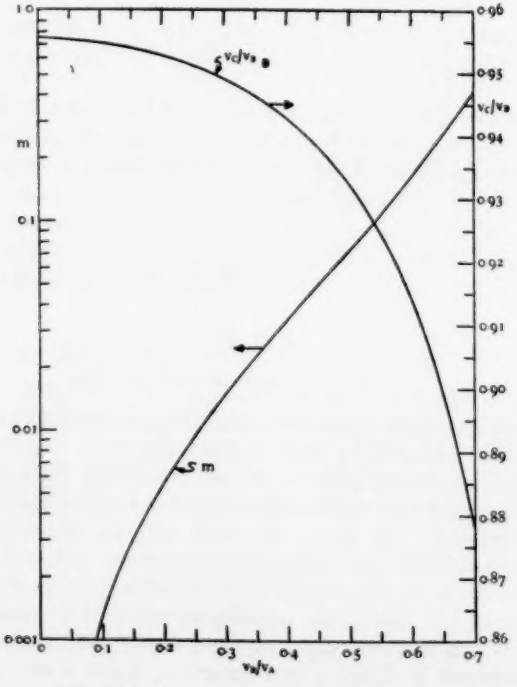

FIG. 1. The quantities m (log scale) and v_C/v_B versus v_B/v_A.

It will be noted that the abscissa extends only from 0 to 0·7. The ratio v_B/v_A may be expressed for isotropic material as

$$(v_B/v_A) = [(1-2\nu)/2(1-\nu)]^{\frac{1}{2}}, \tag{11}$$

where ν is Poisson's ratio. For an incompressible body $\nu = \frac{1}{2}$ and $v_A = \infty$. The minimum value of ν is zero; thus the maximum value of v_B/v_A is $2^{-\frac{1}{2}}$. The quantity m increases continuously beyond this physical limit, however, and reaches 9·1 for $v_B/v_A = 0{\cdot}95$ and infinity for $v_B/v_A = 1$.

When one or more of the $1/Q_i$'s are appreciably greater than 0·1, the exact complex equivalent of (3) must be solved using (4) and (5) in their exact forms. Solution of the resulting cubic equation with complex coefficients will be difficult but is usually unnecessary since the condition $1/Q_i \leqslant 0{\cdot}1$ is usually well met in most situations of physical interest.

Finally, it should be pointed out that for $v_B/v_A \geqslant 0{\cdot}567008$ there are three real roots of (3) rather than the single one which appears for smaller v_B/v_A. As Jeffreys (1952) has shown, however, it is only the smallest of the three roots which is of physical significance for Rayleigh wave transmission.

3. Acknowledgment

I wish to thank Dr. C. Lomnitz for drawing this problem to my attention and for helpful discussions.

Texas Instruments Incorporated,
6000 *Lemmon Avenue*,
Dallas 9,
Texas, U.S.A.:

1959 *February* 25.

References

Jeffreys, H., 1952. *The Earth*, third edition, pp. 35–36 (Cambridge: University Press).
Knopoff, L. & MacDonald, G. J. F., 1958. *Rev. Mod. Phys.*, **30**, 1178.
Lomnitz, C., 1957. *J. Appl. Phys.*, **28**, 201.
Press, F. & Healy, J., 1957. *J. Appl. Phys.*, **28**, 1323.

Research Note

An Earth Model and the Reduction of Gravity Observations for use in Stokes's integral

J. C. Bhattacharji

(Received 1959 February 23)

Summary

Application of Dr Hunter's Earth model in the reduction of gravity observations for use in the Stokes integral is discussed. An attempt is made to make it clear that there are practical difficulties in utilizing the new surface anomaly designated by Dr Hunter as $g-\gamma_E$, in the Stokes integral, for the purpose of determining ultimately the figure of the Earth.

Dr Hunter derives his Earth model from the actual Earth by smoothing its topography without change of total mass. What is actually required is to compute the weighted average values H of the actual heights h of the land topography (or $-0{\cdot}615$ times the depths of the ocean bed) for a sufficient number of control points, each average height being over a region of 150 km radius. These computed values enable us to draw the contours of average height, which actually define the Earth model. It is thus "bounded by a surface of gentle and slowly varying slopes" never exceeding 1/100 even in the worst cases of rugged topography, which have but negligible effects on gravity. It is, therefore, considered advantageous to reduce an observed gravity value to the surface of the Earth model, that is, to a point having its height equal to the weighted average height over a region of 150 km radius, by means of the usual Bouguer reduction and then to compare it against the theoretical value of gravity reduced to the same height by the free-air method in order to obtain the gravity anomaly designated by Dr Hunter as $g-\gamma_E$. The disturbing effect of the more irregular part of the Earth's actual topography, having been removed as above, the surface anomaly $g-\gamma_E$ becomes necessarily more regular than either $g-\gamma_A$ or $g-\gamma_B$ and, therefore, as representative of the unseen anomalies of masses as any other isostatic anomaly derived by heavy reductions. Moreover, the surface of the Earth model being very smooth compared with that of the real Earth, the gravity values once reduced to the spherical surface of the layer of thickness H, limited only to 150 km radius, do not require appreciable corrections to be applied for any departure of this spherical surface from the actual surface of the Earth model, while by reducing them to the smoothed surface of the latter the anomaly $g-\gamma_E$ becomes comparable with similar anomalies anywhere in the world without requiring any assumptions of internal densities of the Earth. This is surely a great advantage. So far there is no difficulty.

But things are entirely different with the geoid. The geoid is affected significantly by the superficial transfers of masses within and beyond the limit of 150 km radius, and is, therefore, not a level surface of the Earth model. "Corresponding to the Earth model will be a co-geoid—a level surface of the same potential as that of the geoid." Now according to the Helmert's second method of condensation, all matter external to the co-geoid can be condensed into a surface lying in the same co-geoid by reducing the gravity value on the surface of the Earth model by the free-air method using the normal rate of change of gravity with height above the co-geoid, along with the Geländereduktion added to it, which in the case of the Earth model is apt to be inappreciable. The vertical separation between the actual co-geoid and the ideal co-geoid after condensation is also negligible. So after the transfer of the external matter, either co-geoid encloses the attracting matter of the Earth model, thereby reducing the co-geoid to a bounding equipotential surface, and the corresponding gravity anomaly on being reduced to the same surface, may be used correctly in Stokes's integral to give the height of the co-geoid above the reference spheroid. It is thus essential to compute the vertical separation between the geoid and the co-geoid (or the consequent indirect effect of gravity) which is required for reducing not only the gravity anomalies to the co-geoid after condensation, but also the height of the co-geoid derived directly from Stokes's integral to the required height of the geoid above the reference spheroid, by considering only the topographical effect due to the superficial transfers of masses. Now the mass-transfers for the Earth model being only superficial, visible features having been removed to fill visible hollows, the shift of the centre of mass and of the rotation axis are likely to be negligible but the deformation of the geoid, on the other hand, is quite significant and what is still worse, the actual computation of the corresponding vertical separation between the geoid and the co-geoid due only to the topographical effect of the mass-transfers, is very much complicated in the absence of considerations of the effect of isostatic compensation, which in fact considerably reduces the large topographic effect increasing normally with distance. It is also quite clear, from Lambert and Darling's tables for computing the deformation of the geoid on the Hayford system based on the hypothesis of complete isostatic compensation, that the resultant geoidal effect of distant masses or of their displacements is an easily computable small quantity inappreciably affected by any possible error of estimation of distant topography or of their displacements and is therefore obtainable with sufficient accuracy, though the effects of topography and compensation considered separately are large quantities significantly and almost equally affected by a slight change in position or amount of distant masses and are, as such, bound to be extremely inaccurate, even if computed with all necessary care and with difficulties involved in such reductions. This is surely an unfortunate position but cannot be avoided if our object is to utilize Dr Hunter's surface anomalies in determining ultimately the height of the geoid above the reference spheroid. This will be made more clear from the following example of the topographic and the isostatic reductions of the deformation of the geoid for a Himalayan station about 8·5 km in height, on the basis of the hypothesis of complete compensation at a depth of 113·7 km.

In this example the mean heights of zones refer to the estimated mean heights of Hayford zones in the actual Earth. These are likely to differ from the corresponding values on the Earth model, the discrepancies becoming more predominent in regions of rugged topography but decreasing slowly with distance.

Example

Computation of the deformation of the geoid on Hayford system

Hayford Zone	Mean height of zone in km	Topographic effect in cm	Compensation effect in cm	Resultant effect in cm
A–G	7·00	94	−17	77
H	6·60	82	−17	65
I	6·00	165	−41	124
J	5·80	227	−68	159
K	6·02	408	−153	255
L	5·70	619	−294	325
M	4·35	1466	−920	546
N	3·73	1700	−1340	360
O	3·20	2464	−2205	259
18	2·86	677	−634	43
17	2·79	802	−762	40
16	2·76	988	−950	38
15	2·69	1240	−1204	36
14	2·64	1633	−1601	32
13	2·54	4079	−4036	43
12	2·44	4494	−4467	27
11	2·32	6113	−6112	1
10	0·450 3·036	6317	−6329	−12
9	−0·075 2·229	4691	−4703	−12
8	−1·012 1·769	4727	−4700	27
7	−1·812 0·915	−741	746	5
6	−2·452 0·487	−5770	5797	27
5	−3·475 0·240	−16811	16885	74
4	−3·571 −0·153	−26282	26382	100
3	−4·019 −1·257	−48996	49196	200
2	−2·726	−41406	41583	177
1	−2·807	−8005	8043	38
A–1		−105030	108080	3050

To take account of the topographic effect of such discrepancies is again not only difficult but also practically unobtainable with the desired accuracy even after heavy reductions.

Thus it would seem clear that the promise held by this new surface anomaly $g-\gamma_E$ in the field of geodesy has got its limitations and as such may not lead us far in the realization of our objective of determining the figure of the Earth.

10 *Raipun Road,*
Dehra Dun (*U.P.*),
India.
1959 *February* 18.

References

Graaff-Hunter, J. de, 1958. Discours Presidential, Tactics of Progressive Geodesy, *Bulletin Géodésique*, **47**, 28–36.

Lambert, W. D., 1930. The reduction of observed values of gravity to sea level, *Bulletin Géodésique*, **26**, 107–175.

Lambert, W. D. & Darling, F. W., 1936. Tables for determining the form of the geoid and its indirect effect on gravity, U.S. Coast and Geodetic Survey, Special Publication No. 199.

Letter to the Editors

Magnetic "Cleaning"

E. Irving

On the basis of demagnetization experiments with 14 specimens from one rock formation in southern France, As & Zidjerveld (1958) conclude (p. 318) that "from these demagnetization experiments it follows that the pole determinations that are based on measurements of remanent magnetization in rock from which the disturbing magnetization of the present Earth's field has not been removed should be treated with reserve."

Now the mean direction ($D = 216$, $I = -24$) of the specimens studied by As and Zidjerveld after removal of the secondary component (that produced by the present Earth's field) is in broad agreement with those published earlier by Roche (1957) who gives $D = 210$, $I = -16$ as the mean of five pyromeride specimens and $D = 185$, $I = -13$ for three dolerite specimens collected from the same rock formation. No reference is made to this earlier work. Moreover the pole position they give (47 N 144 E) agrees very well with that obtained from work on other Permian formations of Europe without magnetic "cleaning": Exeter traps 43 N 164 E (Creer 1955); Montcenis sandstone 38 N 162 E, St. Wendel sandstone 45 N 175 W, Nideck rhyolites 43 N 168 E (Nairn 1957); Oslo porphyries 46 N 165 E, (Rutten & others 1957); Lavas 36 N 175 E, sediments 37 N 163 E and intrusives 32 N 174 E of Ayrshire (Du Bois 1957, Armstrong 1957); Upper Permian of N.W. Russia 45 N 178 E (Khramov 1958). The agreement is very good when it is remembered that each pole determination is subject to errors of the order of 10°, and that each of the formations is not exactly contemporaneous and so small polar movements between the times represented by each are not excluded. These new results given by As and Zidjerveld do not cast suspicion on what has been done previously; on the contrary, they confirm it. In fact this agreement between many determinations from Permian rocks in Europe would seem to be a most convincing confirmation of procedures in palaeomagnetism.

The techniques of magnetic "cleaning" of rocks are providing the means of dissecting out the unwanted secondary components which often mask the primary components in the natural state. Up till now only a few per cent of rocks have been of use, but now our range of vision may be increased many times. The mood is one of optimism for the future, not reserve about the past.

Dept. of Geophysics,
Australian National University,
Canberra, Australia.
1959 *April* 3.

References

Armstrong, D., 1957. *Nature*, **180**, 1277.
As, J. A. & Zijderveld, J. D. A., 1958. *Geophys. J.*, **1**, 308.

Creer, K. M., 1955. Thesis, Cambridge.
Du Bois, P. M., 1957. *Adv. in Phys.*, **6**, 177.
Nairn, A. E. M., 1957. *Bull. Soc. Geol. France*, **7**, 721.
Khramov, A. M., 1958. *Palaeomagnetism and Stratigraphic correlation*, 187.
Roche, A., 1957. *C.R. Acad. Sci. Paris*, **244**, 2952.
Rutten, M. G., Everdingen, R. O. & Zijderveld, J. D. A., 1957. *Geol. Mijnbouw*, **19**, 193.

Note on Progress in Geophysics

Dynamic Processes of Abyssal Sedimentation: Erosion, Transportation, and Redeposition on the Deep-sea floor

Bruce C. Heezen

Summary

The concept of a quiet, nearly motionless, and certainly currentless deep-sea floor lacking the processes of erosion so prevalent in shallower seas was well ingrained in scientific thought until discoveries of the past decade revised this serene and static picture. The new concept is a more dynamic one in which submarine landslides, raging turbidity currents, internal tides, deep-sea current scour, and submarine post-depositional solution and alteration play a part in shaping the sea floor, in disturbing and nurturing its fauna and which produce sedimentary structures and distributions formerly thought to be the exclusive mark of shallow water deposits. The concepts involved are still in a critical state of flux with many conflicting viewpoints as to the processes involved and their relative importance. The development of the major concepts is traced and the principal variant viewpoints are briefly reviewed.

Part 1. Early ideas

The Naked Abyss. "The geological clock may strike new periods; its hands may point to era after era; but, so long as the ocean remains in its basin—so long as its bottom is covered with blue water—so long must the deep furrows and strong contrasts in the solid crust below stand out bold, ragged, and grand. Nothing can fill up the hollows there; no agent now at work, that we know of, can descend into its depths, and level off the floors of the sea." (Maury 1855.)

Thus M. F. Maury eloquently summed up the view generally held a century ago. Remembering the then newly discovered deep-sea oozes he added:

"But it now seems that we forgot the oceans of animalculae . . . whose remains in vast multitudes sink down and settle upon the bottom."

The Unremitting Snowfall. The concept of the great unremitting snowfall which modified and then replaced the original picture of a naked abyss was stated clearly by Rachel Carson:

"When I think of the floor of the deep sea, the single overwhelming fact that possesses my imagination is the accumulation of sediments. I see the steady, unremitting, downward drift of material from above, flake upon flake, layer upon layer—a drift that has continued for hundreds of millions of years, that will go on as long as there are seas and continents."

Large elements of truth are found in both of these seemingly contradictory concepts which is why both have so long endured. To be sure, sedimentation is so slow over vast areas of the ocean floor that the original "grand and imposing" relief mentioned by Maury is, over broad areas of the sea floor, still to be observed only slightly modified by subsequent deposition (Heezen, Tharp & Ewing 1959). Furthermore, the success which students of sediments have had in reading that "epic poem of earth history" contained in the successive layers of sediment further attests to the general validity of the concept of the unremitting snowfall (Phleger 1952, Ericson *et al.*, in press, Broecker, Turekian & Heezen 1958). However, neither of these concepts tells the complete story; nature is considerably more complex than either model.

A Revolutionary Discovery. John Murray announced in an obscure footnote added to a discussion on deep-sea sediments published in 1912 that:

"From his examination of the samples collected on board the *Gauss*, Philippi believed that stratification on the sea floor of today is not the exception but the rule."

This revolutionary discovery led to hypotheses of uplifted and deeply downfaulted, mobile blocks to account for each successive thin stratification. The most perplexing of the stratifications were those which involved an alternation of deep-sea ooze or clay on one hand, with sand and silt of a type previously found only near the shore. As long as only a few such deposits were known (Andree 1920), the problem was not faced straightforwardly, but when, after World War II, dozens upon dozens of examples were brought up in deep-sea piston cores, the problem reached tremendous proportions.

The Atlantic Cable. Maury (1855) discussing the practicability of the proposed telegraph cables wrote with confidence:

"It is an established fact that there is no running water at the bottom of the deep sea. The agents which disturb the equilibrium of the sea, giving violence to its waves and force to its currents, all reside near or above its surface; none of them have their home in its depths." And, therefore, he concluded that if a deep-sea cable were laid it "would lie in cold obstruction, without anything to fret, chafe, or wear, save alone the tooth of time". That this clear statement also contains a large element of truth is shown by the great success of the telegraph cables which have broken infrequently under blue water. However, not long after the first cable was laid, the rude fact that this picture did not tell the whole story became very apparent.

A Rude Awakening. In an early report Benest (1899) wrote:

"Unmistakable evidence, offered in some cable repairs in recent years, has disclosed novel causes of rupture, and has extended our knowledge of the hidden dangers that beset the telegraph wire after it has been assigned to its oozy bed."

Early investigations of the distribution of earthquake epicentres were made with the practical aim of avoiding earthquake belts in laying out future cable routes, for it was early shown that earthquakes and cable breakage were closely related. In his classic paper on "Suboceanic Change" Milne (1897) documented

many cases where a positive relationship was proved. Benest, writing at about the same time, noted the seasonal breakage of cables along certain continental slopes, and thus did not strongly favour the seismic cause of cable interruption. He noticed that many earthquakes failed to produce cable failures; this, together with the seasonal occurrence of breaks led him to suspect a connection with the seasonal floods of nearby streams. His appeal to submarine underground river outlets, a misguided effort, was revived more recently by Douglas Johnson (1939).

The mode of emplacement of deep-sea sands and the cause of deep-sea cable breakage remained independent problems for nearly three-quarters of a century. It has been only in recent time that these two phenomena were related to a common cause.

Part 2. Turbidity currents

The Unifying Concept. Turbidity currents, the concept which provided a unified explanation for these previously unrelated problems was not a brand new theory; but, like so many other concepts in science, it was resurrected after being ignored or rejected for over fifty years. Interest in turbidity currents originally stemmed, not from their relationship to the origin of deep-sea sands, nor from their responsibility for the breakage of cables, but from the explanation of another related mar on the picture of a motionless pristine abyss.

The discovery of submarine canyons had been made originally by wire soundings; but these giant gorges carved into the submerged flanks of the continental blocks became a real enigma when, as the result of careful surveys made with the then newly-developed echo-sounder, it became clear that canyons could be found in large numbers wherever surveys were made on the continental margins. As an explanation, the first and most popular theory involved the drowning of subaerially eroded valleys (Spencer 1903, Shepard 1948). However, this concept rapidly lost favour when it was demonstrated that submarine canyons reached the very bottom of the ocean basins instead of being limited to the upper parts of the continental slope. R. A. Daly (1936) resurrected the original concept of F. A. Forel who had proposed in 1885 that the sublacustrine canyon of the Rhône was cut by currents of sediment-laden water flowing in along the floor of Lake Leman (Lake of Geneva). Inspired by Daly's eloquent appeal Kuenen (1937) and Bell (1942) successfully produced turbidity currents in tanks. Grover & Howard (1938) actually observed weak turbidity flows in Lake Meade Reservoir (Gould 1951).

Muddy Water. Turbidity currents produced by the early experiments flowed at relatively slow speeds, did not erode, and were, in fact, little more than halting underflows of muddy water (Kuenen 1937). Stetson & Smith (1937) believed that the density contrast between turbidity currents and the superadjacent water was so small that a marine turbidity flow could leave the bottom and flow as a turbid interflow when it reached a depth where the density of the water exceeded that of the turbidity current. In later experiments the use of higher density mixtures yielded greater velocities (Kuenen 1950). Although high density turbidity currents had been effectively demonstrated in Kuenen's experiments, scepticism and lack of confidence in the scale factors prevented a general acceptance of the process when projected to full scale. The concept of low-density turbidity currents which leave the bottom to form interflows was also adopted by Menard & Ludwick (1951).

Although they concluded that submarine landslides "are the only likely sources of dense turbidity currents thus far suggested" they had serious reservations, and felt that such turbidity currents resulting from slides "may be tenuous rather than dense". They also concluded that "turbidity currents resulting from suspended sediment in rivers must be rare". Concerning the generation of turbidity currents along the shore they concluded:

"If they exist, marine turbidity currents produced by wave agitations, or any other stirring agent, probably do not have high effective density." . . .

"No means exist for holding the current in place until the suspended sediment becomes very concentrated; therefore, it is unlikely that very dense turbidity currents can be generated even by violent wave and current agitation." . . .

". . . turbidity currents may flow on the ocean surface or within the ocean due to marine density stratification. . . . Surface flows and interflows may be important geologically because they can spread sediment over wide areas."

For this reason they conclude that "marine turbidity current deposits may be difficult to identify".

The concept thus projected was not appealing and most oceanographers and geologists still favoured the picture so eloquently phrased by Maury (1855).

The case for modern high density, high velocity turbidity currents was finally proved by a study involving the explanation of both the breakage of submarine cables and the origin of deep-sea sands.

Full-scale Experiment. In 1952 Heezen and Ewing concluded that the:

". . . events associated with the Grand Banks earthquake of 1929 November 18 may be considered as a full-scale experiment in erosion, transportation, and deposition of marine sediments by a turbidity current in which the submarine telegraph cables served to measure its progress and to give tangible evidence of its force".

Following this earthquake which shook the continental slope south of Newfoundland, all the submarine telegraph cables lying downslope (south) of the epicentral area were broken in sequence from north to south. According to Heezen and Ewing's explanation each successive cable was broken by a turbidity current which had originated as a series of slumps in the epicentral area. The current travelled down and across the continental slope, continental rise, and ocean basin floor and continuing far out onto the abyssal plain, reached a limit well over 450 miles from its source area on the continental slope.

On the continental slope where the bottom gradient is 1:10 to 1:30 the velocity of the current exceeded 50 knots; and out on the abyssal plain where the gradient is less than 1:1500 its velocity, although diminished, still exceeded 12 knots. Subsequent exploration of the area with the piston corer revealed a one-metre thick, uppermost bed of graded silt containing shallow-water microfossils (Heezen, Ericson & Ewing 1954) overlaying abyssal lutite. The thickness of the bed was nearly identical with that calculated by Kuenen (1952) on the basis of the slopes and observed velocities.

This bold challenge to the concept of the motionless, pristine abyss was immediately attacked. Shepard (1954) based his objections largely on the claim that the velocities of 10–50 knots were larger than could be expected, but offered no more serious objections. Kullenberg (1954) misled by some erroneous soundings

claimed that Heezen and Ewing's explanation required the turbidity current to run uphill and over a range of hills, an ability which, he correctly pointed out, could not be attributed to turbidity currents. However, subsequent exploration confirmed Heezen and Ewing's belief that the alleged mountain range was the result of poor contouring of bad soundings. In fact, a survey by Heezen, Ewing & Ericson (1954) revealed nothing but a smooth abyssal plain in the indicated position of Kullenberg's mountains.

One of the strongest critics of the turbidity current concept is Professor Hans Pettersson (1954), the well-known leader of the *Albatross* Expedition. To explain the occurrence on the equatorial Atlantic abyssal plains of graded, deep-sea sands which contained "twigs, nuts, and the bark of dicotyledonous trees" he offered the following alternate to turbidity current deposition:

"In the event that a large island, harbouring vegetation, and with a fairly extensive shelf covered the Mid-Atlantic Ridge northwest of St. Paul's Rocks and became submerged during a catastrophe of seismic-volcanic character a few hundred thousand years ago, material like that found in the *Albatross* cores might have become distributed over the adjacent sea bottom."

Abyssal Plains. Following World War II continuously recording echo-sounders were first extensively used in deep water. One of the first discoveries was that, while most of the deep-sea floor is covered by hills and mountains, large areas in the deepest portions of the ocean are covered by abyssal plains (Heezen, Ewing & Ericson 1954). The origin of these vast flat areas posed a real problem until the concept that turbidity currents were filling the oceanic depressions offered a ready solution (Heezen, Ewing & Ericson 1951). Pettersson and some of his followers including Koczy remained unconvinced, and to this day prefer to explain the abyssal plains as the result of great outpourings of lava (Koczy & Burri 1958).

During the exploration of the abyssal plains, long narrow steep-sided channels were discovered which cut into the abyssal plains. These features, called mid-ocean canyons (Ewing & others 1953), or deep-sea channels (Dietz 1953, Menard 1955) were indeed an enigma to those who believed that the plains are the result of the outpourings of lava. Koczy & Burri (1958), in an attempt to explain the occurrence of features normally ascribed to erosion and deposition in an area where these authors deny the existence of such processes, offered the suggestion that mid-ocean canyons were, in fact, fault-bounded rift valleys, and that their natural levees were instead the sides of tilted fault blocks. This explanation says nothing of the graded sand beds found in the canyon floor, the graded silt beds found on the levees, nor of any of the other streamlike characteristics of the Northwest Atlantic Mid-Ocean Canyon (Ewing & others 1953). Recent magnetic profiles across this Mid-Ocean Canyon failed to reveal an anomaly, a fact which can be added to the list of objections to Koczy and Burri's theory.

Submarine Natural Levees. Submarine natural levees have been observed along the continental slope canyons of southern California (Buffington 1952), as well as along the mid-ocean canyons of the Atlantic (Ewing & others 1953), the Indian Ocean (Dietz 1953), and the deep Pacific (Menard 1955). The largest deep-sea natural levees observed to date are those of the Congo Submarine Canyon (Heezen & others 1957) which in a depth of 2 250 fathoms are 100 fathoms high and over 20 miles wide. It is safe to conclude that the submarine natural levees are of nearly the same origin as the subaerial ones. When turbidity currents overflow

the tops of the canyon walls they suddenly deposit a considerable portion of their load as they abruptly slow down and disperse.

Since the natural levees of the Northwest Atlantic Mid-Ocean Canyon are nearly identical in form with those bounding the deeper parts of the Congo Submarine Canyon, it seems unlikely that they are the result of a radically different process as proposed by Koczy & Burri (1958).

Deep-sea Sands. Ericson, Ewing & Heezen (1952) presented a preliminary account of their study of turbidity-current sediments deposited in the abyssal plains of the North Atlantic. Some of the most dramatic evidence came from two cores taken from the narrow trench abyssal plain which lies at about 4 580 fathoms at the bottom of the Puerto Rico Trench. These cores consisted of abyssal red clay at their base; but each contained a graded bed of calcareous sand, silt and clay which included fragments of the algae *Halimeda*. Since living *Halimeda* requires sunlight this detritus must have originated near the shore.

Over 200 cores have been obtained from the abyssal plains of the North Atlantic. Each core taken in an abyssal plain contained either sands or silts, many with shallow water Foraminifera. Most cores from the flanks of the Mid-Atlantic Ridge, the abyssal hills and the oceanic rises contained only pelagic deposits, although a few at the bases of islands or from the crest zone of the ridge contained coarser material (Ericson & others, in press, Heezen, Tharp & Ewing 1959).

Incredible Coincidence. After the initial shock wore off, a general acceptance of deep-sea turbidity currents as an important process was found in most quarters. Pettersson (1954) admits the possibility of their existence but concludes that:

"The present evidence hardly affords clear proof that turbidity currents have played any dominant part in sculpturing the ocean floor. Both their extension over the deep ocean basin and their velocities of steep slopes appear to have been over-estimated by Heezen and Ewing."

Shepard (1955) now feels that turbidity currents transport sediments, but denies that they have the ability to erode. Unable to accept the high velocities indicated by the Grand Banks sequence of cable brakes, Shepard (1954) suggested that an unrelated series of local and independent submarine landslides had broken the cables. He wrote:

"Is it not possible that slides developed more slowly on the gentle outer slopes and built up pressure gradually against the cables until they broke?" ". . . otherwise the sequence could be explained as at least in part a *coincidence* and in part due to the slower development of slides at an increasing distance from the epicentre."

Jones (1954) also believed the breaks were:

". . . much more likely to have been caused by slumping than by the thin stream of material carried in a turbidity current (flowing at) an *incredible* velocity".

Spontaneous Liquefaction. Encouraged by the objections to the turbidity current hypothesis raised by Shepard and others, but not satisfied with their alternate explanations, Terzaghi (1957) offered a new explanation for the cable breakage which followed the 1929 Grand Banks Earthquake. He supposed that the sediment in the epicentral area and over the whole area of cable breakage to the south

existed in a metastable state. He supposed that the earthquake shock caused spontaneous liquefaction over the epicentral area and that the apparent velocity of the turbidity current was instead:

"... the velocity of the advance of the boundary of the liquefied portion of the sediments underlying the ocean floor and not the velocity at which the slide material moved over the floor".

The only fact he attempts to explain is the velocity indicated by the sequence of cable breaks. He is neither concerned with the problem of how the sediment came to be in the supposed metastable state, nor why the sequence of breaks was downslope and not in all directions from the epicentre. Neither is he concerned with the emplacement of the shallow water sediments in deep water nor the grading of the deposited beds. It is not readily apparent why the passage of such a wave of liquefaction should break submarine cables with at least 10 per cent slack. One might think that the cable would be required to sink thousands of feet into the sediment before breakage would occur. Although it cannot be denied that the mechanism he suggests may locally affect sediments, the weight of evidence seems to definitely point away from Terzaghi's theory of propagation of spontaneous liquefaction as an explanation of the Grand Banks cable breaks.

Undetected Earthquakes. A series of cable failures on the floor of the western Mediterranean essentially similar in distribution and order to the Grand Banks sequence followed the 1954 Orleansville earthquake (Heezen & Ewing 1955). These events further supported the interpretation of the Grand Banks turbidity current and provided additional evidence of the mode of emplacement of the Mediterranean deep-sea sands which Bourcart (1953) had previously interpreted as turbidity-current deposits.

Bourcart & Glangeaud (1956, 1958), however, objected to the interpretation claiming that turbidity currents had broken only the cables on the steep slopes. To explain the later breaks out on the nearly level ocean floor they suggested that undetected or at least unlocated aftershocks had caused the breaks. Apparently impressed by Kullenberg's objections to the computed velocities for the Grand Banks turbidity current, they sought an alternative interpretation not requiring such high velocities. Also misled by bad soundings, they denied the existence of an abyssal plain in the area. Precision soundings, however, have confirmed the existence of the Balearic Abyssal Plain.

The Big Creep. Lombard (1956), referring to the transportation of ancient sediments, and Koczy & Burri (1958), referring to the present deep-sea environment, favour as an alternative to turbidity currents, a slow creep which might require hundreds or thousands of years to traverse a distance that a turbidity current would cross in only a few hours. That slumps, slides and other slower and more massive slope failures occur in the ocean is clear from the evidence of topography, of sediments and of sedimentary structures. But the results of such slow movements are quite different from the graded, well-sorted deposits laid down by turbidity currents travelling at express train speeds over the ocean floor. Koczy (1954) notes that:

"Near the shelf the surface is often undulating because of the presence of the sediment sliding down the continental slope. This movement can be assumed to be very slow."

This slow creep, although certainly of importance over wide areas, cannot be considered as a substitute for turbidity currents, but rather as an additional and independent process (Kuenen 1956).

"*Elevator Tectonics.*" A concept which might be described by the term "elevator tectonics" (or perhaps "lift faulting") has been often employed in the explanation of stratified deep-sea deposits (Cushman 1941, Landes 1952). The latest proponents of this concept are Greenman & Le Blanc (1956) who invoke a 10 000 foot subsidence of the entire central portion of the Gulf of Mexico at the close of the Wisconsin (11 000 years ago) to account for the emplacement of grey silts now found on the floor of the Sigsbee Abyssal Plain. These grey silts have been explained by Ewing, Ericson & Heezen (1958) as the results of turbidity-current deposition of sediment contributed by the Pleistocene Mississippi River. Cores from low knolls rising above the abyssal plain contained only slow, uniformly deposited pelagic sediments. According to Greenman and LeBlanc's explanation, the knoll core stations would have stood more than 150 metres above sea-level until commencement of Recent time. Radiocarbon measurements on the pelagic deposits from the knolls indicated post-glacial rates of deposition of 3 cm per 1 000 years, while the Pleistocene rate in the same cores ranged from 10 to 20 cm per 1 000 years. In contrast, the sediments cored from the abyssal plain showed post-glacial rates of 10 cm per 1 000 years and glacial rates of 60 cm per 1 000 years.

Archipelagic Aprons. Broad, smooth, deep-sea aprons encircle many oceanic islands. Ericson, Ewing & Heezen (1952) reported graded beds of coarse, shallow water detritus from the Bermuda Apron. More recently, Menard (1956) referring to similar features observed in the southwest Pacific, coined the term "*archipelagic apron*". He reasons that while turbidity currents may have smoothed their surface, the aprons owe their existence to extensive outpourings of lava. Since their volume exceeds that of the pedestal they surround, he reasons that turbidity current deposition cannot account for their entire volume and consequently that a gentle rise toward the island pedestals must have existed before the smoothing process started. Such features lacking a smooth surface can be detected near some islands and seamounts but they are excluded by their roughness from the definition of archipelagic aprons.

Tsunami. Bucher (1940) formerly thought that tsunami waves set up by the Grand Banks Earthquake had caused the later sequence of cable breaks. Indeed there seems to be a relationship between tsunami and cable breaks; however, they are probably not cause and effect but both result form the motion of the slump and ensuing turbidity current. Heezen & Ewing (1952) concur with Gutenberg's (1939) view that "principal cause of each tsunami is submarine slumping." However, the turbidity currents themselves probably are also capable of generating tsunami. That tsunami could not be the direct result of earthquakes was proved by the fact that not all large submarine earthquakes produce tsunami. In order to prove that turbidity currents and slumps alone could produce a tsunami, we clearly need to find a tsunami and a related series of cable failures not preceded by an earthquake; or to disprove the concept, to discover a turbidity current lacking an associated tsunami.

Hydrodynamic Considerations. There was considerable feeling that the velocity and extent of the Grand Banks turbidity current were over-estimated. Robert

Stoneley (1957) investigating the problem from the viewpoint of hydrodynamics concluded that "the hypothesis would be much more workable if the current had a thickness of only a few metres rather than over 100 metres suggested by Kuenen's calculations". He found that the question of

"... whether the motion of the current will persist over distances of the order of 1 000 km without being damped out by viscous forces ... hinges on the viscous drag of the stream at high Reynolds numbers. Theoretical and experimental work on arrested saline wedges suggests a much lower drag coefficient than is appropriate for slower speeds, and the extrapolation to high Reynolds numbers again suggests a thinner turbidity current of vertical thickness about 5 metres".

The thickness resulting from Kuenen's (1952) calculations had also seemed excessive from a geological point of view since turbidity-current deposits were not found on slight elevations above turbidity-current blanketed abyssal plains.

Staublawinen. Careful study of snowslides may provide instructive analogies for the understanding of the behaviour of slumps and turbidity currents. Roher (1954) who fired small charges in the air a half-metre above the snow surface, triggered snowslides in a small Alpine valley (Grat des Sazmartinhorns). He cast lines of coloured dye on the snow and by observing with both pressure gauges set in the snow and coloured motion picture photography, was able to differentiate between turbulent and laminar slides. He found that in laminar slides the velocity did not exceed 32 km/hr. The sides of a laminar slide were sharp; and when it stopped, the slide left a cone of sediment on the valley floor. Under certain snow conditions the laminar flows, after moving about 100 metres, would undergo a quick transition (usually during less than 30 metres of movement) and flow in a turbulent manner. In the same valley where laminar flows travelled at 32 km/hr, turbulent flows of 114 km/hr were observed. The velocity of turbulent flows timed in a variety of locations ranged from 85 km/hr to 305 km/hr. The deposits of dyed turbulent flows were spread out evenly on the valley floor with the dye evenly mixed through the deposit. The transition along the sides of turbulent flows was a gradual one. In one case the suction produced in the air by the passing of a fast moving flow pulled men from one side into the slide. In Staublawinen the snow mixes with air, while in turbidity current sediments mix with water; and although the two may not be directly analogous, their comparison may help in the better understanding of high velocity turbidity currents.

Requirements of Turbidity Currents. Turbidity currents first of all require sediment, just as rivers require water, without it they do not exist. Turbidity currents require a trigger mechanism; this can be supplied by earthquakes, hurricanes impinging on the shore, high bedload discharge of rivers; and lacking a trigger mechanism, turbidity currents probably can occur after long continued deposition simply by slope failure resulting from over-steepening of a depositional slope. Finally, turbidity currents require a slope. The optimum conditions for the generation of a turbidity current probably would be a large body of fine, well-sorted sand triggered by an earthquake on a steep slope.

Heezen (1956) studying cable failures from various parts of the world has found evidence for several different trigger mechanisms. Besides earthquakes, hurricanes have, in at least one instance, produced a turbidity flow off Cape Hatteras. One of the most interesting types of trigger mechanism is that related

to the high bedload transport at the mouths of rivers. Potentially, such a source should have a greater geologic importance since both the trigger effect and the source of sediments are supplied by the river. In such an area repeated flows from a single source could build up a submarine abyssal cone, and at the same time repeated currents down the same path on the continental slope could erode a canyon. Significant periodic changes in depth have been observed at the heads of submarine canyons by Shepard (1948), Zenkovich (1958), Heezen (1956) and others.

It was found that cable failures in the submarine canyon of the Magdalena (Heezen 1956) occurred after prominent changes had taken place in the depth and shape of the river mouth. These changes in turn had occurred only during the highest flood stages of the river. A similar pattern was also observed off the Congo. Both rivers have a common characteristic in their lack of a modern subaerial delta. The delta sediments in both cases are to be found in the alluvial cones at the mouths of their submarine canyons; and indeed, exploration in both areas has disclosed graded beds containing a large proportion of terrestrial organic remains as well as tree leaves and wood. A dramatic fact associated with the 1935 cable failure off the Magdalena was recorded when grass, still green, was brought up wrapped around the damaged cable which lay in 750 fathoms, 12 miles seaward from the river mouth.

Abyssal Life and Petroleum. The occurrence of carbonaceous deposits in the deep-sea alluvial cones led to speculation on the effect of this material on the nutrition of the abyssal fauna (Heezen, Ewing & Menzies 1955, 1957). It was reasoned that turbidity flows would have two radically contrasting effects on the abyssal fauna. Rapid deposition of a thick bed of sediment over the abyssal floor must have a tremendous destructive effect, smothering by burial much of the indigeneous fauna. In contrast, the large windfalls of organic debris brought to the deep-sea by turbidity currents must support a greater productivity than the normal, slow, pelagic deposition.

Repeated turbidity currents from an organic-rich source build an organic-rich submarine deposit containing both the transported organic debris and the trapped and entombed abyssal fauna.

Another important effect of turbidity currents on petroleum occurrence is independent of the bottom fauna. Orr, Emery & Grady (1958) found that while the content of chlorophyll derivatives in sediment immediately below turbidity current deposited sands was anomalously high, that of the sands themselves was anomalously low. The turbidity currents which brought in the sands were apparently derived from a source low in organic matter and thus in this case only the blanketing effect of the turbidity current deposit is seen.

Turbidity currents flowing into an anaerobic basin (such as the Cariaco Trench, Heezen & others 1958), may provide sandy source beds and impermeable clay cap beds for future oil fields. In this case the source of the oil is the planktonic remains. It seems likely that much of the oil in the productive Maracaibo basin was formed and trapped in this manner.

Since the geologist's key to the past is the present, the implications of submarine turbidity currents as regards paleogeographic reconstructions are tremendous. No longer can scattered shallow water fossils be considered evidence of shallow-water deposition, nor does evidence of strong currents indicate shallow depths. Even ripple marks, long considered an absolute proof of shallow water origin, have been found as deep as 2 000 fathoms.

Modern Geosynclines. Turbidity currents are gradually filling the modern deep-sea trenches. Turbidity-current smoothed trench (abyssal) plains have now been reported from every trench which has been sounded in detail. Trenches bound most of the circumference of the Pacific Ocean, but in the Atlantic such marginal topographic trenches are exceedingly rare. However, wherever seismic-refraction studies have been made at the base of the continental slope a deep trough of lower velocity material ascribed to unconsolidated sediments and sedimentary rock has been found paralleling the base of the continental slope. These former trenches were probably filled largely by turbidity current sediment. They constitute in all probability, the modern geosynclines which quietly await the process of orogeny which through deformation and uplift, may eventually turn them into folded mountains.

The effect of turbidity currents over a long period of geologic time is to fill in the hollows of the deep-sea floor by building vast abyssal plains, and to erode canyons into the continental slopes. Of course, if the rate of subsidence of the marginal trenches exceeds the rate of deposition, broad basin floor abyssal plains would not form since all turbidity current deposits would be trapped in the trenches. The effect of turbidity currents in the deep sea produces a topography essentially similar to that produced by periodic downpours in desert mountains. The coalescing alluvial fans resemble the continental rise, and the playas resemble the abyssal plains.

Continued Acceptance. Turbidity current deposits have been described from the modern basins of sedimentation off southern California by Gorsline & Emery (1959). These modern turbidity-current deposits have been compared by them to those described by Natland & Kuenen (1951) and others from the filled sedimentary basins of southern California. Considerable attention has been given to these deposits since the analogous deposits in the filled basins are productive of petroleum.

Menard (1955) has employed the turbidity current hypothesis to explain the smooth topography, and the canyons, and the deep-sea channels of the North Pacific. Locher (1952, 1954) and Phleger (1951) who studied the lithology and fauna of the deep-sea sands from the equatorial Atlantic became convinced of their turbidity-current origin. Bourcart (1953) and Dupliax & Calleux (1956) described deep-sea sands from the abyssal plains of the Mediterranean which they identified as the deposits of turbidity currents. The concept has found an increasingly greater application in palaeogeographical reconstruction and a host of recent papers have appeared which we will not attempt to review here. It will suffice to say that Kuenen, his associates, and his students as well as many other independent workers have had considerable success in identifying ancient turbidity-current deposits throughout the world.

Over-enthusiasm. Unfortunately, the turbidity-current concept has been occasionally overworked even in regard to recent deposits. By invoking turbidity-current action Rigby & Burckle (1958) attempted to explain the emplacement of thin beds (millimetres thick) of fresh-water diatoms found in cores of mid-equatorial Atlantic eupelagic sediment. This explanation is no less ridiculous than the theory proposed by Malaise (1957) who believes them to be deposits laid down in ponds during a recent and complete emergence of the Mid-Atlantic Ridge. The Congo River at present carries fresh-water diatoms hundreds of miles offshore. Kolbe (1957a, 1957b) points out that they are also blown hundreds

of miles to sea by the wind. To emplace diatoms on the Mid-Atlantic Ridge as suggested by Rigby & Burckle (1958) would require turbidity currents to climb over 3000 metres in 500 miles travelling all the way over an intensely rugged bottom, an ability not attributable to turbidity currents. Rigby and Burckle do not doubt that surface currents, or perhaps the wind, can transport diatoms as far as the core stations on the Mid-Atlantic Ridge, but they do not believe, for some unspecified reason, that ocean currents could deposit and concentrate beds of fresh-water diatoms.

The geological record contained in the ancient sediments is sufficiently complex that other misapplications will undoubtedly occur.

Part 3. Erosion at depth

A New Surprise: Abyssal Ripples. When photographs of the deep sea floor were first taken in appreciable numbers the frequent discovery of ripple marks and scour marks was simply astounding. In 1948 a well-known physical oceanographer, upon seeing a picture of ripple marks at 400 fathoms was so amazed that he seriously suggested to the writer that the ripples were fossil and had been formed before a local subsidence of the sea floor. Ripples were found in many localities inaccessible to downslope movements. It is improbable that turbidity currents are related in any general way to the processes forming the ripples seen in bottom photographs. Actually, the ripples should not have come as a surprise since early studies of sediments taken from submarine peaks and in deep straits in depths ranging down to 2000 fathoms had revealed winnowing of the finer particles (Murray & Renard 1891). In fact, Agassiz (1888) early recognized that current scour could be effective to depths down to at least 650 fathoms. He concluded that:

". . . the bottom of the Gulf Stream along the Blake Plateau is swept clean of slime and ooze, and is nearly barren of animal life".

Weber, in 1900, later noted coarse sand and rock bottom to depths of 1500 metres in the passages between the Indonesian Islands. But concerning these findings Grabau (1913) concluded that:

"It is probable that we have here a prevention of sedimentation by the removal of the particles before they reach the bottom, rather than any effect of eroding work of the currents at such depth."

Ripple marks and scour marks have been found on every seamount photographed to date (Menard 1952, Heezen, Tharp & Ewing 1959). Ripple marks have been observed on the crest of the Mid-Atlantic Ridge down to 2000 fathoms (Elmendorf & Heezen 1957). They have also been observed on the continental slopes to similar depths. The deepest photographs of the North Atlantic abyssal floor had indicated probable scour marks in 3200 fathoms depth (Dietz 1952, Elmendorf & Heezen 1957). The deepest Atlantic photographs recently taken revealed rock bottom, at 4000 fathoms in the Romanche Trench portion of the Mid-Atlantic Rift Valley (Cousteau 1958). These sharper topographic features are being scoured by ocean currents which remove the finer sediment and produce the ripple marks. The direction of these currents has not been determined, although a collection of oriented photographs might go far to solving the problem. It must be supposed that the sediment eroded from these peaks by the currents is deposited

in their lee. A study of these deposits may produce evidence of the direction of the deep currents and the nature of their variations in late Tertiary, Pleistocene and Recent time.

Deep Currents. Wüst (1935, 1957) concluded that relatively strong bottom currents swept along the continental slope off eastern South America. His calculations indicated a 5–20 cm/s western boundary current in the South Atlantic. The same range of velocities was recently measured in the North Atlantic western boundary current through the use of neutral floats (Swallow & Worthington 1957).

Ocean-bottom photographs of rock outcrops and ripple marks taken on the continental slope shows the eroding capability of this current (Northrop & Heezen 1951, Heezen & others 1959). Dietrich (1957) and Cooper (1955) have described bolses of cold Norwegian sea water which flow through the Denmark Strait and descend to the depths of the Atlantic at velocities of 10 to 30 cm/s. Strong currents have been calculated from the fine systematic observations made by J. B. Tait (1956) in the Shetland Channel.

It has been suggested that the bolses of cold water flowing across the northern margins of the Atlantic may be related in some way to the turbidity currents which built or eroded the northwest Atlantic Mid-Ocean Canyon (Ewing & others 1953).

Except where shallow-water benthonic organisms are found incorporated in the deposit, it may be difficult to distinguish in every case the effects of bottom scour from the deposits of turbidity currents.

More must be learned of the causes and further effect of these strong bottom currents which have denuded the crest of a large part of the Mid-Atlantic Ridge to depths of 2 000 fathoms (Heezen & others 1959). These currents wear so gradually that transatlantic submarine cables crossing the crest of the ridge often last 25 years or more before their armour wires are finally worn through. Thus, this incessant motion must never become too violent or the cables would snap more frequently.

Internal Tides. Internal tides have been observed during all oceanographic anchor stations made in deep water. Defant (1950) concluded that:

"Internal tides are as common as tides at the surface of the ocean . . ." "The amplitude . . . and the water transport connected with them are much larger than those of normal surface tides."

In view of this it seems likely that internal tides could be responsible for the abyssal ripple marks observed in deep-sea photographs.

Swallow (1955, 1957) reported eleven direct measurements of deep currents made in the eastern Atlantic with neutrally buoyant floats. Residual non-tidal components of 22 cm/s down to 1 cm/s were measured in depths ranging from 340 to 2 900 m. A tidal current varying from 7·3 to 10·0 cm/s was found superimposed on a net current of 2·4 cm/s in one observation at 800 m depth. However, in measurements made at greater depths the tidal component, if present, could not have exceeded 5 cm/s. Swallow suggests therefore:

"Possibly the contribution from internal waves becomes less important at greater depths, so that the remaining tidal current may be near the theoretical value of about 3 cm/s derived on the assumption that the tidal current is uniform over the whole depth."

If Swallow's tentative conclusion is further confirmed it would appear that the deep ripples and bottom scour must be the work of currents related to the general circulation of the ocean rather than to the work of currents induced by the tides.

Homogenized History. Evidence of deep-sea erosion, transportation and deposition by bottom currents comes from the fine studies of the minute, fragile tests of silicious Radiolaria and diatoms found in mid-Pacific abyssal red clays. The long, red clay cores of the *Albatross* Expedition were chosen for detailed study since, based on estimates of sedimentation rates, they were thought to contain the undisturbed record of most of the late Tertiary. At the time Riedel (1957) began his investigation of the Radiolaria, he

"expected that the assemblages in the tops of the cores could be used to determine the areal distribution of various species at the present day, while samples from lower levels of the cores would show, in an orderly manner, the development of present-day species through at least Pleistocene and Recent time."

However, the results of his study forced him to conclude:

"that the situation is actually more complicated than was expected. Late Tertiary Radiolaria were found to be reworked into Recent sediments, and evidence of disconformities was found in the sediment sequences. Re-examination of some of the samples from the *Challenger* Expedition showed that Tertiary sediments outcrop on the deep-sea floor. Erosion, and reworking of older Radiolaria into younger sediments, obscure phylogenetic developmental sequences in the long sediment cores . . ."

The "epic poem" contained in these layers of sediment had, it seemed, been frequently reduced to a font of jumbled type as cryptic to read as a typesetter's pie.

Kolbe (1957a, 1957b) who found pre-Quaternary diatoms in several Pacific and Indian Ocean cores, concluded that their presence is "unimportant" and "accidental, although no plausible explanation of the occurrence can be given". Riedel, however, "speculated that a more or less continuous agency (? current) was transporting Radiolaria on or near the sea floor" and that "the transporting agency has acted either continuously, or at such short intervals as to obscure intermittance".

In the light of Riedel's conclusions, it is not surprising that difficulty was encountered in the stratigraphic interpretation of the chemical analyses of these cores (Berrit & Rotschi 1956), and that, in general, the ionium and radium methods of dating of deep-sea sediments have been more often a failure than a success (St. Kroll 1955, Volchok & Kulp 1957). Probably the most important result of the later studies has been the conclusion that conditions of uniform, undisturbed, unreworked sedimentation required by these dating methods only rarely prevail on the deep-sea floor.

Radiocarbon evidence. The top samples of deep-sea cores generally show an apparent radiocarbon age of the order of a few thousand years. Even when the "zero age" for the top of the core is extrapolated from several dates determined deeper in the core, ages are found averaging 2 500–3 000 years. It has been claimed that this discrepancy results from the action of bottom burrowers which

churn the sediment bringing older material to the surface. Others believe that sedimentation underwent a recent drastic diminution. Isotopic fractionation during sedimentation, decomposition and diagenesis has also been suggested.

The age determined for the fine fraction of a sample is generally greater than the age of the coarse fraction, and the age of the organic part is generally less than that of the carbonate portion. However, these generalizations frequently do not hold.

Broecker, Ewing & Heezen (in press) attribute the finite zero age of top samples at least in part to the continuous erosion and redeposition of sediment. Sediment suspended in the water or wafted along the bottom is believed to be continuously reworked into the modern sediment. In addition, they believe that loss of sediment during coring and churning by bottom burrowers are also significant contributory factors in many cases. However, the fact that similar finite zero ages are found in varve-like sediment rapidly deposited in anaerobic basins (Heezen & others 1958) indicates that these factors are insufficient as a general explanation.

Sub-bottom Echoes. The character of the echo returned to the echo sounder from the deep-sea floor can be examined in great detail by use of the high-resolution Precision Depth Recorder.

The echo may be sharp and discrete, diffuse and prolonged, single, double or multiple. Over distances of a few hundred yards, the bottom may appear absolutely smooth or completely disrupted on a minute scale.

Sub-bottom echoes are frequently observed in deep-sea echograms. In some cases the sediment horizon responsible for the sub-bottom echo has been identified by coring or drilling. Worzel (1959) has correlated a prominent sub-bottom echo in the east tropical Pacific with a 2–4 inch thick bed of volcanic ash. Heezen & others (1958) have correlated a prominent sub-bottom echo with the base of the Recent anaerobic layer in the Cariaco Trench. Gorsline & Emery (1959) have mapped turbidity-current beds in the San Pedro Trough. In areas of particle by particle deposition where one or two prominent, 5–20-fathom deep sub-bottom echoes can be traced over a wide area they typically show deepening in the small depressions, thinning over gentle rises, and are totally absent on steeper inclines, indicating that due to gentle scour sedimentation has been greater in the depressions.

The gentle but continuous wafting suggested by Riedel in explanation of the distribution of Radiolaria would seem to be a satisfactory explanation of these configurations. In other areas the simple sub-bottom echo, while still detectable, became intensely disturbed, possibly suggesting that the bed is intermittent or has been folded.

The occurrence of a series of closely-spaced reflectors on an otherwise smooth bottom (Heezen & others 1959, Plate 5) may indicate deep-sea dunes (2 400 fathoms) produced by strong bottom scour. Echogram profiles taken in depths of 300 fathoms beneath the Gulf Stream were interpreted in a similar manner.

Photographs of manganese nodules (Dietz 1952, Elmendorf & Heezen 1957) taken in great depths of the Atlantic Ocean floor, and more recently on the Easter Island Ridge of the southeast Pacific (Revelle 1958) tell us that sedimentation in these areas is virtually at a standstill. Pettersson has estimated their rate of concretionary growth at 1 mm in 1 000 years on the basis of measurements of radium. Regardless of their actual rate of growth, which may be one-tenth or one-hundredth of that amount (Goldberg 1958) it must be exceedingly slow for Tertiary sharks' teeth often form their nuclei. Features in the sediment around

the nodules resemble scour marks. Thus the gentle scour and reworking of the abyssal red clay is supported both by the study of cores and by examination of the bottom photographs.

Archaic Fauna. That the bottom currents were not always so strong, so fast, or so cold, is shown by the frequent discovery of early Tertiary calcareous oozes beneath the red clay of the eastern Pacific (Arrhenius 1952). In several areas where now less than a few per cent of the carbonate falling onto the modern sea floor escapes solution, in the Eocene and Oligocene seas over seventy per cent of the carbonate remained. Oxygen-isotope measurements have been interpreted by Emiliani & Edwards (1953) to indicate cooling of 12 °C in the Pacific bottom water since Eocene time. However, regardless of the various assumptions of the isotope method, the existence of the high carbonate deposits itself is indicative of a comparable change of temperature or rate of circulation.

The conclusion of Menzies & Imbrie (1958) that the deep-sea fauna contains fewer rather than, as formerly held, a greater number of archaic types is probably the result of the apparently relatively wide variation in the rates and modes of circulation of the abyssal waters as contrasted to the almost uniform water conditions in the near surface environments. The close uniformity of variables in the deep-sea with depth and geographical location had misled earlier investigators to assume that the deep-sea was an environment unvarying over long periods of time. But it now seems that the properties of the deep-sea most important to living organisms, namely, oxygen, temperature and nutrients, have varied widely throughout geologic time.

Some problems

Solution: The Big Lollipop. In addition to mechanical processes of erosion, deposition and mixing by slumps, turbidity currents, deep-sea currents and tidal oscillations, the sediments of the deep-sea floor undergo chemical alteration and solution before, during and after burial. It is frequently incorrectly assumed that once buried the components of deep-sea sediments remain locked in the ocean depths, permanently removed from the bio-geochemical cycle. The interstitial waters gradually forced from the sediment during compaction probably deliver some components back to the sea water (Emery & Rittenberg 1952). Volcanic glasses are devitrified and altered to clays and carbonates. Calcareous sediments are dissolved not only while sinking through the water, but after burial, since the mechanical processes active on the sea floor favour solution and alteration.

In addition to currents and waves, the benthic fauna continually stirs the sediments. Bottom photographs show abundant trails and tracks criss-crossing the sea floor. Often the bottom is studded with small cones a few inches across built by burrowing organisms (Heezen & others 1959). Sediment cores characteristically show burrow mottling.

With abundant evidence of erosion, reworking and redeposition by bottom currents, we now must conclude that carbonate, silica and other components may re-enter the bio-geochemical cycle after millions of years residence beneath the deep-sea floor.

Geochemical balance calculations generally encounter difficulty in regard to the high proportion of calcium in sedimentary rocks (Kuenen 1950). In explanation it has been suggested that no carbonate deposits could have formed in the

Palaeozoic ocean due to the lack of lime-secreting plankton; but Bramlette (1958) points out that cocoliths which make up the bulk of modern pelagic carbonate sediments, probably were present in Palaeozoic seas. However, the evidence of reworking, erosion and resolution of carbonate sediments long entombed beneath the sea floor may ease the problem since it need not be assumed that the calcium in deep-sea sediments is permanently lost from the geochemical cycle.

"*Moholes.*" One of the major problems of deep-sea sedimentation, indeed probably the most perplexing question in regard to the origin of the ocean floors is the thinness of the deep-sea sediments as determined by the seismic-refraction method. Over most of the Pacific (Raitt 1956, Hill 1957) the unconsolidated sediment and sedimentary rock has a thickness of less than a half kilometre; in the Atlantic the average thickness of deep-sea sediments (Ewing & Ewing 1959) is only slightly greater. If sedimentation at rates at all comparable to those measured for post-glacial time by radioactive decay are applied to this thickness, we come to the startling but dubious conclusion that the oceans were formed in late Palaeozoic, late Mesozoic, or early Tertiary time; the exact date depending on our particular choice of average rates. This calculation allows for only pelagic sedimentation and takes no account of turbidity-current additions to the thickness. If we cannot assume that throughout most of geologic time the marginal trenches trapped the turbidity-current deposited sediments, the discrepancy becomes much greater. As an explanation of this apparent discrepancy, the solution of deposited sediment, the submergence of most of the present lands with attendant decreased erosion, and the lack of Palaeozoic plankton all have been suggested; but the problem of the extreme thinness of the sediments has become nonetheless evasive and intriguing. The answers to these problems may be provided by core samples obtained during the drilling in the deep-sea floor of the exploratory holes to the Mohorovičić discontinuity (Gaskell 1958). However, in view of the many phenomena which can continue to jumble the record, great care must be exercised in the choice of drilling sites to better our chances of obtaining a readable record.

Conclusion

We now can view the vast abyss with somewhat less mystery and more real understanding. The picture of an unremitting snowfall of sediment which softly casts a thin veil over the rugged, grand and imposing relief of the deep-sea must be tempered with occasional, sometimes frequent, turbidity flows, which, like snow avalanches in the Alps, sweep down and smother the relief of the lower slopes. Just as winds striking the mountains drive the snow from the peaks, so the ocean currents sweep the sediment from the higher and bolder submarine mountains.

Just as wind and water shape the land so do the submarine currents of water and mud, by erosion, by solution and by scour shape the ocean floor. To be sure, erosion dominates on the land, as does deposition in the deep sea.

Acknowledgments

Discussions with Maurice Ewing, David Ericson, Wallace Broecker and Robert Menzies of the Lamont Geological Observatory have greatly aided the writer in forming the opinions expressed in this review. In addition, conversations with

W. H. Bucher, R. S. Dietz, K. O. Emery, H. Gould, F. F. Koczy, Ph. H. Kuenen, B. Kullenberg, H. W. Menard, F. P. Shepard, K. K. Turekian, G. Wüst and with many others have been quite helpful.

Lamont Geological Observatory,
Columbia University,
Palisades, New York.
(*Lamont Geological Observatory Contribution No.* 345).

References

Agassiz, A., 1888. *Three cruises of the* Blake, Vol. I, Harpers, New York, 220 pp.

Andree, D., 1920. *Geologie des Meeresbodens*, Gebrüder Borntraeger, Berlin, 689 pp.

Arrhenius, G., 1952. Sediment cores from the East Pacific. *Rep. of Swedish Deep-Sea Expedition, V* (1, 2, 3 & 4).

Bally, A., 1957. Turbidity currents—a list of selected references, *J. Alberta Soc. Petrol. Geol.*, **5,** 89–98.

Bell, H. S., 1942. Density currents as agents for transporting sediments, *J. Geol.*, **50,** 512–547.

Benest, H., 1899. Submarine gullies, river outlets, and fresh-water escapes beneath the sea level, *Geog. J.*, **14,** 394–413.

Berrit, G. R. & Rotschi, H., 1956. Chemical analyses of cores from the central and west equatorial Pacific, *Rep. of Swedish Deep-Sea Expedition, VI*, (2), 51–58.

Bourcart, J., 1953. Sables "néritiques" a 2750 m de profondeur au large de Bougie (Algérie), *C. R. Acad. Sci., Paris*, **236,** 738–740.

Bourcart, J. & Glangeaud, L., 1956. Perturbations sous-marines et courants de turbidité du Seisme d'Orléansville, *C. R. Acad. Sci., Paris*, **242,** 1504–1506.

Bourcart, J. & Glangeaud, L., 1958. Perturbations sous-marines et courants de turbidité resultant du tremblement de terre d'Orléansville, *Bull. d'Information C.O.E.C.* (*Paris*), X (10), 642–656.

Bowden, K. F., 1954. The direct measurement of subsurface currents in the oceans, *Deep-Sea Res.*, **2,** 33–47.

Bramlette, M. N., 1958. Significance of coccolithophorids in calcium-carbonate deposition, *Bull. Geol. Soc. Amer.*, **69,** 121–126.

Bramlette, M. N. & Bradley, W. H., 1942. Geology and biology of North Atlantic deep-sea cores, *U.S. Geol. Survey Prof. Paper*, **196,** 1–32.

Broecker, W. S., Ewing, M. & Heezen, B. C., in press. Evidence of an abrupt change in climate close to 11 000 years ago.

Broecker, W. S., Turekian, K. K. & Heezen, B. C., 1958. The relation of deep-sea sedimentation rates to variations in climate, *Amer. J. Sci.*, **256,** 503–517.

Bucher, W. H., 1940. Submarine valleys and related geologic problems of the North Atlantic, *Bull. Geol. Soc. Amer.*, **51,** 489–512.

Buffington, E. C., 1952. Submarine natural levees, *J. Geol.*, **60,** 473–479.

Carson, R., 1951. *The sea around us.* Oxford Univ. Press, New York, 230 pp.

Clarke, F. W., 1924. *The data of geochemistry*, 5th ed. U.S. Geol. Survey Bull. **770,** 841 pp.

Cooper, L. H. N., 1955. Deep-water movements in the North Atlantic as a link between climatic changes around Iceland and biological productivity of the English Channel and Celtic Sea, *J. Marine Res.*, **14,** 347–362.

Cousteau, J., 1958. *Calypso* explores an undersea canyon, *Nat. Geogr. Mag.*, **113**, (3), 373–396.

Cushman, J. A., 1941. A study of the Foraminifera contained in cores from the Bartlett Deep., *Amer. J. Sci.*, **239**, 128–147.

Daly, R. A., 1936. Origin of submarine canyons, *Amer. J. Sci.*, **31**, 401–420.

Defant, A., 1950. On the origin of internal tide waves in the open sea, *J. Marine Res.*, **9**, 111–119.

Dietrich, G., 1957a. *Allgemeine Meereskunde.* Gebrüder Borntraeger, Berlin, 492 pp.

Dietrich, G., 1957b. Ozeanographische Probleme der deutschen Forschungsfahrten im Internationalen Geophysikalischen Jahr 1957–58, *Deutschen Hydrogr. Z.*, **10** (2), 41–61.

Dietz, R. S., 1952. Geomorphic evolution of continental terrace. *Bull. Amer. Assoc. Petrol. Geol.*, **36**, 1802–1819.

Dietz, R. S., 1953. Possible deep-sea turbidity-current channels in the Indian Ocean, *Bull. Geol. Soc. Amer.*, **64**, 375–378.

Duplaix, S. & Calleux, A., 1956. Sur quelques sables des fonds de 1850 á 4270 m de la Méditerranée, *C. R. Acad. Sci., Paris*, **244**, 104–106.

Elmendorf, C. H. & Heezen, B. C., 1957. Oceanographic information for engineering submarine cable systems, *Bell System Tech. J.*, **26**, 1047–1093.

Emery, K. O. and Rittenberg, S. C., 1952. Early diagenesis of California basin sediments in relation to origin of oil, *Bull. Amer. Assoc. Petrol. Geol.*, **36**, 735–806.

Emiliani, C. & Edwards, G., 1953. Tertiary ocean-bottom temperatures, *Nature (London)*, **171**, 887–888.

Ericson, D. B., Ewing, M. & Heezen, B. C., 1951. Deep-sea sands and submarine canyons. *Bull. Geol. Soc. Amer.*, **62**, 961–965.

Ericson, D. B., Ewing, M. & Heezen, B. C., 1952. Turbidity currents and sediments in the North Atlantic, *Bull. Amer. Assoc. Petrol. Geol.*, **36**, 489–512.

Ericson, D. B., Ewing, M., Wollin, G. & Heezen, B. C., in press. Atlantic deep-sea cores. *Geol. Soc. Amer., Memoir.*

Ewing, J. I. & Ewing, W. M., 1959. Seismic refraction measurements in the Atlantic Ocean basins, Mediterranean Sea, on the Mid-Atlantic Ridge and in the Norwegian Sea, *Bull. Geol. Soc. Amer*, **70**, 291–318.

Ewing, M., Ericson, D. B. & Heezen, B. C., 1958. Sediments and topography of the Gulf of Mexico, pp. 995–1058 in Weeks, L., Editor, *Habitat of Oil*, Amer. Assoc. Petrol. Geol., Tulsa, 1384 pp.

Ewing, M., Heezen, B. C., Ericson, D. B., Northrop, J. & Dorman, J., 1953. Exploration of the Northwest Atlantic Mid-Ocean Canyon, *Bull. Geol. Soc. Amer.*, **64**, 865–868.

Forel, F. A., 1885. Les ravins sous-lacustre des fleuves glaciaires, *C. R. Acad. Sci., Paris*, **101**, 725–728.

Gaskell, T. F., 1958. Drilling deep holes into the earth, *Proc. R. Inst. Gr. Brit.*, Part II, **37**, 189–209.

Goldberg, E. D. & Arrhenius, G., 1958. Chemistry of Pacific pelagic sediments, *Geochim. et Cosmochim. Acta*, **13**, 153–212.

Gorsline, D. S. & Emery, K. O., 1959. Turbidity current deposits in San Pedro and Santa Monica basins off southern California, *Bull. Geol. Soc. Amer.*, **70**, 279–290.

Gould, H. R., 1951. Some quantitative aspects of Lake Mead turbidity currents, *Spec. Pub. Soc. Econ. Paleont. Mineralog.*, **2,** 34–52.

Grabau, A. W., 1913. *Principles of stratigraphy.* Seiler, New York, 1185 pp.

Greenman, N. N. & Le Blanc, R. J., 1956. Recent marine sediments and environments of northwest Gulf of Mexico, *Bull. Amer. Assoc. Petrol. Geol.*, **40,** 813–847.

Grover, N. C. & Howard, C. S., 1938. The passage of turbid water through Lake Mead, *Trans. Amer. Soc. Civil Eng.*, **103,** 720–790.

Gutenberg, B., 1939. Tsunamis and earthquakes, *Bull. Seismol. Soc. Amer.*, **29,** 517–526.

Heezen, B. C., 1956a. Origin of submarine canyons, *Scient. Amer.*, **195,** 36–41.

Heezen, B. C., 1956b. Corrientes de turbidez del Rio Magdalena, *Bol. Soc. Geog. Colombia*, **51** & **52,** 135–143.

Heezen, B. C., Ericson, D. B. & Ewing, M., 1954. Further evidence for a turbidity current following the 1929 Grand Banks earthquake, *Deep-Sea Res.*, **1,** 193–202.

Heezen, B. C. & Ewing, M., 1952. Turbidity currents and submarine slumps, and the Grand Banks earthquake, *Amer. J. Sci.*, **250,** 849–873.

Heezen, B. C. & Ewing, M., 1955. Orleansville earthquake and turbidity currents. *Bull. Amer. Assoc. Petrol. Geol.*, **39,** 2505–2514.

Heezen, B. C., Ewing, M. & Ericson, D. B., 1951. Submarine topography in the North Atlantic, *Bull. Geol. Soc. Amer.*, **62,** 1407–1409.

Heezen, B. C., Ewing, M. & Ericson, D. B., 1954. Reconnaissance survey of the abyssal plain south of Newfoundland. *Deep-Sea Res.*, **2,** 122–133.

Heezen, B. C., Ewing, M. & Menzies, R. J., 1955. The influence of submarine turbidity currents on abyssal productivity, *Oikos*, **6,** 170–182.

Heezen, B. C., Ewing, M., Menzies, R. J. & Broecker, W. S., 1958. Date of stagnation of the Cariaco Trench, *Bull. Geol. Soc. Amer.*, **69,** 1579.

Heezen, B. C., Ewing, M., Menzies, R. J. & Granelli, N. C., 1957. Extension of the Congo Submarine Canyon, *Bull. Geol. Soc. Amer.*, **68,** 1743.

Heezen, B. C., Tharp, M. & Ewing, M., 1959. The floors of the oceans: I, The North Atlantic, *Geol. Soc. Amer. Spec. Paper*, **65,** 126 pp.

Hill, M. N., 1957. Recent geophysical exploration of the ocean floor, pp. 129–163 in Ahrens, L. H. & others, Editors, *Physics and chemistry of the earth.* Pergamon, London, 259 pp.

Houot, G. S., 1958. Four years of diving to the bottom of the sea, *Nat. Geogr. Mag.*, **113** (5), 715–731.

Johnson, D., 1939. *Origin of submarine canyons.* Columbia Univ. Press, New York, 216 pp.

Jones, O. T., 1954. The characteristics of some Lower Palaeozoic marine sediments, *Proc. Roy. Soc. A.*, **222,** 372–332.

Koczy, F. F., 1954. A survey of deep-sea features taken during the Swedish Deep-Sea Expedition. *Deep-Sea Res.*, **1,** 170–184.

Koczy, F. F. & Burri, M., 1958. Essai d'interpretation de quelques formes du terrain sous-marin, *Deep-Sea Research*, **5,** 7–17.

Kolbe, R. W., 1957a. Diatoms from equatorial Indian Ocean cores, *Rep. of Swedish Deep-Sea Expedition*, IX (1), 1–50.

Kolbe, R. W., 1957b. Fresh-water diatoms from Atlantic deep-sea sediments, *Science*, **126,** 1053–1056.

Kröll, V. S., 1955. The distribution of radium in deep-sea cores, *Rep. of Swedish Deep-Sea Expedition*, X (1), 1–32.

Kuenen, P. H., 1937. Experiments in connection with Daly's hypothesis on the formations of submarine canyons. *Leidsche Geol. Med.*, **8,** 327–335.

Kuenen, P. H., 1950. *Marine Geology*. Wiley, New York, 568 pp.

Kuenen, P. H., 1952. Estimated size of the Grand Banks turbidity current, *Amer. J. Sci.*, **250,** 874–887.

Kuenen, P. H., 1956. The difference between sliding and turbidity flow, *Deep-Sea Res.*, **3,** 134–139.

Kuenen, P. H. & Migliorini, C. I., 1950. Turbidity currents as a cause of graded bedding, *J. Geol.*, **58,** 1–127.

Kullenberg, B., 1954. Remarks on the Grand Banks turbidity current, *Deep-Sea Res.*, **1,** 208–210.

Landes, K. K., 1952. Our shrinking globe, *Bull. Geol. Soc. Amer.*, **63,** 225–240.

Locher, F. W., 1954. Ein Beitrag sum Problem der Tiefseesande im westlichen Teil des aquatorialen Atlantiks, *Heidelberger Beiträge z. Mineralogie u. Petrographie*, **4,** 135–150.

Lombard, A., 1956. *Géologie sédimentaire; les séries marines*. Masson, Paris, 722 pp.

Malaise, R., 1957. Oceanic bottom investigations and their bearings on geology, *Geol. Fören., Stockholm*, **79,** 195–224.

Maury, M. F., 1855. *Physical geography of the sea*. Harpers, New York, 389 pp.

Menard, H. W., 1952. Deep ripple marks in the sea, *J. Sed. Petrol.*, **22,** 3–9.

Menard, H. W., 1955. Deep-sea channels, topography, and sedimentation, *Bull. Amer. Assoc. Petrol. Geol.*, **39,** 236–255.

Menard, H. W., 1956. Archipelagic aprons, *Bull. Amer. Assoc. Petrol. Geol.*, **40,** 2195–2210.

Menard, H. W. & Ludwick, J. C., 1951. Applications of hydraulics to the study of marine turbidity currents, *Soc. Econ. Paleont. Mineralog. Spec. Pub.*, **2,** 2–13.

Menzies, R. J. & Imbrie, J., 1958. On the antiquity of the abyssal fauna, *Oikos*, **9,** 192–210.

Milne, J., 1897. Suboceanic changes, *Geogr. J.*, **10,** 129–146 and 259–289.

Murray, J. & Hjort, J., 1912. *Depths of the ocean*. John Murray, London, 821 pp.

Murray, J. & Renard, A. F., 1891. *Report on the scientific results of the voyage of* H.M.S. Challenger, 1873–76. Neill, Edinburgh, 525 pp.

Natland, M. L. & Kuenen, P. H., 1951. Sedimentary history of the Ventura Basin, California, and the action of turbidity currents, *Soc. Econ. Paleont. Mineralog. Spec. Pub.*, **2,** 78–107.

Northrop, J. & Heezen, B. C., 1951. An outcrop of Eocene sediment on the continental slope. *J. Geol.*, **59,** 396–399.

Orr, W. L., Emery, K. O. & Grady, J. R., 1958. Preservation of chlorophyll derivatives in sediments off southern California, *Bull. Amer. Assoc. Petrol. Geol.*, **42,** 925–962.

Pettersson, H., 1954. *The ocean floor*. Yale Univ. Press, 179 pp.

Pettersson, H., 1955. Manganese nodules and oceanic radium, *Deep-Sea Res.*, **3** (supplement), 335–345.

Phleger, F. P., 1951. Displaced Foraminifera faunas, *Soc. Econ. Paleont. and Mineral. Spec. Pub.*, **2,** 66–75.

Raitt, R. W., 1956. Seismic-refraction studies of the Pacific Ocean basin, Part I, Crustal thickness of the equatorial Pacific, *Bull. Geol. Soc. Am.*, **67,** 1623–1640.

Revelle, R., 1958. The Downwind Expedition to the South-east Pacific. *Trans. Amer. Geophys. Un.*, **39,** 528–429.

Revelle, R., Bramlette, M., Arrhenius, G. & Goldberg, E. D., 1955. Pelagic sediments of the Pacific, *Geol. Soc. Amer. Spc. Paper*, **62,** 221–236.

Riedel, W. R., 1957. Radiolaria, a preliminary stratigraphy, *Rep. of Swedish Deep-Sea Expedition, VI* (3), 59–96.

Rigby, J. K. & Burckle, L. H., 1958. Turbidity currents and displaced freshwater diatoms, *Science*, **127,** 1504.

Roher, E., 1954. Staublawinen-ja oder nein?, *Die Alpen*, **3,** 62–69.

Rubin, M. & Suess, H. E., 1955. U.S. Geol. Survey radiocarbon dates II, *Science*, **121,** 481–488.

Shepard, F. P., 1948. *Submarine geology*. Harpers, New York, 348 pp.

Shepard, F. P., 1954. High velocity turbidity currents, a discussion, *Proc. Roy. Soc. A.*, **222,** 323–326.

Spencer, J. W., 1903. Submarine valleys off the American coast and in the North Atlantic, *Bull. Geol. Soc. Amer.*, **14,** 207–226.

Stetson, H. C. & Smith, J. F., 1937. Behavior of suspension currents and mud slides on the continental slope, *Amer. J. Sci.*, **35,** 1–13.

Stoneley, R., 1957. On turbidity currents, *K. Nederl. Geol. Mijnb. Gen.*, **18,** 279–285.

Swallow, J. C., 1955. A neutral-buoy float for measuring deep current, *Deep-Sea Res.*, **3,** 74–81.

Swallow, J. C., 1957. Some further deep current measurements using neutrally-buoyant floats, *Deep-Sea Res.*, **4,** 93–104.

Swallow, J. C. & Worthington, L. V., 1957. Measurements of deep currents in the western North Atlantic, *Nature* (*London*), **179,** 1183.

Tait, J. B., 1956. Recent oceanographical investigations in the Faroe-Shetland Channel, *Proc. Roy. Soc. Edinburgh*, **64,** 239–289.

Terzaghi, K., 1957. Varieties of submarine slope failures, *Norw. Geotech. Inst. Pub.*, **25,** 1–15.

Volchok, H. L. & Kulp, J. L., 1957. The ionium method of age determination, *Geochim. et Cosmochim. Acta*, **11,** 219–246.

Weber, M., 1900. Die niederländische SIBOGA Expedition zur Untersuchung der marinen Fauna und Flora des Indischen Archipels, *Petermann's Geog. Mitt.*, **46,** 187.

Worzel, J. L., 1959. Extensive deep-sea sub-bottom reflections identified as white ash. *Proc. Nat. Acad. Sci.*, **45,** 349–355.

Wüst, G., 1957. Quantitative Untersuchungen zur Statik und Dynamik des Atlantischen Ozeans; Stromgeschwindigneiten und Strommengen in den Tiefen des Atlantischen Ozeans. *Deutscher Atlantischen Exped.* Meteor, 1925–29, Wiss. Erg., VI (2), 420 pp.

Zenkovich, V. P., 1958. *Shores of Black and Azov Seas.* State Geographic Editions, Moscow, 371 pp.

Reports of Discussions

Geophysical Discussion of the Royal Astronomical Society

A discussion on **The Characteristics of the Antarctic Ice Sheet** was held in the rooms of the Society on 1959 February 27. The meeting was arranged jointly by the Royal Astronomical Society and the British Glaciological Society under the chairmanship of Dr J. F. Nye.

After welcoming and introducing the other speakers *Dr Nye* gave an outline of the theoretical aspects of the problems presented by large ice sheets. The mechanical behaviour of an ice sheet is governed by two opposing forces: the weight, which tends to squeeze the ice out sideways, and the resistance to outward flow provided by the rock bed. These two forces are approximately balanced. Two substantial sources of heat affect the temperature distribution within the ice. Heat flows into the bottom of the ice sheet from the earth itself and heat is generated at the bottom of the ice sheet by friction between the ice and the rock bed over which it moves. If the minor effects of transverse convection are ignored both sources of heat tend to raise the temperature of the lowest layers. As the plasticity of ice is sensitive to small changes in temperature, it follows that the plasticity of the ice sheet is greatest near the bottom. The shearing stress in the ice increases linearly with the depth and hence the shear distortion takes place predominantly in the lowest layer and analysis has shown that the movement may equally well be regarded as slipping on the bed or as very intense shear in the lowest layer. The two principal features of the motion are thus a very slow squeezing down partly or entirely compensated by the accumulation of new snow and giving a strain rate of about 10^{-4}/yr, and a faster outward movement giving a shear rate greater than 10^{-2}/yr in the bottom layer. In a steady state the total outward flow of ice is just sufficient to balance the accumulation of new snow. A simple model shows that the steady state thickness of the ice sheet is proportional to only the 5th or 6th root of the accumulation and so the height of the ice sheet will be very insensitive to even long term fluctuations in the rate of accumulation, and calculations of the form of an ice sheet can be made with fair accuracy without a knowledge of the accumulation. Field measurements on a large ice sheet should aim at elucidating the topography, ice thickness, and rate of accumulation.

The second speaker was *Ingénieur Hydrographe B. Imbert* who is in overall charge of the French I.G.Y. Expeditions to the Antarctic and who himself led the second French I.G.Y. Expedition to Terre Adélie. M. Imbert presented the results obtained along a traverse running 300 miles inland from Base Dumont d'Urville to a southernmost point south of Base Charcot at an altitude of 2 509 m. During the southern summer 1957–58 seismic reflection results were obtained at twenty-five stations along this route and during the next summer seventy gravity stations were occupied and glaciological work was carried out.

A twelve channel recording camera and filter with pass bands of 5–100 c/s were employed in the seismic work. From the coast to an altitude of 480 m reflections were obtained with shots fired on the surface but farther inland it was

necessary to bury the charges and at the southernmost point, where the ice was 2 990 m thick, a charge of 1 kg was used at a depth of 18 m. Larger charges gave no improvement. Difficulties were experienced from the cold surface layers of the snow which tend to spoil transmission and from persistently strong winds averaging 30 knots. It was impossible to record in winds greater than 38 knots. In spite of this the typical reflection records passed round by M. Imbert were of a very high quality. The results of the seismic work showed that the undulating bedrock is largely below sea-level along the line of the traverse. The average depth is 40 m below sea-level but a maximum depression of 600 m below sea-level was recorded. M. Imbert suggested that a broad valley observed near Charcot is occupied by a glacier flowing to the north-east because instruments levelled at Charcot gradually became tilted in this direction.

In establishing the topography of the ice sheet for the gravity and seismic traverses heights were estimated barometrically but the atmospheric pressure was checked independently by radio-sonde methods. The estimated accuracy of the heights obtained is ± 15–20 m. The results of the gravity traverse are not yet available. The profile of the ice sheet along the line of the traverse is given by the ellipse

$$\left(\frac{h}{2{\cdot}68}\right)^2 + \left(\frac{550 - x}{550}\right)^2 = 1$$

where x is the horizontal distance in kilometres inland from Dumont d'Urville and h is the height in metres of the ice surface above sea-level. The r.m.s. error in h is 25 m.

Glaciological work was carried out by the French expedition. Fifty-seven stakes were set up on the traverse of 483 km and were observed during the two subsequent summers. More detailed observations of accumulation were made at Charcot. The results showed that the rate of accumulation falls off from a value of 36 cm of water equivalent per year near the coast to 10 cm per year at the southernmost point. The observed surface densities lay between 0·38 and 0·48 g/cm^3. The mean temperature of the ice at Charcot was −38 °C at a depth of 16 m.

In answer to *Dr T. F. Gaskell* the speaker stated that multiple explosion shots fired above the snow surface did not improve the records sufficiently to justify the increased expenditure of explosive. *The Chairman* enquired what was the magnitude of the tilting observed at Charcot and M. Imbert estimated that it was a few minutes of arc per fortnight. *Dr H. Lister* noted that the rate of accumulation observed at Charcot was high and enquired whether the station was in a topographic trough. M. Imbert said that the station was not in a trough but agreed that accumulation rates were greatest in troughs.

The third speaker, *Mr J. G. D. Pratt*, described the seismic and gravity traverse carried out by the Commonwealth Trans-Antarctic Expedition. Mr Pratt said that, like M. Imbert, he had found a range of 5–100 c/s adequate for the seismic recording equipment but that it had been necessary to fit a heater into the camera. Lack of time had prevented him from burying the shots more than 12 m below the surface and as this produced no great improvement the shots were sometimes fired on the surface. A slide showed records obtained at the South Pole where there is a discrepancy between Mr Pratt's estimate of the depth to the bedrock and the estimate based upon a single American observation. Mr Pratt pointed out the reflection which he ascribed to the bedrock and the subsequent reflection

which the American observers had chosen. He said that his own estimate of the depth, which agrees with the results of neighbouring seismic stations and with the gravity profile, should be accepted in preference to the very much greater American estimate. Mr Pratt showed a profile of the ice sheet from South Ice on the Weddell Sea side of the Pole to the Plateau Depot on the Ross Sea side. The results obtained by the Trans-Antarctic Expedition showed that along the line of their route the rock bed was almost everywhere above sea-level. On the Weddell Sea side there are two depressions comparable with Lake Baikal, for example, but on the Ross Sea side of the Pole the bedrock is substantially higher, due probably to the fact that the route of the Expedition was parallel with the known mountain range fringing the Ross Sea and probably lay over the buried foothills of the range.

The results of a refraction line shot at South Ice were used to find the variation in the velocity of compressional waves with depth in the ice. It was found that the velocity increased in the surface layers from 0·5 to 4 m/s at a depth of 80–90 m Below this the velocity was uniform. The observed rate of increase in velocity in the surface layers was used to calculate an accurate value for the correction due to the depth of shot and it was shown that this correction could have been made with sufficient accuracy by the usual assumption of a linear increase in velocity with depth in the surface layer. Although the snow surface was undulating no correlation was found between the observed arrival times of the refracted waves and the topography. This was interpreted as meaning that the valleys are underlain by softer snow in which the lower velocity counterbalances the effect of the shorter path which the sound has to follow.

Shackleton Base was built on an ice shelf. Reflection shots were fired near the Base to try to determine the thickness of the floating ice. Reflections were obtained from the sea bed but no reflections were obtained from the bottom of the ice shelf. However the travel times for a ray refracted at the ice–water interface and reflected at the sea bed can be expressed as a power series in terms of the horizontal distance from shot to detector and Mr Pratt has shown that a unique solution of the thickness of the ice shelf can be obtained in this way.

The results of the gravity measurements were used to confirm the general correctness of the seismic profile. Altitudes were measured barometrically and errors from this source amount to ± 25–50 mgal. The estimated errors due to drift are about 5 mgal. Bouguer anomalies have been calculated taking the ice thicknesses indicated by the seismic profile and assuming a rock density of 2·1 g/cm^3. The fact that there are no outstanding anomalies is taken to indicate that the seismic profile is substantially correct. However there is a mean anomaly of -200 mgal which cannot be explained away by the uncertainties of the measurements and suggests that Antarctica, like Scandinavia, has not yet recovered from the depression caused by the burden of a much larger ice sheet which covered the continent in the past.

The last of the four speakers was *Dr H. Lister*, who described the glaciological results obtained by the Trans-Antarctic Expedition. In order to determine the mass balance of the ice sheet as a whole it is necessary to know how the average annual rate of accumulation varies from the centre of the continent to the periphery. The average annual rate of accumulation at the coast was estimated as equivalent to about 30 cm of water per year by observing the layering in the shelf ice cliff. In order to observe the accumulation during the year at Shackleton Base and at "Southice" strings and graduated pegs were fixed to the snow surface

between stakes. This was done every fortnight. At the end of the winter the strings were dug out and the fortnightly accumulation measured. In order to find the rate of accumulation in past years, observations were made of the layering in pits and boreholes and the hardness of the snow layer was measured by means of the Rammsonde device. The annual layering is marked by variations in grain size hardness, and density, but it is not easy to be certain of the identity of the individual, layers. In pits and boreholes at "Southice" Dr Lister was able to recognize the annual layering back to the year 1895 with some confidence and the mean rate of accumulation obtained was about 10 cm/yr. On the trans-continental journey 10 boreholes penetrated through twenty annual layers and 40 more penetrated five layers. Zones of hard sastrugi and areas of broad undulations were encountered on the Polar Plateau. The mean rate of accumulation found on the plateau was 8–10 cm/yr but as much of the route of the expedition lay in a topographic trough this figure is probably a little greater than average. In the coastal mountains and on the shelf ice the observed rate was 16 cm/yr rising to 26 cm/yr near the sea. The low accumulation observed as Shackleton—10 cm/yr—was explained as being due to loss of drift snow over the nearby ice cliff. Making due allowance for the shape of the continent Dr Lister calculated a mean annual rate of accumulation of 13·1 g/cm^2 yr for the whole Antarctic ice sheet.

Photographs and observations were made to determine the distribution of drift snow above the surface and led to a figure of 0·1 g/cm^2 yr for the loss from the whole continent due to drift blown out to sea. Assuming a mean flow rate of 200 m/yr for the edge of the ice sheet Dr Lister arrived at a mass balance for the continent of 13·1 g/cm^2 yr accumulation and 10·1 g/cm^2 yr total loss due to evaporation (1·0 g), deflation (0·1 g), calving of icebergs (4·0 g), and melting, largely at the ice/sea interface (5·0 g). He said that there was probably a closer approximation to balance than these figures would suggest.

Mr Pratt pointed out that it was curious that the tracks of drift particles shown on the photographs were all parallel, indicating that all the particles were at the same point on their trajectories. *Dr H. H. Lamb* of the Meteorological Office asked what were the estimated errors of the points on the curve showing annual snow accumulation at "Southice" since 1898. Dr Lister said that the standard deviation of a single observation was 3½ g but that the actual error probably amounted to 50 per cent.

In the discussion which followed the papers *Dr T. F. Gaskell* asked how it might be possible to reconcile Dr Lister's results which suggest net accumulation with Mr Pratt's gravity results which suggest net loss. *Mr Pratt* said that the gravitational results indicate a long term retreat, whereas the glaciological results apply to a short period of only a few years and may indicate a minor fluctuation. *The Chairman* suggested that the rate of flow of the ice sheet should be taken as greater than 200 m/yr and *Professor J. H. Zumberge* said that he had measured a flow rate of about 10 metres per day on the Ross Ice Shelf. *Dr Lister* said that it would not be sufficient to double the estimate of 200 m/yr which he had taken but that the high flow rate of about 1 000 m/yr suggested by Professor Zumberge would be enough to remove the discrepancy between accumulation and loss which his figures had indicated. *Professor Zumberge* asked why the low figure of 1 g/cm^2 yr had been taken for evaporation. *Dr Lister* replied that he had actually observed rime accumulation rather than evaporation. He thought that there is insufficient heat available for much sublimation and that 1 g/cm^2 yr was a generous estimate of the loss from the continent as a whole due to evaporation. Professor

Zumberge mentioned measurements of summer meltwater on land, made in the McMurdo Sound area, but Dr Lister thought that this melting merely balanced the excessive snowfall which occurred near the sea.

The Chairman asked what was the significance and history of the large-scale surface undulations observed on the polar plateau. Dr Lister said that in the walls of the pit dug at "Southice" a regular fluctuation in grain size had been observed and that this had been ascribed to the migration of large sastrugi with a frequency of about one per 1½ metres of accumulation. This was comparable with the surface undulations which have a wavelength of about 12km and a mean amplitude of 20 to 25m. *The Chairman* pointed out that these undulations may have a profound effect on the motion of the ice sheet. They represent fluctuations in slope comparable with the average slope itself and extending over distances comparable with the thickness of the ice sheet. Since the shear stress on the bed is proportional to the surface slope and on Weertman's theory the sliding velocity is proportional to the square of the stress, the undulations may result in a system of random velocities, perhaps greater than the mean velocity, superimposed on the smoothly varying outward velocity. This might invalidate measurements of the velocity of flow made in the field. *Mr G. R. Elliston* asked whether it would be possible to measure the grain size in a pit at the crest of an undulation in order to see how long the crest had persisted. *Dr Lister* replied that the random variation would make this impossible. Replying to Dr Zumberge he said that the undulations were asymmetric in profile on the Ross Sea side of the Plateau. *Mr Hollingworth* asked why the undulations did not smooth themselves out and what was the mechanism of their motion. Replying, the speakers agreed that bad sastrugi were found on the flanks of the undulations and that these might interfere with the flow of air and be responsible for the soft snow and greater accumulation found in the troughs.

The Chairman thanked the speakers and the contributors to the discussion and adjourned the meeting at 18h 20min.

The Geological and Geophysical Results of the cruises of R.R.S. *Discovery II* during 1958 May–July

A symposium concerned with the geophysical and geological investigations of the ocean floor during 1958 from R.R.S. *Discovery II* was held at the Department of Geodesy and Geophysics at Cambridge on March 4th. The expedition, which was a joint venture of the Department of Geodesy and Geophysics and the National Institute of Oceanography, lasted approximately three months and during this time investigations of the ocean floor were made in three separate areas. The first was in the neighbourhood of a small sea-knoll in latitude 41°15′N and longitude 14°30′W, near the western boundary of the Iberian Abyssal Plain which lies at a depth of about 5 300m. The main object of the cruise in this neighbourhood was the measurement of deep ocean currents; this was not a full-time occupation and allowed time and opportunity for detailed investigations of the topography and magnetic field of the abyssal plain and neighbouring sea mounts in an area approximately 60 miles from north to south by 100 miles from east to west. Seismic refraction shooting experiments, heat flow measurements, coring, dredging and bottom photography were also successfully undertaken.

The dredging over the sea-knoll and over the sea-mounts to the westward

provided a large collection of rocks which were not erratics and which, there was good reason to suppose, were *in situ*. Bottom photography had shown the existence of outcropping rock and the samples from any one haul were largely of the same type. The rocks from the sea-knoll were rotted basaltic lavas which were more or less manganese coated; this coating in some cases was entering cracks in the rock and causing the rocks to fracture. Weathering of this type has not hitherto been observed. Only small samples of unaltered glass were obtained but these will be adequate for chemical analysis; sections of these rocks have been made and are at present being studied.

The lavas from the sea-mounts were less altered and of a different type from the others. Petrographical work on these rocks is now being undertaken. Measurements of the radioactivity, the magnetic susceptibility and the elastic properties are also to be made in the future.

The seismic results in the area suggested that the Mohorovičić discontinuity was at a relatively small depth. The combined results from three stations showed that on the abyssal plain a thin layer (about 200 m) of sediments covered a layer which, with an assumed velocity of 4 km/s, was 2·7 km in thickness. This overlay the typical oceanic "basaltic" layer of velocity 6·8 km/s and thickness 1·3 km. The Mohorovičić discontinuity lay at a depth of 9·5 km below sea-level and the velocity below was 8·1 km/s.

Various minor features were observed to stick up through the abyssal plain and the sediments collecting on their slopes were fine clay and foraminiferal tests. This material was markedly different from that in the cores from the abyssal plain which were loaded with coarse quartz sand and fragments of metamorphic rocks.

The total magnetic force contours of the area showed a restricted correlation with the topography. The central sea-knoll had a clear anomaly associated with its northern end, and the sea-mounts to the west likewise caused greatly increased magnetic roughness. Other features on the abyssal plain, however, had no anomalies associated with them and conversely there were a number of magnetic anomalies dissociated from topographic features. From these measurements it was not possible to decide whether the anomalies were caused by rocks immediately below the sediments or by deeper rocks.

The precision echo sounder developed by the National Institute of Oceanography, and which was first used on this expedition, allowed great detail of the fine structure of the abyssal plain to be studied. It was found to slope upwards towards its boundaries to the north and east with slopes of a few parts in 10 000. This had been deduced from earlier work.

The second area of investigation lay in the region between the Biscay and the Iberian abyssal plains. This area was selected since it appeared from the slopes of the plains that there must be a channel or channels interconnecting the two plains through the saddle separating them and that sediment was transported from the Biscay plain to the Iberian plain. The depth difference between these plains is about 200 m. Two channels were located on the Biscay side of the saddle; these joined into a single channel approximately halfway between the plains and then bifurcated into two at the Iberian plain end. The total distance between the plains is about 30 miles. The gradients in the beds of the channels are high at their top ends, slopes of 1 in 10 existing near the spill-over from the Biscay plain. Lower down, the channels have relatively small gradients and near the region where they join the gradient is in fact reversed. It is postulated that turbidity currents from the Biscay plain acquire sufficient kinetic energy when passing down

the steep slope to sweep over this region of slightly reversed gradient before travelling far out into the Iberian plain. Core samples from the bed of the valley were of coarse material in comparison with that obtained from the areas elevated above the abyssal plains.

The third area of investigation was centred at a position 42½°N, 11½°W and has provisionally been named Galicia Bank. It is an elevated plateau of depth about 700 m separated from Cape Finisterre by a channel of depth greater than 2000 m. To the north lies the Biscay abyssal plain and to the south-west the Iberian plain. The plateau which is about 30 miles in length from north to south and 20 miles in width from east to west is bounded by steep escarpments to the east and to the west. Magnetic measurements show that, compared with measurements made over sea-mounts further from the continental boundary, the rocks must have a relatively very low magnetic susceptibility. In this respect the rocks appear to resemble rocks of the continental shelf more closely than those of the deep ocean. Seismic measurements indicate that the plateau is covered with a thin layer of unconsolidated material overlying rocks with velocity 4·8 km/s. This layer is approximately 4 km in thickness and lies above a layer of velocity 7·1 km/s. From these velocities it is not possible to identify the rocks; they are not, however, inconsistent with what might be found in a column of continental rocks. Dredging in the area produced a collection of stones which, to date, have not been closely inspected. They included a considerable number of metamorphic rocks, some basic lavas and some limestones. It is not yet certain that these rocks are *in situ*; it is possible that they are erratics.

During the expedition numerous unoriented cores up to 7 m in length were obtained for palaeomagnetic measurements. The measurements are not yet complete but it appears from the preliminary results obtained from three cores taken from the flanks of a small sea-mount in the Iberian abyssal plain that they are magnetically stable. Correlation between the magnetic properties from core to core is not immediately obvious; future measurements may nonetheless show that it exists. The mean value of the inclination of the magnetic vectors in these cores is not appreciably different from what would be expected if the present inclination and the associated variation of direction of the Earth's magnetic field had persisted throughout the time of deposition of the core. The intensity of permanent magnetization of the core material is directly associated with the water content which is itself associated with the quantity of clay minerals present. It appears that the increase of the proportion of clay results in an increase in water content. Extraction of the magnetic minerals and a closer study of the lithology of the cores will take place in the future.

During the expedition two refuelling visits were made in Lisbon and a very large magnetic anomaly was located in shallow water a few miles outside the mouth of the Tagus. A survey of the area showed that the anomaly could be produced by a dipole buried at a depth of approximately 2 km below the sea floor. This dipole could be caused by a spherical mass of magnetic rocks of maximum radius 2 km centred at a depth of 2 km. The minimum susceptibility of such a mass of rocks must be exceptionally high. The anomaly was associated with magnetic compass deviations of about ±4°.

Those participating in the Symposium were: Dr M. N. Hill, Sir Edward Bullard, Mr T. D. Allan, Mr M. J. Keen and Mr D. H. Matthews, from the Department of Geodesy and Geophysics, and Dr A. S. Laughton from the National Institute of Oceanography.

РЕЗЮМЕ ДОКЛАДОВ, В ПЕРЕВОДЕ НА РУССКИЙ ЯЗЫК

СДВИГОВЫЕ КОЛЕБАНИЯ ЗЕМЛИ И СВЯЗАННЫЕ С ЭТИМ ВОПРОСЫ

Х. Такэути

Методами вариационного исчисления проводится решение задачи колебаний сдвига для упругих сфер, в которых меняются плотности и упругие константы, а также решается задача для плоских волн Лява в среде с вертикальной неоднородностью.

Показана эффективность методов применительно к решенным задачам; получена кривая фазовой скорости для модели Земли по Буллену (см. фиг. 1). Соответствующие распределения смещений показаны на фиг. 2.

ИСКАЖЕНИЯ, ВНОСИМЫЕ СЕЙСМОГРАФАМИ В СИГНАЛЫ ЗЕМЛЕТРЯСЕНИЙ ИМПУЛЬСНОГО ВИДА

М. Ландисман, И. Сато, и. М. Юинг

Для изучения аппаратурных искажений, вносимых приборами с различными постоянными в сигналы импульсного вида—как теоретически заданных, так и полученных экспериментальным путем — используется метод вычисления сейсмограмм, полученных при любом сейсмографе для произвольного непрерывного движения почвы. Вычисления сводятся к решению уравнения движения системы маятник-гальванометр четвертого порядка типа Рунге-Кутта. Изменение постоянных приборов дает существенно различные сейсмограммы для различных практически интересных случаев.

Для выяснения причин кажущегося различия между наблюдениями Сато и данными наблюдений Беньоффа и Пресса за групповой скоростью длиннопериодных волн Лява были сравнены вычисленные сейсмограммы длиннопериодных волн Лява G_1, для толчка 1 февраля 1938 года в Новой Гвинее с их же записью на линейном деформографе. Результаты такого изучения совпадают с данными Сато о том, что график групповой скорости волн Лява совершенно прямолинеен в широком диапазоне периодов в несколько сотен секунд. Искажение, вносимое приборами, увеличение которых быстро возрастает с периодом, совершенно достаточно для того, чтобы маскировать любую незначительную дисперсию, которая может быть связана с такого рода импульсными сигналами.

ОПРЕДЕЛЕНИЕ ТЕМПЕРАТУР В НЕНАРУШЕННЫХ ПЛАСТАХ ПО НАБЛЮДЕНИЯМ В ГЛУБОКИХ РАЗВЕДОЧНЫХ СКВАЖИНАХ

Л. Р. Купер и С. Джонс

В процессе бурения скважины температура окружающих ее слоев нарушается за счет циркуляции бурового раствора и после остановки бурения жидкость в скважине и прилегающие к ней слои приобретают первоначальную температуру ненарушенных слоев. Восстановление температурного равновесия скорее всего происходит у забоя скважины, где нарушение было наименьшим. На основании этого положения можно проводить температурные наблюдения после остановки бурения на выходной день. Для того, чтобы на достигнутых глубинах можно было вычислить из этих наблюдений значения температур, используется решение тепловой задачи в случае цилиндрической симметрии с начальными условиями, определяемыми тепловыми параметрами жидкости и окружающей среды.

Разработана новая и недорогая аппаратура, использующая принцип термистора для температурных измерений, которая успешно опробована до глубин 1060 м в скважине

Хоптон Пул в районе Каннок Чейс. Описано оборудование и даны измеренные температуры ненарушенных пластов, вскрытых скважиной Хоптон Пул. Приведена серия наблюдений температуры бурового раствора на различных глубинах, полученная в течение нескольких дней спустя после окончания бурения скважины и показано, что эти результаты не могут рассматриваться как надежные данные о температуре ненарушенных пластов.

ФУНКЦИИ ПОГЛОЩЕНИЯ ВОЛН РЭЛЕЯ В СРЕДЕ С МАЛЫМИ ПОТЕРЯМИ

Дж. Росс Макдоналд

Выведена простая формула, характеризующая специфические факторы поглощения для рэлеевских продольных и поперечных волн в материалах, обладающих малыми потерями. Представлены результаты вычислений и таблицы, которые позволяют получить неизвестный фактор поглощения из двух известных для других типов волн. Результаты приложимы к любому, реальному отношению двух или трех фазовых скоростей.

КРАТКОЕ СООБЩЕНИЕ

МОДЕЛЬ ЗЕМЛИ И РЕДУКЦИЯ НАБЛЮДЕНИЙ СИЛЫ ТЯЖЕСТИ ДЛЯ ЕЕ ИСПОЛЬЗОВАНИЯ В ИНТЕГРАЛЕ СТОКСА

Дж. Ч. Бхаттачарджи

Обсуждается приложимость модели Земли д-ра Хюнтера в поправках при использовании формулы Стокса для гравитационных наблюдений. Сделанапопытка выяснения практических трудностей при использовании в интеграле Стокса для определения фигуры Земли нового вида поверхностной аномалии вида $g-\gamma_E$, предложенной доктором Хюнтером.

О ПРОГРЕССЕ В ГЕОФИЗИКЕ

ДИНАМИЧЕСКИЕ ПРОЦЕССЫ ГЛУБОКОВОДНОГО ОСАДКООБРАЗОВАНИЯ ЭРОЗИЯ, ДВИЖЕНИЕ НАНОСОВ И ПЕРЕОТЛОЖЕНИЕ НА ГЛУБОКОВОДНЫХ УЧАСТКАХ МОРЯ

Б. С. Хизен

До исследований последнего десятилетия господствовало представление о глубоководном осадкообразовании, как подобном осадкообразованию на мелководье: спокойное, почти лишенное движения, не подвергающееся воздействию течений и процессов эрозии. В настоящее время это представление пересмотрено. Процессы, происходящие на морском дне, рассматриваются как динамические, находящиеся под сильным воздействием мутьевых потоков, внутренних приливных волн, глубинных течений, растворения ранее образовавшихся наносов,—играющих роль в изменении формы морского дна, разрушении и создании его фауны. Эти процессы создают распределение и структуру осадков, которые прежде считались образованными на мелководье. Новое представление находится в стадии критической разработки, при наличии противоречивых взглядов на относительное значение тех или иных процессов. Показывается развитие новых представлений и описываются варианты принципиально различных точек зрения на этот вопрос.

Geophysical Journal

INSTRUCTIONS TO AUTHORS

Хонтон Пул в районе Галиок Чейс. Описано оборудование и даны измеренные температуры неперфорированных пластов, вскрытых скважиной Хонтон Пул. Приведена серия наблюдений температуры бурового раствора на различных глубинах, полученная в течение нескольких дней спустя после окончания бурения скважины и показано, что эти результаты не могут рассматриваться как надежные данные о температуре неперфорированных пластов.

ФУНКЦИИ ПОГЛОЩЕНИЯ ВОЛН УПРУГОСТИ В СРЕДЕ С МАЛЫМИ ПОТЕРЯМИ

Дж. Росс Макдональд

Выведена простая формула, характеризующая специфические факторы поглощения для релеевских продольных и поперечных волн в материалах, обладающих малыми потерями. Представлены результаты вычислений и таблицы, которые позволяют получить неизвестный фактор поглощения из двух известных для других типов волн. Результаты приложимы к любому, реальному отношению двух или трех фазовых скоростей.

БРАТНОЕ СООБЩЕНИЕ

МОДЕЛЬ ЗЕМЛИ И РЕДУКЦИИ НАБЛЮДЕНИЙ СИЛЫ ТЯЖЕСТИ ДЛЯ ЕЕ ИСПОЛЬЗОВАНИЯ В ИНТЕГРАЛЕ СТОКСА

Дж. Ч. Беннетт-мл.

Обсуждается приложимость модели Земли д-ра Хейтера в поправках при использовании формулы Стокса для гравитационных наблюдений. Сделан анализ выяснения практических трудностей при использовании в интеграле Стокса для определения фигуры Земли нового вида поверхностной гармоники вида $\sin^2 2\varphi$, предложенной доктором Хейтером.

О ПРОГРЕССЕ В ГЕОФИЗИКЕ

ДИНАМИЧЕСКИЕ ПРОЦЕССЫ ГЛУБОКОВОДНОГО ОСАДКООБРАЗОВАНИЯ ЭРОЗИЯ, ДВИЖЕНИЕ ВАЛОВ И ПЕРЕОТЛОЖЕНИЕ НА ГЛУБОКОВОДНЫХ УЧАСТКАХ МОРЯ

Б. С. Хизен

До исследований последнего десятилетия господствовало представление о глубоководном осадкообразовании как подобном осадкообразованию на мелководье, спокойное, почти лишенное движения, не подвергающееся воздействию течений и процессов эрозии. В настоящее время это представление пересмотрено. Процессы, происходящие на морском дне, рассматриваются как динамические, находящиеся под сильным воздействием мутьевых потоков, внутренних приливных волн, глубинных течений, растворения ранее образовавшихся илистых, играющих роль в изменении формы морского дна, разрушении и создании его фауны. Эти процессы создают распределение и структуру осадков, которые прежде считались образованными на мелководье. Новое представление находится в стадии критической разработки, при наличии противоречивых взглядов на относительное значение тех или иных процессов. Показывается развитие новых представлений и описываются варианты принципиально различных точек зрения на этот вопрос.

Geophysical Journal

RECOMMENDATIONS TO AUTHORS

1. Authors are advised to follow the general suggestions for the preparation of scientific papers given in *Notes on the preparation of papers to be communicated to the Royal Society* and in *The printing of mathematics* by T. W. Chaundy, P. R. Barrett and C. Batey (Oxford University Press, 1954). In particular the abbreviations for the names of periodicals used in the *Geophysical Journal* are those given in *Notes on the preparation of papers . . .* and the symbols, signs and abbreviations are those recommended for British scientific publications by the Symbols Committee of the Royal Society.

2. Papers should be typewritten with double spacing and on one side of the paper only. Two copies, one of them the top copy, should be submitted. All papers must be accompanied by a summary; summaries are not required for *Letters to the Editors*.

3. Tables are printed without rules. They should be numbered serially with Arabic numerals. Table headings should be brief. Units should be placed at the head of the column. Tables should be typed on separate sheets and their positions in the text indicated on the copy.

4. Illustrations, especially photographs, should be kept to a minimum, and the same information should not in general be given in both tables and illustrations. Line drawings should be in dense black ink on smooth white board or transparent tracing film. Original drawings must not be lettered; lettering should be indicated on copies or photoprints which must be supplied in addition to the originals. Wherever possible, lettering should be kept outside the diagram so that it may be set in type. Diagrams should be drawn at twice to three times the size at which they will be printed. The maximum dimensions for diagrams, when reduced and with their lettering and captions, are 8 in by 5 in. A wide variety of flat tints of dots, lines and shadings can be applied to line drawings by the blockmaker. Photographs for reproduction should be unmounted glossy prints and should be accompanied by lettered prints.

5. References should be quoted in the form recommended by the Royal Society but authors may also quote titles of papers if they wish. References in the text are made in the form (Smith 1940).

6. Authors whose work involves much mathematics should follow carefully the recommendations in *The Printing of Mathematics*.

7. The Editors will be glad to advise authors on any special points of difficulty arising in the preparation of papers for the *Journal*.

Contents

PAGE

H. TAKEUCHI, Torsional oscillations of the Earth and some related problems 89

M. LANDISMAN, Y. SATO and M. EWING, The distortion of pulse-like earthquake signals by seismographs 101

L. R. COOPER and C. JONES, The determination of virgin strata temperatures from observations in deep survey boreholes 116

J. ROSS MACDONALD, Rayleigh-wave dissipation functions in low-loss media 132

Research Note

J. C. BHATTACHARJI, An Earth Model and the reduction of gravity observations for use in Stokes's integral 136

Letter to the Editors

E. IRVING, Magnetic "cleaning" 140

Note on Progress in Geophysics

BRUCE C. HEEZEN, Dynamic processes of abyssal sedimentation: erosion, transportation, and redeposition on the deep-sea floor 142

Reports of Discussions

The characteristics of the Antarctic Ice Sheet (R.A.S. Discussion of 1959 February 27) 164

The geological and geophysical results of the cruises of R.R.S. *Discovery II*, 1958 May–July (Cambridge Discussion of 1959 March 4) 168

Russian translations of summaries of original papers 171

РЕЗЮМЕ ДОКЛАДОВ, В ПЕРЕВОДЕ НА РУССКИЙ ЯЗЫК 171

Printed in Great Britain by J. W. Arrowsmith Ltd., Bristol